Repair of DNA-protein crosslinks in mammalian cells

A DISSERTATION

SUBMITTED TO THE FACULTY OF THE

UNIVERSITY OF MINNESOTA

BY

Lisa Nicole Chesner

IN PARTIAL FULFILLMENT OF THE REQUIREMENTS

FOR THE DEGREE OF

DOCTOR OF PHILOSOPHY

Advisor: Colin Campbell, PhD

July 2018

Acknowledgements

First and foremost, I would like to thank Dr. Colin Campbell for his constant guidance and support throughout my degree. I am very grateful for all the opportunities he provided to help me grow as a scientist such as teaching in his classes, mentoring students in lab, and attending conferences. I feel very fortunate to have worked with such a caring mentor who constantly challenges himself and, in doing so, inspires his students to do the same.

Next, I would like to thank my thesis committee chair, Dr. Jill Siegfried, and members Dr. Natalia Tretyakova and Dr. Carol Lange for their advice and input throughout my degree. It has been a privilege to work with outstanding female scientists who have helped paved the way for future women researchers. I also want to acknowledge Dr. Natalia Tretyakova for her collaboration throughout this project and helpful feedback she has provided on my work and manuscripts.

Finally, I would like to thank Dr. David Ingbar and Dr. Peter Bitterman for inviting me to join the Department of Medicine's NHLBI T32 training grant. This grant has graciously provided me with the opportunity to network with clinicians and scientists in my field as well as allowed me to expand my knowledge at weekly seminars and international conferences.

Dedication

I would like to dedicate this work to my parents, Robert and Patricia Chesner, from whom I received a strong work ethic and desire to help others. I feel truly blessed to have been brought up in an environment filled with love and support. I thank my father for picking up additional work in the winters snow plowing, even if it meant getting up at 3am and working twenty-hour days, so that his children would have the opportunity to go to college. I thank my mother for staying home with me and my brother, always helping me with my homework, and ingraining in me a love for reading. I can only hope that one day I will be able to live up to the examples they have set as wonderful parents when I raise my own children.

I would also like to dedicate this work to my fiancé, Jay Sekhon, who has been an immovable beam of support throughout my graduate career. His confidence in me has never once wavered and has helped me prevail through this challenging process. I feel very lucky to have found a man who is willing to move across the country so I can follow my dreams and has never once stopped encouraging me to do so.

Finally, I dedicate this thesis to the young girls doing science experiments in their parents' basement. May it be the start of an exciting adventure to gain a better understanding of yourself and the world around you.

Abstract

The work below describes a new assay called strand-specific primer extension-quantitative polymerase chain reaction (SSPE-qPCR) used to study the repair of DNA-protein crosslinks in mammalian cells. DNA-protein crosslinks (DPCs) are bulky lesions which disrupt important cell processes such as transcription and replication. They are formed by endogenous molecules such as formaldehyde and exogenous damaging agents such as ionizing radiation. However, the repair mechanisms associated with their repair are still unclear. **Chapter 1** of this document provides background information on the formation, biological consequences, current models, and methods used to study DPC repair. **Chapter 2** describes the SSPE-qPCR assay and its uses/limitations for studying the repair of plasmids containing DPCs or other polymerase-blocking adducts transfected into mammalian cells. **Chapter 3** describes results generated using this assay to assess the role of nucleotide excision repair in DPC repair and highlights the versatility of the SSPE-qPCR assay. **Chapter 4** extends observations made in Chapter 3 by using SSPE-qPCR to examine repair of DPC-containing plasmids in the presence of a homologous donor. It also provides evidence for homologous recombinational repair of DPCs in mammalian mitochondria. Overall, this work provides additional insight into the mechanisms of DPC repair in the nucleus and mitochondria using a quantitative, flexible assay that has not been available previously.

Table of Contents

List of Tables

List of Figures

Abbreviations

DNA-protein crosslinks (DPCs)

Nucleotide excision repair (NER)

Homologous recombination (HR)

Strand-specific primer extension-quantitative polymerase chain reaction (SSPE-qPCR)

Microhomology-mediated end joining (MMEJ)

8-oxo-2’-deoxyguanosine (8-oxo-dG)

Human oxoguanine glycosylase 1 (OGG1)

Base excision repair (BER)

deoxynucleotide triphosphates (dNTPs)

non-homologous end-joining (NHEJ)

Chapter 1

Introduction

I. DNA-PROTEIN CROSSLINK FORMATION

DNA-protein crosslinks (DPCs) are formed when cellular proteins become covalently linked to DNA[1,2]. Studies using mass spectrometry have identified hundreds of proteins that are capable of being crosslinked to DNA[3-5]. With numerous potential crosslinking sites per protein, it is not surprising that thousands of DPC variations are produced on DNA. DPCs are commonly characterized by two classes: **enzymatic and nonenzymatic[6] (Figure 1.1).**

Enzymatic DPCs are reaction intermediates formed when an enzyme is covalently linked to DNA. Normally, these enzymes reversibly bind to DNA. However, upon exposure to a crosslinking agent, the enzyme becomes trapped to the DNA[7-9]. Examples of such enzymes include DNA topoisomerases which transiently interact with DNA to relieve torsion stress but can become trapped onto DNA by inhibitors such as camptothecin[10,11]. DPCs can also be formed during base excision repair[12]. Glycosylases remove damaged bases and form a Schiff base intermediate in which the repair protein is linked to the abasic site[13]. Oxidation of these sites by reactive oxygen species or free radicals results in a covalent bond between the protein and DNA backbone[14]. DNA polymerases can also be crosslinked to abasic sites via oxidation[15]. Other repair enzymes, such as methyltransferases, which remove alkyl groups from DNA, form DPCs upon exposure to carcinogens like 1,2,3,4-diepoxybutane[16-21]

Nonenzymatic DPCs are more common than enzymatic DPCs and can involve any protein in the vicinity of DNA. These proteins are crosslinked upon

exposure to exogenous agents such as ionizing radiation, UV light, cigarette smoke, and chemotherapeutics[1,22,23]. Endogenously produced metabolites such as reactive aldehydes can also form DPCs. Reactive aldehydes are produced during the oxidation of ethanol to acetaldehyde, metabolism of amino acids, and histone demethylation at chromatin[24,25]. These aldehydes possess electrophilic carbons which can react with the primary amine of a DNA base, and following dehydration, form a Schiff base. This intermediate can then form a stable amide bond with the arginine or lysine of a nearby protein to create a DNA-protein crosslink. Reactive oxygen and nitrogen species produced during cellular respiration can also react with DNA bases to create electrophilic lesions which subsequently induce DPCs[26].

Due to their bulky nature and ability to distort the DNA helix, DPCs block the progression of replication and transcription machinery[27,28]. They also interfere with the ability of chromatin remodeling factors to access DNA and have been associated with the formation of double-strand breaks[29,30]. DPCs of various sizes have been shown to be mutagenic in human cells, resulting in genome instability and cellular toxicity[31]. Despite the frequent occurrence of these lesions, the exact mechanism(s) involved in DPC repair are still not fully understood. Multiple approaches have been taken to gain insight into the repair pathways involved.

II. DPC REPAIR DETECTION METHODS

a. Hypersensitivity of repair mutants

DNA-protein crosslinks were first noted in *Escherichia coli* following exposure to ultraviolet light and linked to cellular toxicity by Smith et al. in 1962[32]. To gain insight into the repair pathways involved in DPC repair, researchers assessed the sensitivity of bacteria repair mutants to DPC-forming agents. Results from these experiments implicated a role for the nucleotide excision repair (NER) pathway and homologous recombination (HR) pathway[33,34] in DPC repair.

The nucleotide excision repair pathway (NER) is the primary pathway for the removal of bulky DNA lesions, such as pyrimidine dimers formed by UV light[35]. Its basic steps consist of damage recognition, dual incisions by endonucleases, resynthesis of the excised DNA, and ligation[36]. Eukaryotic NER is divided into two sub pathways: global genomic NER (GG-NER) and transcription-coupled NER (TC-NER) which differ in damage recognition[37] **(Figure 1.2).** Global genomic NER employs the DNA-damage binding (DDB) protein and XPC-Rad23B complex to scan the genome to recognize helix distortions[38,39]. On the other hand, transcription-coupled NER is initiated by the stalling of RNA polymerase at a DNA lesion and recruits XPG and CSB to the site of damage[40]. Individuals with Cockayne Syndrome (CS) possess mutations in TC-NER and are hypersensitive to UV irradiation while patients with the autosomal recessive syndrome xeroderma pigmentosum (XP) suffer from extreme sun sensitivity and an increased likelihood of developing cancer[41,42].

Following recognition, these pathways converge, using the same helicases (XPB and XPD) and transcription factor (TFIIH) to unwind the DNA, followed by the endonucleases XPG and XPF/ERCC1 to make excisions on either side of the damage[43,44]. Finally, DNA polymerase delta and epsilon fill in the gap, which is an average of 30 nucleotides, and is sealed by DNA ligase[45,46].

Homologous recombination is known to repair double-strand breaks[47]. In mammals, HR occurs in the S and G2 phases of the cell cycle when homologous, sister chromatids are available and consists of two primary models: double Holliday junction and synthesis-dependent strand annealing[48,49] **(Figure 1.3).** In both models, a double-strand break occurs, and the MRN complex (Mre11, Rad50, and Nbs1) binds to either side of the break which subsequently recruits the ataxia telangiectasia mutated (ATM) kinase. Next, the DNA ends are resected to form 3' overhangs by the MRN complex and CtIP and is then coated by the RPA protein[50]. Next, BRCA2 (part of the BRCA1-PALB3-BRCA2 complex) recruits RAD51 to replace RPA and begins the search for homology[51,52]. Once found, the 3' overhang invades the recipient DNA, forming a displacement loop (D-loop), and is extended by DNA polymerase, creating a Holliday junction[53]. In the double Holliday junction pathway, the 3' overhang on the other side of the double-strand break also forms a D-loop[54,55]. Both loops are then cut by nicking endonucleases and sealed by DNA ligase, resulting in either crossover or non-crossover products[56]. In synthesis-dependent strand annealing, the invading 3' overhang is extended along the homologous donor and anneals to the other 3'

overhang of the damaged strand[57]. Following annealing, any small flaps of DNA are removed, and the repaired DNA is sealed with ligase, resulting in non-crossover products[58,59].

Formaldehyde is a DPC-inducing agent commonly used in hypersensitivity assays of repair mutants. Bacterial mutants deficient in the NER and HR pathways have been shown to be hypersensitive to formaldehyde[33,34]. *Saccharomyces cerevisiae* mutants deficient in the NER pathway were also shown to be sensitive to formaldehyde by Chanet et al. in 1976[60,61]. Interestingly, studies performed by McCullough et al. demonstrated that the contribution of HR and NER can differ depending on the dose and duration of drug exposure. Low-dose, chronic exposure of formaldehyde in *Saccharomyces cerevisiae* showed the greatest sensitivity in clones mutated in the HR pathway while high-dose, acute treatment was more toxic to NER-deficient mutants[62]. Hypersensitivity assays in DNA repair mutants were also used to assess DPC repair in mammalian cells. Studies performed in Chinese hamster ovary cells showed that clones deficient in the NER gene XPF were the most sensitive to formaldehyde treatment and accumulated double-strand breaks[63]. Additionally, Xeroderma pigmentosum patients, who possess mutations in the NER pathway, are known to be hypersensitive to formaldehyde and UV light[63,64].

A limitation to these hypersensitivity experiments is that agents that create DPCs, like formaldehyde, invariably produce other types of DNA damage such as DNA-DNA crosslinks and strand breaks which could contribute to enhanced

sensitivity[65]. Therefore, other methods have been established to distinguish between ‘protein-bound’ DNA and ‘free DNA’ to examine DPC repair mechanisms.

b. Quantification of protein-linked DNA on chromosomal DNA

Zhitkovich et al. developed a modified radioactive assay from Liu et al. to recover DNA-protein complexes from intact cells following the exposure to chromate, cisplatin, and formaldehyde[66,67]. Following drug treatment, cells are lysed with SDS, which will bind to protein (but not DNA). Upon the addition of potassium chloride, potassium displaces the sodium and forms an insoluble KSDS precipitate which can be recovered by centrifugation. Thus, the amount of DNA in the pellet is a direct quantification of ‘protein-linked’ DNA and can be measured by radioactivity or fluorescence. Results from Zhitkovich et al. detected a five-fold increase in DPCs following exposure to cisplatin, ten-fold increase to formaldehyde, and significant accumulation of DPCs in white blood cells following animal exposure to chromate. Thus, demonstrating the use for this K-SDS assay to detect accumulation of DPCs following drug treatment.

Another strategy used to isolate ‘protein-linked’ DNA is to run the cellular lysate through a nitrocellulose filter to bind ‘protein-linked DNA’ and allow ‘free DNA’ to run through. The ‘protein-linked DNA’ retained on the filter can then be quantified using fluorescence or radioactivity. Oleinick et al. used this technique to analyze DPCs formed in hamster cells following exposure to ionizing

radiation[68]. Results from these experiments showed an enrichment of DPCs on actively transcribing DNA, suggesting that DPCs may form preferentially in regions of the genome where chromatin is unwound.

Comet assays can also be used to estimate DPC formation in cells. In this assay, cells are embedded in a thin agarose gel on a microscope slide, lysed, and subjected to electrophoresis. This allows broken DNA to migrate away from the nucleus, forming a comet “tail”. The DNA is then stained with a fluorescent dye to visualize the tail length. The extent of DNA damage is directly proportional to the length of the tail[69]. Comet tails made due to DPC formation can also be reversed by pretreating samples with proteinase K. Studies performed by Merk and Speit, showed a connection between formaldehyde-induced DPC formation and removal with cytotoxicity, but this association maybe fluctuate for different types of crosslinks[69]. Conversely, comet assay studies did not show a difference between wild-type, NER-deficient, and HR-deficient cells in the removal of protein-bound DNA induced by formaldehyde[70]. Ide et al. used fluorescein isothiocyanate (FITC) to label protein-linked DNA and measured fluorescence following cell treatment with formaldehyde. Results from these experiments also showed no difference in DPC repair dynamics between wild-type and mammalian cells deficient in the NER gene XPA[71].

Maizels et al. developed a rapid approach to DNA adduct recovery (RADAR) assay to quantify protein-linked DNA by immunodetection[72,73]. This assay used chaotropic salts and detergents to separate ‘protein-linked’ DNA from

‘free-DNA’ and preserved epitopes needed for antibody recognition of the desired protein. Studies using this method recovered Topoisomerase I (Top1)-DNA adducts trapped by the chemotherapeutic camptothecin from as little as 60ng of DNA, highlighting its use for analyzing small numbers of cells.

Significant insight has been gained into DPC induction and removal following exposure to crosslinking agents using methods, such as those above, to separate ‘free-DNA’ from ‘protein-bound’ DNA. However, most of these assays do not provide details on the type of protein or nature of the chemical crosslink that is trapped onto DNA. Therefore, mass spectrometry has been used to quantify the formation and removal of specific types of DPCs, as well as to identify proteins that are crosslinked to DNA by various drug treatments.

c. Mass Spectrometry

Mass spectrometry-based proteomics has been used to conduct analysis of DPCs formed by crosslinking agents such as formaldehyde, diepoxybutane, nitrogen mustards, cisplatin, ionizing radiation, and reactive oxygen species[4,5,8,17,18,58,74,75]. Following drug treatment, chromosomal DNA is purified and proteins are released from the backbone by heating and resolved on a SDS-PAGE gel. Proteins are then excised and extracted from the gel using tryptic digestion or filters. Finally, proteins are digested to peptides using trypsin and identified using MS/MS fragmentation and proteomic software. Tretyakova et al. identified proteins crosslinked by the carcinogen 1,2,3,4-diepoxybutane (DEB)

and identified 152 proteins crosslinked to DNA. The largest percentage of proteins crosslinked to DNA had known DNA/RNA binding activity, followed by cell motility proteins, proteins involved in cellular homeostasis, and mRNA processing proteins.

To quantify DPCs using mass spectrometry, cell culture media can be depleted of native amino acids and replaced with isotopically labelled arginine and lysine. These 'heavy cells' are then treated with a crosslinking agent in parallel with normal, 'light cells' and combined after treatment[76]. High performance liquid chromatography-tandem mass spectrometry (HPLC-MS/MS) is then used to quantify the peptides. Tandem mass tags reacted with lysine and arginine residues on the ends of tryptic peptides have also been used to quantify chromosomal DPCs. In these experiments, control and experimental samples are labelled with unique isotope tags and can be distinguished on higher-performance liquid chromatography/electrospray ionization tandem mass spectrometry (HPLC-ESI-MS/MS)[77,78]. Recently, these studies have been used to assess the formation of DPCs in cardiomyocytes following ischemia/reperfusion injury[79].

To provide absolute quantification of DPCs on chromosomal DNA, isotope-dilution tandem mass spectrometry assays have been used to compare DPC accumulation in cultured cells or blood[80,81]. In these studies, amino acid-nucleoside or nucleobase standards are synthesized and isotopically labeled. Known amount of these standards are then spiked into each sample to be

quantified by HPLC-ESI-MS/MS. Tretyakova et al. quantified the formation and removal of DPC-containing DNA from cells treated with nornitrogen mustard[82] and showed higher adduct accumulation in NER-deficient cells compared to wild-type.

Although valuable information has been generated using mass spectrometry analysis of DPCs[83], these assays can be expensive and time consuming. Therefore, researchers have also utilized plasmid-based approaches to gain insight into DPC repair[84]. This method is useful in examining the repair of defined lesions at a specific site following transfection into cells proficient and deficient in DNA repair pathways.

d. Plasmid-based assays

To analyze the repair of DPC-containing plasmids, proteins can be enzymatically trapped or synthetically crosslinked to plasmid DNA and then incubated with extracts or transfected into cells[85,86]. Baker et al. enzymatically trapped the repair protein methyltransferase onto plasmid DNA and used a host cell reactivation assay to quantify its repair[87]. In this assay, the DPC blocks the transcription of a reporter gene, luciferase, which luminesces in the presence of a substrate. Changes in luminescence can then be quantified on a plate reader, and repair of the DPC is correlated with an increase in luminescence. Results from these experiments indicated a role for the NER pathway in DPC repair. Advantages to using host cell reactivation assays are that they can quantitate repair of specific

types of DPCs. However, since this assay relies on gene transcription, it is incapable of detecting repair events earlier than 24 hours post-transfection. Additionally, it is incapable of distinguishing from repair of a DPC and polymerase bypass of a lesion. Therefore, residual proteins or peptides that are still present on DNA, but have been bypassed by the transcription machinery, would be quantified as a repaired adduct.

To gain further insight into the bypass of specific lesions on DNA, synthetic adducts can be created on DNA duplexes and incubated with different polymerases to study the efficiency with which the polymerase can extend a complementary primer[88]. This strategy is useful because it allows one to manipulate the type of crosslink and polymerase to gain insight into its biological effects in *vivo*[84]. For example, it can be used to better understand which DNA adducts completely block replication and which lesions are able to be bypassed[19,20]. Bypassed lesions can be especially important if they are associated with error-prone DNA synthesis and the development of mutations in *vivo*[86,89].

e. Strand-specific primer extension-quantitative polymerase chain reaction (SSPE-qPCR)

The work herein describes a new plasmid-based assay to quantify the repair of DPC-containing plasmids using qPCR[90]. This method creates site-specific DPCs on plasmids by either enzymatic trapping or synthetic crosslinking of proteins to

DNA. DPC-containing plasmids are then transfected into repair proficient and deficient mammalian cells and repair quantified after various time points. This assay is fast, low cost, and can quantify repair events as early as 2 hours post-transfection. Using this method, new insight has been generated into the mechanisms of DPC repair and previous inconsistencies clarified regarding the role of the nucleotide excision repair (NER) pathway and homologous recombination (HR)[91] in DPC repair (see Chapter 3).

III. PROTEOLYSIS IN DPC REPAIR

It has been shown that larger DPCs are unable to be excised by the NER pathway unless proteolyzed to a smaller DNA-peptide crosslink. Studies performed in bacteria indicated that NER was incapable of excising lesions larger than 14 kDa and that these bulkier proteins were instead repaired by homologous recombination[61,92]. Similarly, Baker and Chesner both reported increased repair of DPC-containing plasmids by the NER pathway following degradation of a ~40 kDa DPC with trypsin to a smaller DNA-peptide crosslink[87,91]. Since hundreds of proteins of various sizes can be crosslinked to DNA, it is logical to suggest that proteolysis of larger DPC lesions plays an important role in DPC repair.

In 2014, Jentsch et al. identified a yeast (*S. cerevisiae*) metalloprotease called Wss1 (weak suppressor of 3mt3) to act specifically on the protein component of DPCs[93]. This group used a synthetic interaction screen with cells

lacking Wss1 and Tdp1 (tyrosly-DNA phosphodiesterase 1), an enzyme which catalyzes the removal of topoisomerase 1-DNA trapped complexes. Cells deficient in both Wss1 and Tdp1 grew slowly and were hypersensitive to camptothecin. Wss1 was also shown to cleave topoisomerase 1 in *vitro* and was capable of auto-cleavage when incubated by itself. However, the protease did not cleave proteins that did not possess DNA-binding activity. They also observed that strains lacking Wss1 and the HR pathway were more sensitive to formaldehyde compared to strains deficient in the NER pathway. Additionally, cells lacking Wss1 displayed higher numbers of Rad52-foci and elevated recombination levels when exposed to formaldehyde. These results demonstrated that in the absence of Wss1, recombination becomes a predominant DPC repair pathway. This led the authors to hypothesize that DPCs are repaired prior to replication by NER but that upon entering S phase, DPCs are repaired by HR or proteolyzed by Wss1 to facilitate translesion synthesis.

Jentsch later conducted BLAST searches in other species for proteins with high sequence similarity to the *Saccharomyces cerevisiae* protein Wss1. In humans, the Spartan (SPRTN or DVC1) protein was identified. Like Wss1, SPRTN binds zinc and was shown to be a DNA-dependent protease linked to DNA replication[6,94-99]. Patients with mutations in the SPRTN gene suffer from an autosomal recessive disease called Ruijs-Aalfs syndrome (RJALS)[100]. Characteristics of this disease include premature aging, chromosomal instability, and early onset hepatocellular carcinoma. At the cellular level, their cells undergo

slower replication and show higher numbers of stalled forks and double-strand breaks. Ramadan et al. has proposed that SPRTN is a constitutive part of the replication machinery and moves with the replisome during DNA synthesis[100]. However, mice with homozygous null alleles for SPRTN die early in embryonic development, making it difficult discern its role in the repair of DPCs in *vivo*.

The proteasome has also been investigated in DPC protein degradation. However, contradictory results have made its role unclear. For example, bacterial mutants deficient in cytosolic ATP-dependent proteases showed no effect on cell survival when treated with DPC-forming agents[61]. In *Xenopus* egg extracts, depletion of ubiquitin pools, but not proteasome inhibition, prevented DPC proteolysis during replication[101]. Baker et al. saw decreased repair of a DPC-containing plasmid using the proteasome inhibitor MG132 in hamster cells while Ide et al. observed no difference in the ubiquitination of DPCs recovered from human cells treated with formaldehyde with or without MG132[87,92]. Since proteasome inhibitors like MG132 deplete the nuclear ubiquitin pool, it is difficult to resolve these discrepancies and determine whether the proteasome is directly involved in DPC ubiquitination/repair.

Although progress has been made in detailing the mechanisms regulating DPC repair, many questions remain. Repair pathways such as nucleotide excision repair, homologous recombination, and proteolysis have all been implicated to play a role. However, it is still unknown how the cell initiates DPC repair of one pathway over another and whether double-strand break repair

pathways such as the Fanconi anemia pathway, non-homologous end-joining, and microhomology mediated end-joining are involved[30,102-104]. Fanconi anemia patients, who possess mutations in Fanconi anemia repair pathway, have been shown to be hypersensitive to DPC-inducing chemotherapeutics[105-107]. However, the involvement of the Fanconi pathway in DPC repair has yet to be established[102]. Additionally, relatively little is known about DPC repair mechanisms in the mitochondria. This gap in our knowledge of DPC repair could be used to provide insight into resistance mechanisms of DNA-damaging chemotherapeutics.

IV. DPC REPAIR IN MITOCHONDRIA

a. Mitochondrial genome **(Table 1.1)**

The human mitochondrial genome (mtDNA) is 16 kb long and densely packed with genetic information encoding complexes for the electron transport chain[108]. It provides the cell with energy in the form of ATP, enzymes for lipid biogenesis, and is involved in other key cellular processes[109]. It contains one origin of replication on each DNA strand, two promoters (one for each strand), and lacks DNA histones[110]. Instead, mtDNA is organized into nucleoids that carries six to ten copies of DNA[111,112]. Most mitochondrial proteins are nuclear encoded and imported into the mitochondria[113]. Similar to nuclear DNA, mitochondrial DNA is also exposed to alkylation and hydrolytic damage, adduct formation from

endogenous and exogenous agents, as well as mismatched bases and strand breaks[114].

Table 1.1: Characteristic comparison of the nuclear and mitochondrial genome in eukaryotic cells[115,116].

Characteristic	Nuclear genome	Mitochondrial genome
Size	3.3 x 10^9 bp	16,569 bp
# of DNA molecules/cell	46 per diploid cell	Thousands/cell
# of encoded genes	20-30,000	37
Gene density	1 per 40,000 bp	1 per 450 bp
Mode of inheritance	Mendelian	Maternal
% coding DNA	3%	93%
Transcription	Genes transcribed individually	All genes transcribed at the same time

b. Mitochondrial DNA repair pathways

Mitochondrial DNA is constantly exposed to external and internal damaging agents capable of forming alkylation damage, hydrolytic damage, DNA adducts, mismatched bases, strand breaks, and oxidative damage[117-123]. Because mitochondria are a major source of reactive oxygen species, the most well-studied type of mtDNA damage is oxidative damage, which is repaired by the base excision repair pathway[124-126]. In 1974, Clayton et al. discovered that

mitochondria are unable to repair UV-induced pyrimidine dimers and lacked the NER pathway[127]. Following exposure to UV light, radioactive thymidine was not incorporated into isolated mitochondria from mice and human cells, and the damaged DNA was incapable of replication. Miyaki et al. showed that mitochondria were also unable to repair alkyl damage induced by two different carcinogens[128]. Double-strand break repair pathways such as homologous recombination and end-joining have also not been well-established in the mitochondria[129].

Restriction endonucleases targeted to the mitochondrial genome showed that yeast rely on ligase Cdc9p to repair double-strand breaks[130]. Work by Thyagarajan et al. showed that mitochondrial protein extracts catalyzed homologous recombination of plasmid DNA substrates in a conservative process that did not involve nuclease-mediated strand-annealing[131]. HR has also been shown in yeast and plant mtDNA but was only detected in low frequencies following exposure to endonucleases in mice[132-134]. Mitochondrial protein extracts can join blunt-ended plasmid DNA but with low efficiency[135,136]. Non-homologous end-joining also been observed in mitochondrial extracts and shown to rely on a C-terminally truncated form of the Ku80 end-binding protein[137]. Microhomology-mediated end joining (MMEJ) of duplex oligonucleotides possessing double-strand breaks has also been observed in mitochondrial extracts. These results showed that repair increased in portion to the length of microhomology and that the smallest amount of end-joining activity occurred with a duplex containing 5

nucleotides of homology on either side of the double-strand break[138]. While mitochondrial double-strand break pathways remain under investigation, other DNA repair pathways such as mismatch repair, single-strand break repair, and base excision repair have been more frequently observed in mitochondria[108,139].

c. Mitochondria DNA degradation

Hundreds to thousands of copies of the mitochondrial genome is present in each cell. Therefore, it is reasonable that loss of mtDNA may not necessarily be detrimental to the cell. This turnover process involving the degradation and replacement of mtDNA by replication was first observed by Gross and Rabinowitz in 1969[140]. Others have shown that cells are tolerant to both chronic and acute mitochondrial DNA reduction as well as full elimination[140-142]. Thus, it is logical to hypothesize that degradation of severely damaged mtDNA could be used as a unique maintenance mechanism of the mitochondrial genome[143,144]. However, evidence for this model has yet to be directly shown and is still incomplete.

d. DPCs in mitochondria

DNA-protein crosslinks have been shown to form on mitochondrial DNA[145]. Enzymatic trapping of polymerases to DNA due to oxidative damage have been observed in purified protein and mitochondrial extracts from Hela cells. However, it is unclear whether DPCs also undergo proteolytic processing in the

mitochondria, as is hypothesized in the nucleus. The mitochondria possess their own E3-ubiquitin ligases, but they are located in the outer membrane and so are unlikely to be involved in DNA repair[146]. It also is unknown whether the translesion synthesis machinery is available in mammalian mitochondria and would be capable of bypassing smaller DNA-peptide crosslinks[147].

e. Mitochondria DNA damage and disease

A correlation of oxidative stress and reduced mitochondria function has been found in several neurological disorders[148,149]. For example, patients with Kearns-Sayre Syndrome have spontaneously inherited mtDNA deletions and suffer from cerebellar ataxia, proximal muscle weakness, and cardiac conduction abnormalities[150]. Other pathologies associated with mtDNA damage include diabetes, cardiovascular and liver disease, as well as aging and cancer[151-154]. Mitochondria also regulate apoptosis by controlling the translocation of pro-apoptotic proteins from the intermediate space to the cytosol. This process can be inhibited in cancer cells *via* the overexpression of anti-apoptotic proteins. Mitochondria have also become an attractive target for drug therapy[155-157]. For example, doxorubicin-resistant osteosarcoma has been shown to overexpress the drug efflux transporter ABCB1/P-glycoprotein. However, chemically modified mitochondria-targeted doxorubicin was shown to decrease tumor growth, increase apoptosis, and was less cardiotoxic than normal doxorubicin in these cells[158].

V. CLINICAL APPLICATIONS

The largest class of chemotherapeutics are DNA-damaging agents which induce different types of DNA damage in cancer cells and interrupt the cell cycle, leading to cell death[159-161] **(Table 1.2).** Within this class of drugs, crosslinking agents are arguably the most widely used. Crosslinking agents such as cisplatin, cyclophosphamide, and doxorubicin are used to treat a variety of cancers such as breast, brain, and prostate cancer[162-164]. However, cancer cells can exhibit resistance to these agents, resulting in therapeutic failure and patient death. It is known that elevated repair pathways contribute to drug resistance[165,166]. Therefore, there is a need to fill the gap of what molecular pathways are involved in the repair of drug-induced DNA damage. Identification of these pathways can lead to a better understanding of drugs resistance and the development of new therapies that target repair pathways[167].

DNA-protein crosslinks are one of the toxic lesions created by these crosslinking drugs, however, the least is known about their repair mechanisms[168]. Therefore, it is unknown how the repair of DPCs contributes to harmful side effects and resistance mechanisms of these drugs. Once the cellular response to DPC damage has been elucidated, altered expression of repair proteins can be examined in chemo-resistance cells. Identification of drug-resistance biomarkers could then be used to influence decisions in chemotherapeutic treatment or lead

to the development of new therapeutics that target DPC repair proteins. Inhibition of repair pathways involved in chemo-resistance can prevent repair, leading to cell death and enhanced efficacy to improve clinical outcomes.

Table 1.2. Classification and uses of DNA-damaging chemotherapeutics[169].

Drug Type and Name	Uses
Nitrogen Mustards	
Chlorambucil	Lymphocytic leukemia, lymphomas, and cancer of the breast and ovaries.
Cyclophosphamide	Breast cancer, prostate cancer, and non-Hodgkin's lymphoma.
Ifosfamide	Testicular cancer, lymphoma, lung cancer, and sarcomas.
Mechlorethamine HCl	Hodgkin's disease, solid tumors, and pleural effusion caused by cancer of the lung.
Melphalan	Multiple myeloma, melanoma, and cancers of the breast, ovary, and testes.
Temozolomide	Refractory anaplastic astrocytoma.
Nitrosoureas	
Carmustine	Hodgkin's disease, multiple myeloma, melanoma, and brain tumors.
Lomustine	Advanced Hodgkin's disease and brain tumors.
Streptozocin	Pancreatic islet cell tumor and cancer of the lung.
Alkyl Sulfonates	
Busulfan	Myelocytic leukemia.
Alkylating-Like Drugs	
Altretamine	Ovarian cancer. Also used for breast, cervix, colon, endometrial, head/neck, and lung cancers; lymphomas.
Carboplatin	Recurrent ovarian cancer.
Cisplatin	Ovarian and testicular cancer, cancer of the bladder, head and neck, and endometrium.
Oxaliplatin	Metastatic colorectal cancer, ovarian cancer, head and neck cancer, and malignant melanoma.
Dacarbazine	Metastatic malignant melanoma, sarcomas, neuroblastoma, and refractory Hodgkin's disease.
Thiotepa	Breast and ovarian cancer.

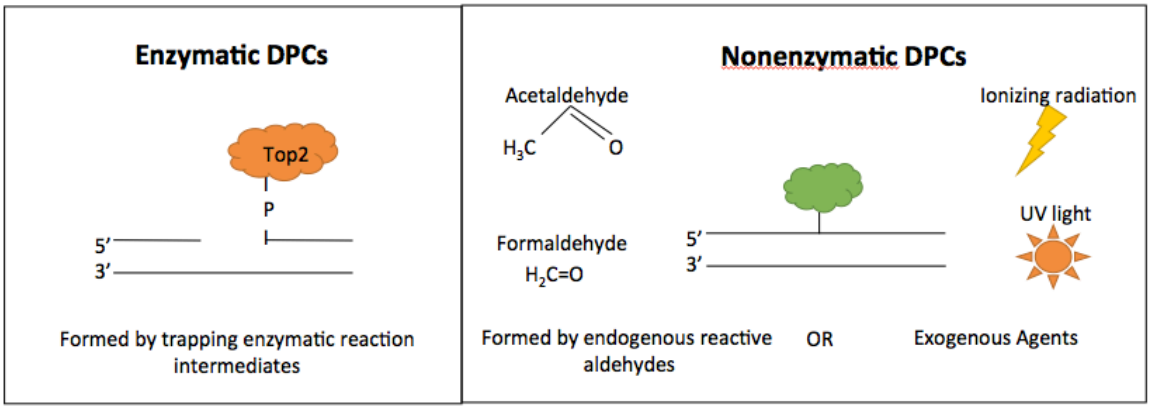

Figure 1.1. Classification of DNA-protein crosslinks[6].

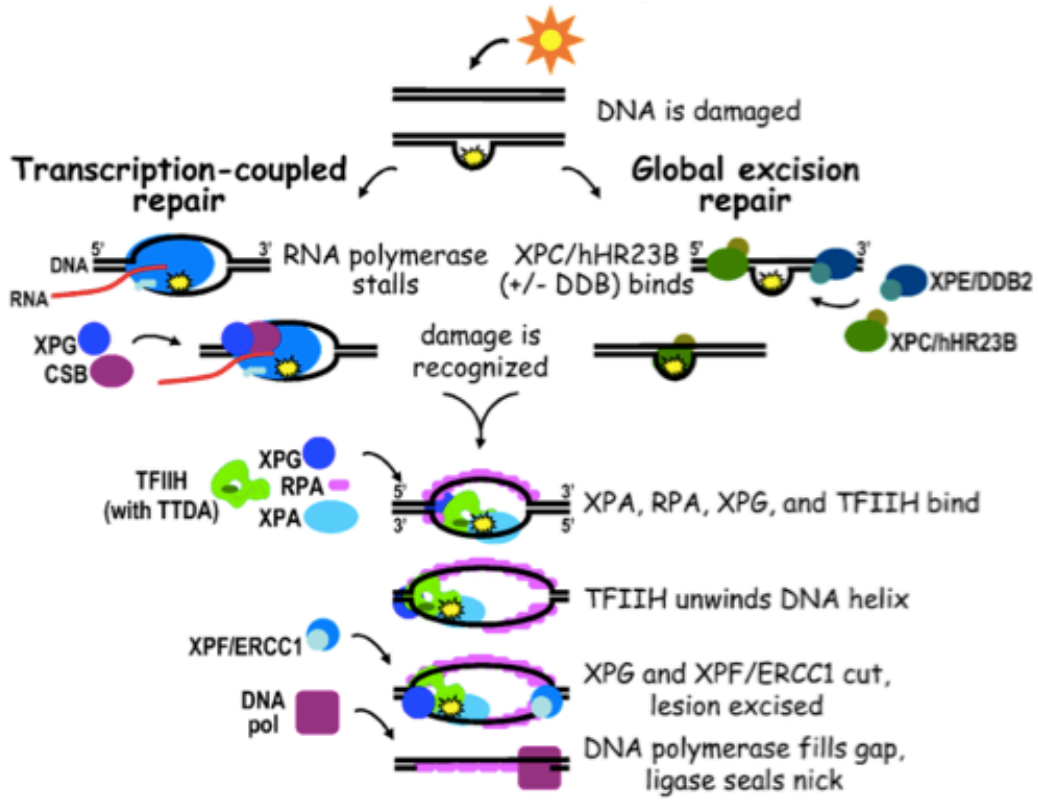

Figure 1.2. Eukaryotic transcription-coupled and global genomic nucleotide excision repair pathway[170].

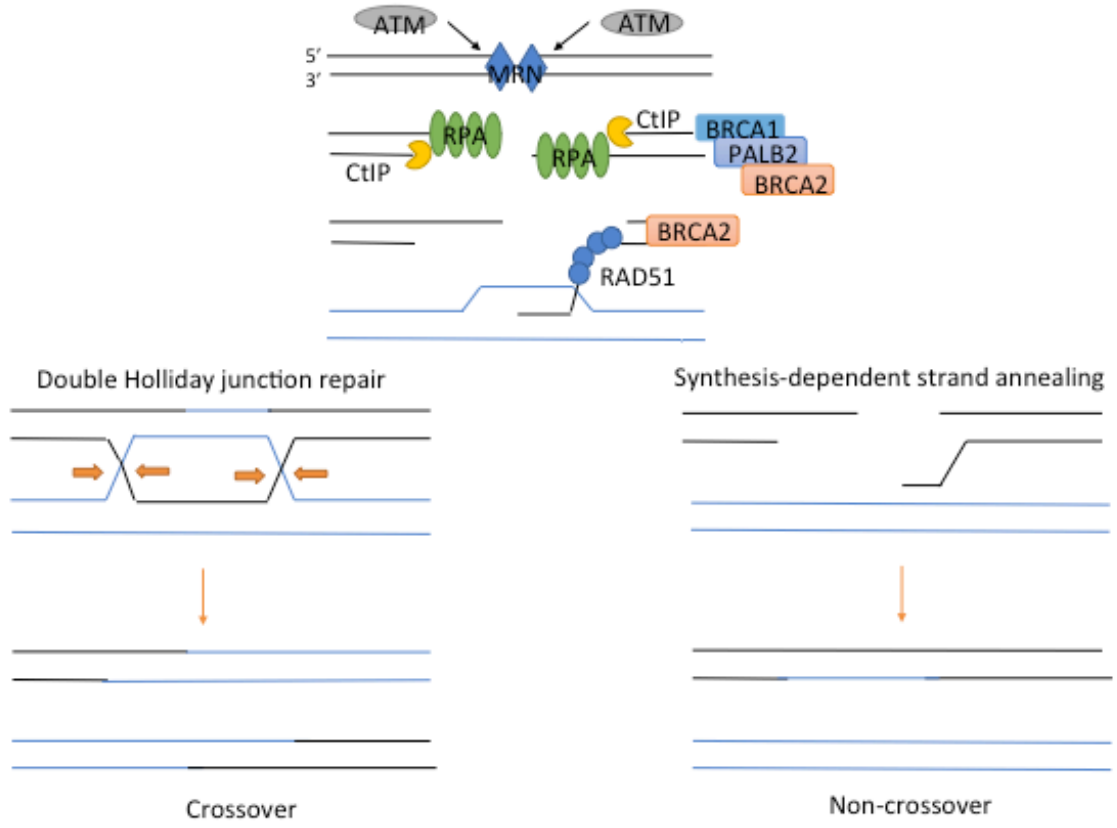

Figure 1.3. Eukaryotic homologous recombinational repair of a double-strand break resolved by double Holliday junction repair or synthesis-dependent strand annealing[53].

Chapter 2

A Simple, Rapid, and Quantitative Assay to Measure Repair of DNA-protein Crosslinks Transfected into Mammalian Cells

Lisa N. Chesner and Colin Campbell

Department of Pharmacology, University of Minnesota

Content adapted from published article: Chesner, LN., Campbell, C. A Simple, Rapid, and Quantitative Assay to Measure Repair of DNA-protein Crosslinks on Plasmids Transfected into Mammalian Cells. *J. Vis. Exp.* (133), e57413, doi:10.3791/57413 (2018).

I. PREFACE

The purpose of this method is to provide a flexible, rapid, and quantitative technique to examine the kinetics of DNA-protein crosslink (DPC) repair in mammalian cell lines. Rather than globally assaying removal of xenobiotic-induced or spontaneous chromosomal DPC removal, this assay examines the repair of a homogeneous, chemically defined lesion specifically introduced at one site within a plasmid DNA substrate. Importantly, this approach avoids the use of radioactive materials and is not dependent on expensive or highly-specialized technology. Instead, it relies on standard recombinant DNA procedures and widely available real-time, quantitative polymerase chain reaction (qPCR) instrumentation. Given the inherent flexibility of the strategy utilized, the size of the crosslinked protein, as well as the nature of the chemical linkage and the precise DNA sequence context of the attachment site can be varied to address the respective contributions of these parameters to the overall efficiency of DPC repair. Using this method, plasmids containing a site-specific DPC were transfected into cells and low molecular weight DNA recovered at various times post-transfection. Recovered DNA is then subjected to strand-specific primer extension (SSPE) using a primer complementary to the damaged strand of the plasmid. Since the DPC lesion blocks Taq DNA polymerase, the ratio of repaired to un-repaired DNA can be quantitatively assessed using qPCR. Cycle threshold (CT) values are used to calculate percent repair at various time points in the

respective cell lines. This SSPE-qPCR method can also be used to quantitatively assess the repair kinetics of any DNA adduct that blocks Taq polymerase.

II. INTRODUCTION

Described herein is a PCR-based assay termed Strand-Specific Primer Extension-Quantitative Polymerase Chain Reaction (SSPE-qPCR). The purpose of this method is to quantify DNA-protein crosslink (DPC) repair on plasmid DNA transfected into repair deficient and proficient mammalian cells. This assay is rapid, quantitative, extremely flexible, and directly measures repair activity. While this report focuses on the use of this methodology to study repair of DPCs, results presented below illustrate that repair of any lesion that blocks Taq polymerase can be studied using this methodology.

The rationale behind the development of this method is to gain insight into the mechanisms through which mammalian cells repair DPCs. Unlike other types of DNA damage, DPCs are massively diverse.[1,24] Studies have demonstrated that hundreds of cellular proteins can become crosslinked to DNA and that for each protein there are, in principle, numerous amino acid side chains that could become covalently attached to cellular DNA.[3] In addition, there are numerous chemical attachment points for proteins onto the DNA backbone, including several positions on the nucleotide bases as well as on the ribose sugar.[8,171] This chemical diversity raises the prospect that distinct biochemical pathways may be

relied upon to repair different types of DPCs. It was with this concern in mind that the SSPE-qPCR assay was developed.

Several techniques have been developed to gain insight into the molecular biology of cellular DPC repair. The following provides an overview of the major approaches that have been developed, with a summary of the major strengths and weaknesses each possess. It is worth stressing that while this summary focuses on studies of DPC repair in mammalian cell culture systems, significant contributions to the current model of DPC repair have been made using microbial and cell-free systems that are not discussed in this manuscript.

Perhaps the easiest strategy that can be taken to gain insight into the genetics of DPC repair is to assess the respective sensitivity to cell death observed in wild-type and mutant cells exposed to agents that induce DPCs.[9,64] This strategy is relatively fast, inexpensive, and doesn't require specialized expertise beyond the ability to perform basic cell culture techniques. Counterbalancing these advantages are numerous limitations to this approach including the following. **First**, the assay does not directly measure DNA repair. The working assumption underlying this strategy is that inactivating mutations in genes encoding relevant DNA repair proteins result in an accumulation of DNA damage that triggers programmed cell death. However, mutations in genes encoding non-DNA-repair proteins could, in principal, enhance (or reduce) cellular sensitivity to xenobiotic-induced cell death. **Second**, agents that create DPCs invariably induce other types of DNA damage (one exception is 5-aza-2'-

deoxycytadine, but this agent also depletes cellular methyltransferase levels[172]). Consequently, it is conceivable that enhanced cellular hypersensitivity to the agent in question may reflect defects in repair of interstrand crosslinks or other lesions. **Third**, as was mentioned above, DPCs represent a vastly heterogeneous class comprised of different types of chemical crosslinks, involving different protein partners. It is possible that while repair of one or more sub-types of these lesions may be altered in a particular genetic background, this difference may not be sufficient to significantly alter cellular hypersensitivity to death induced by this agent. In summary, while this strategy represents an attractive starting point, the limitations outlined above highlight the importance of pursuing other, more direct methods to study the kinetics of DPC repair.

Several related approaches have been developed to achieve this objective. For instance, investigators have developed methods to distinguish between 'free' DNA and 'protein-bound-DNA.[173-175] Using these approaches, it is possible to compare steady-state levels of DPCs or following exposure to a DPC-producing agent in different genetic backgrounds. The two strategies that have been most widely used involve separating DPC-containing DNA from free DNA using either a nitrocellulose membrane binding strategy or KCl/SDS precipitation.[66,68] In the former approach cells are lysed and passed through a nitrocellulose filter. Because nitrocellulose binds protein, the filter retains protein-linked DNA, permitting free DNA to pass through. In the latter strategy protein-bound DNA is separated from free DNA since SDS binds to protein but not DNA,

and can be precipitated by addition of KCl. Consequently, protein-linked DNA becomes insoluble while unbound DNA remains in solution. DPC-containing DNA can then be quantitated using radiolabeled thymidine (if cells were initially metabolically labeled) or by a DNA-selective fluorescent dye like Hoechst 33258. These methods are reproducible and require a small number of steps. However, they do not provide information regarding the nature of the chemical crosslink through which protein is attached to DNA. Furthermore, it is important to note, these assays may over-estimate DPC repair by falsely scoring incomplete repair, i.e. proteolytic processing to smaller DNA-peptide crosslinks that may not be as easily trapped or precipitated, as bona fide DNA repair.

Comet assays can be used to visualize DPC formation in cells.[69] In these experiments, the presence of DPCs decrease DNA migration which can then be reversed by pretreating with proteinase K. Therefore, the length of the tail can be used to estimate DPC formation. However, as mentioned above, DPC-forming drugs create other types of DNA damage which could alter tail length. This protocol is also highly technical and requires expertise and training in confocal imaging.

Mass spectrometry can be used to study DPC repair kinetics following treatment with crosslinking agents.[4,17,82] These experiments treat cells with DPC-forming agents and isolate DNA-protein crosslinks via biotin capture or phenol: chloroform (1:1) extraction. Mass spectrometry can then be used to identify the crosslinked proteins or quantitate the amount of DPCs formed over time. The

major advantage of this approach is the nature of the data produced. One can precisely catalog the types of proteins that become crosslinked following exposure to a xenobiotic, however, this protocol is expensive, time consuming, and is limited by the type of crosslink that can be detected.

Maizels *et. al* developed a sensitive 'RADAR' (rapid approach to DNA adduct recovery) assay to quantitate immunodection of DNA-protein adducts as well as a ELISA-based RADAR assay.[72,73] These assays are especially useful for trapping DNA-protein intermediates that transiently form in cells and generate samples suitable for mass spectroscopy to identify new protein adducts. This immunodection assay relies on the availability of antibodies to capture the DNA-protein crosslink and, therefore, may not be capable of detecting degraded DNA-peptide adducts that form during repair. Recently, a specific DPC repair pathway linked to DNA replication and a DNA-dependent metalloprotease Spartan was discovered in which DNA-protein crosslinks are proteolyzed to smaller peptides during repair. [94,176] Inherited mutations in this gene are associated with Ruijs-Aalfs syndrome in humans, a disease characterized by genomic instability, premature ageing and liver cancer.[22] Mice with genetically engineered Spartan gene defects display similar phenotypes.[98,100]

Host-cell reactivation of transcriptional activity has been used to study the repair of defined lesions present on transfected plasmid DNA substrates.[85,87] In these experiments, plasmid containing DPCs (or other types of DNA lesions) that block the transcription of a reporter, such as luciferase, are transfected into cells.

Luminescence measurements taken 24-72 h later are then correlated with DPC repair. However, these indirect repair assays are incapable of detecting repair events earlier than 24 h post-transfection and cannot distinguish between RNA polymerase bypass of partially repaired substrates and complete repair.

Each of the methods described above has advantages and has contributed to the current model of DPC repair. However, the SSPE-qPCR assay circumvents several of the limitations associated with these other approaches and consequently can provide more specific insight into DPC repair mechanisms. For example, the SSPE-qPCR assay can directly measure repair of site-specific DPCs on DNA in intact mammalian cells. This method is versatile and has been used to obtained repair results following transfection in hamster and human cell lines. Transfection of the plasmid can be performed using lipofection or electroporation in cultured mammalian cell lines. It also ensures that only repair of defined DNA-protein crosslinks is measured and not other types of DNA damage induced by most DPC-forming agents. The SSPE-qPCR is easy to perform, inexpensive, and rapid. Results obtained using this assay have detected repair events as early as 2 h post-transfection. Using this method, variables that may influence DPC repair outcomes can be studied in a manner that is sensitive and efficient. For example, the role of transcription in DPC repair has yet to be rigorously evaluated. Due to the flexibility of the SSPE-qPCR assay, the crosslinking site of the DPC can be manipulated to address this question. In addition, introduction of an origin of replication into the DPC-bearing plasmid can

be used to address the influence of replication on DPC repair. Additionally, multiple crosslinks can be created on the plasmid to examine differences in repair of a single DPC versus multiple crosslinks. These are questions that would be difficult to answer using chromosomal DNA but can easily be addressed using the SSPE-qPCR assay. Overall, the SSPE-qPCR assay requires purified, plasmid DNA in microgram quantities containing a lesion of a known location. Adducts besides DPC can be used in this assay, however, the lesion must be capable of blocking extension by Taq polymerase.

III. PROTOCOL

1. Generation of DPC-containing plasmid DNA

1.1) Combine 80 pmol of oligonucleotide containing an 8-oxoguanine residue (20 μL) with 10 units of T4 polynucleotide kinase (1μL) in 10X ligase buffer (5 μL). Add water to reach a total volume of 50 μL and incubate at 37 °C for 30 min in a heated water bath.

1.1.1) Combine the phosphorylated oligonucleotide (50 μL), 80 pmol of single-stranded DNA (80 μL), 100 units Taq polymerase (20 μL) in 10X Taq reaction buffer (25 μL), 100 mM ATP (20 μL), 10 mM dNTPs (20 μL), NEB buffer 2 (25 μL), and 8 μg BSA (20 μL) to total 260 μL. Incubate the sample in a PCR machine set at 75 °C for 15 min followed by 37 °C for 5 min. Next, add 60 units of T4 polymerase (20 μL), 8000 units ligase (20 μL), 100 mM ATP (20 μL), 10 mM

dNTPs (20 μL), NEB buffer 2 (15 μL), and 8 μg BSA (20 μL) to total 375 μL. Incubate the reaction overnight at 37 °C **(Figure 2.1A).**

1.2) Create a 50:50 buffer-saturated phenol: chloroform mixture. Add equal volumes of each component, mix, and spin in a table-top centrifuge at 15K x g for 5 minutes. Chloroform drives water out of the buffer-saturated phenol to form two layers: an upper, aqueous layer and a bottom, organic layer. Add 375 μL of the lower, organic layer to the primer extension reaction, mix, and spin in a table-top centrifuge at 15K x g for 5 minutes. **CAUTION:** Phenol and chloroform are hazardous substances and precautions should be taken to avoid contact with the eyes or skin.

1.2.1) Following centrifugation, carefully extract the top layer and mix with ammonium acetate added to a final concentration of 0.3 M followed by 2 volumes of 100% ethanol. Store the solution at -20°C for a minimum of 30 minutes or overnight.

1.2.2) Spin the sample in a table-top centrifuge at 15K x g at 4°C for 10 min. Remove the supernatant and wash the pellet in 1 mL of 70% ethanol. Spin the sample in a table-top centrifuge at 15K x g at 4°C for 5 min. Remove the supernatant and resuspend the pellet in 100 μL of water.

1.3) Combine 50 μL of DNA from the previous step with 16 μL 6X gel-loading dye, and 34 μL water and subject to electrophoresis on a 0.8% low-melt agarose gel containing 0.5 μg/mL ethidium bromide. Run the gel at 2 V/cm on a 10-cm gel

for 6 h in 1X TAE buffer. Excise the supercoiled band using a razor blade and weigh the gel slice **(Figure 2.1A). Note:** It can be helpful to run a positive control to serve as a marker for where the covalently closed, supercoiled DNA migrates. **CAUTION:** Ethidium bromide is a mutagen and precautions should be taken to avoid contact with the skin. Also, it is important to minimize the time that the plasmid sample is exposed to UV to reduce the formation of UV photoproducts.

1.3.1) Digest the gel slice by adding 10% β-agarase reaction buffer for every mg of gel weight. Incubate at 65 °C for 10 min and cool to 42 °C. Add 10 units of β-agarase and incubate at 42 °C for 1 h.

1.3.2) Following incubation, measure the volume and add ammonium acetate to a final concentration of 0.3 M and chill on ice for 15 min. Centrifuge at 15K x g for 15 min at room temperature, collect the supernatant, and add 2 volumes of isopropanol. Chill at -20 °C overnight.

1.3.3) Centrifuge the purified, supercoiled DNA for 10 min at 15K x g in a table-top centrifuge at 4 °C and resuspend the pellet in 40 μL of water.

1.4) Crosslink 12 pmol (15 μL) of DNA to 36 pmol of oxoguanine glycosylase (1 μL) in buffer containing 100 mM NaCl (3 μL), 1 mM $MgCl_2$ (3 μL), 20 mM Tris-HCl pH 7.0 (6 μL), and 10 mM sodium cyanoborohydride (2 μL) to reach a final volume of 30 μL at 37 °C for 30 min.[177] Remove 1 μL of crosslinked sample and dilute in 500 μL of water to serve as a 0 h data point and analyze on PCR in step 3.

2. KCl/SDS precipitation

2.1) To visualize crosslinking efficiency, restriction digest 1 μg of the crosslinked plasmid with 1 μL *Bsp*DI in 10x buffer at 37 °C for 1 h to generate two different sized DNA fragments. One fragment will be crosslinked to protein (4.4 kb) and the other will not (2.8 kB), **(Figure 2.1B).**

2.1.1) Divide the samples in half, add SDS to both to a final concentration of 0.5%, and incubate at 65 °C for 10 min.

2.1.2) Add KCl (final concentration 100 mM) to one of the samples and incubate on ice for 5 min.

2.1.3) Centrifuge both samples at 12K x g for 5 min at 4 °C and run the supernatants on an agarose gel to estimate percent conjugation of protein to DNA.[66] Note: KCl/SDS precipitation is used for quality control, not substrate preparation.

3. Transfection into mammalian cells

3.1) One day prior to transfection, plate 0.5 X 10^6 cells/well in a 6-well plate. The next day, mix 1.5 μg (30 μL) of the DPC-containing plasmid (from step 1.6) with 300 μL of serum-free culture media. In another tube, mix 12 μL of lipofectamine reagent and 300 μL of serum-free culture media. Combine 300 μL of diluted DNA with 300 μL of diluted lipofectamine and incubate for 5 min at room temperature.

Add 250 μL of the complexes to each of two wells and allow to incubate for a minimum of 1 h.

3.1.2) Following incubation, remove media, add 1 mL of 0.6% SDS/0.01 M EDTA, and incubate at room temperature for 10-15 min. Scrape the cells using a rubber policeman and transfer to a 1.5 mL microfuge tube. Add 200 μL of 5 M NaCl (final concentration of 1 M), invert gently 5 times, and incubate at 4 °C overnight.[178]

3.1.3) Centrifuge the samples at 15K x g in a table-top instrument at 4 °C for 30 min, collect the supernatant, ethanol precipitate as described above, and resuspend in 50 μL of water.

4. Strand-specific primer extension-qPCR

4.1) Mix together 1 μL of recovered DNA from each time point *(including 0 hr)*, 2X sybr green master mix (30 μL), 27 μL of water, and 1 μL (100 pMol) of primer complementary to the damage strand of the plasmid (Primer R, **Figure 2.2**). Perform PCR using the following conditions: Initial pre-melt for 10 min at 90 °C, followed by 8 cycles of: 90 °C, 15 seconds, 65 °C, 1 minute. At the completion of cycle 8 add 1 μL (100 pMol) of the second primer to total 60 μL (Primer L, **Figure 2.2).**[179] *(see Table of Materials for reagent details)*

4.1.2) Mix 1 μL of *unamplified* recovered DNA from each time point *(including 0 hr),* 2X sybr green master mix (30 μL), 27 μL of water, and 1 μL of each primer (100 pMol) to total 60 μL.

4.1.3) Load a 96-well PCR plate with the samples from 4.1 and 4.2 (20 μL/well, in triplicate) and perform qPCR for 30 cycles using the conditions described above.

4.1.4) Average the CT values from each set of triplicate samples. Subtract the CT values generated in 4.1 from 4.2 to obtain the delta CT value for each sample. Subtract the 0 h time point from the delta CT value to remove any background. (See Representative Results section for a detailed description.)

4.1.5) Convert the delta CT value into percent repair using the formula: percent repair=$(2^{\Delta CT}/2^3)$ x 100.

IV. REPRESENTATIVE RESULTS

To utilize the SSPE-qPCR assay to assess cellular DPC repair a sufficient quantity (*μg amounts*) of high-quality DPC repair substrate must be prepared. To obtain this product, an oligonucleotide containing an 8-oxoguanine residue was annealed to complementary single-stranded DNA, primer extended, and gel purified to ensure that only covalently, closed circular product was used for transfections **(Figure 2.1A).** This report focuses on substrates in which borohydride-trapping is used to create a covalent crosslink between recombinant

human oxoguanine glycosylase and a ribose unit on a double-stranded circular plasmid molecule, although analogous approaches can be used to obtain chemically diverse DPC substrates. The oxoguanine glycosylase/borohydride trapping strategy is especially attractive given the extremely high efficiency of the crosslinking reaction. As shown in **Figure 2.1B**, KCl/SDS precipitation performed on a DPC substrate that had been digested into two fragments selectively and nearly quantitatively depleted the DNA fragment harboring the DPC. These results support the conclusion that essentially 100% of the plasmid substrate molecules contain a protein crosslink.

The SSPE-qPCR assay described in the Protocols section utilizes cycle threshold (CT) values generated by qPCR to calculate the percent of DPC repair following transfection in mammalian cells. As **Figure 2.2** illustrates, the protein crosslink blocks Taq polymerase from extending the 'R' primer annealed to the DPC-containing strand. A second, critical feature of this assay is the incorporation of eight rounds of strand-specific primer extension (SSPE) reactions (using the R primer) prior to performing the qPCR assay. While undamaged (or repaired) DNA will be extended during these SSPE reactions, creating a binding site for the downstream 'L' primer, damaged DNA (or incompletely repaired DNA) will not be extended. Consequently, SSPE increases the abundance of each undamaged (or repaired) strand by eight-fold. This means that repaired samples in which the SSPE step has been performed prior to qPCR will display a cycle threshold (CT) value that is three units lower than

that obtained for an identical sample in which SSPE was not performed prior to qPCR **(Figure 2.2).** The three-unit difference in CT values observed for the two treatments, referred to as Δ CT, reflects the fact that $8=2^3$. This delta CT value can be used to calculate cellular DNA repair activity by using the formula: percent DNA repair= $(2^{\Delta CT}/2^3)$ X 100. Control experiments confirmed that a delta CT value of approximately 3 was consistently observed when undamaged substrate plasmids were subjected to SSPE-qPCR (data not shown).

Table 2.1 depicts example CT values that were generated from DPC-containing plasmid substrates that were recovered from Chinese hamster lung fibroblasts 3 and 8 h post-transfection (A), as well as from time zero samples, i.e. samples that were prepared as described in the Protocol section, but not transfected into cells (B). The table also provides the ΔCT, and percent repair values (calculated using the formula $2^{\Delta CT}/2^3$x 100) obtained from these samples. As illustrated in **Table 2.1A**, the percent repair calculated from samples harvested 3 and 8 h post-transfection was 66% and 93%, respectively. These values are then subtracted from that obtained from analysis of the 0 h sample to determine percent repair. **Table 2.1B** depicts CT values for two different 0 hr samples in which efficient crosslinking was or was not achieved prior to transfection. Efficiently crosslinked sample resulted in a delta CT value of 0.8 whereas a poorly crosslinked sample resulted in a delta CT value of 2.5. To date, it has not been possible to precisely determine the source of the 0.8 background signal in the efficiently crosslinked 0 h sample. It is unlikely that this background

reflects a low level of either spontaneous DPC removal, or is due to a low level of Taq polymerase 'bypass' synthesis through the DPC lesion. Because extensive experimentation performed on highly purified single-stranded M13 substrate consistently yielded a delta CT value of approximately 0.8, i.e. essentially identical to this 'background' extension seen in DPC-containing substrates. Consequently, it is likely that there is a small degree of mis-priming of the 'R' primer during SSPE that results in the generation of a small amount of product that can subsequently be amplified when the 'L' primer is added and qPCR performed. Efforts to eliminate this background by manipulating PCR conditions have, to date, failed to remedy this defect. However, the subtraction strategy described above permits one to accurately estimate DPC repair activity. It is worth noting that inefficient crosslinking of the protein onto the plasmid will result in an elevated background value. This is depicted in the sample data provided in **Table 2.1B** where inefficient protein-DNA crosslinking resulted in a higher delta CT value for time 0. Therefore, control experiments are invariably performed prior to initiating transfections and substrates with delta CT values elevated above the 0.8 threshold level are discarded. As mentioned in the qPCR protocol, each sample is divided into 3 wells to ensure pipetting consistency. These replicates are then averaged to obtain the CT value for that sample. Replicates that deviate more than +/- 0.1 are eliminated from the data set. If all three replicates deviate more than +/- 0.1 from each other, the SSPE-qPCR assay is redone until consistent values are obtained. Experience shows that at least 3 independent

transfections must be performed to obtain reliable average values that can then be subjected to statistical analysis to determine the influence of various parameters on DPC repair efficiency.

Table 2.1: Calculating percent repair using CT values generated from SSPE-qPCR. (A) Repair of a DPC-containing substrate transfected in V79 Chinese hamster lung fibroblasts 3 and 8 h post-transfection. (B) SSPE-qPCR of 0 h samples not transfected into cells. In one sample the efficiency of the crosslinking reaction between DNA and oxoguanine glycosylase was high (this sample yielded a low delta CT value) while in the other sample the efficiency of protein crosslinking was low (this sample yielded a relatively high delta CT value). See text of Representative Results for details.

Table A

Time	- Primer extension	+ Primer extension	Δ CT	Percent Repair ($2^{\Delta CT}/2^3$x 100)
3 h	23.5	21.1	2.4	66
8 h	29.4	26.5	2.9	93

Table B

Time	- Primer extension	+ Primer extension	Δ CT	Percent Background ($2^{\Delta CT}/2^3$x 100)
0 h	15.4	14.6	0.8	22
0 h	15.4	12.9	2.5	71

V. DISCUSSION

The strand-specific primer extension-qPCR method offers numerous advantages over other approaches by examining the repair of a homogenous population containing a single, defined DPC lesion. It is noteworthy that in addition to controlling the identity of the protein and the type of chemical crosslink used to connect the protein to the DNA, one can easily manipulate the sequence context into which the DPC lesion is introduced. We have explored the influence on DPC repair of introducing the lesion on either the template or coding strand of a plasmid downstream of an active promotor locus. Similarly, we are in the process of investigating the influence on DPC repair of replication using a M13 plasmid containing an SV40 origin of replication transfected into HEK293T cells. The assay described herein directly measures DPC repair, as opposed to other strategies such as host cell reactivation that indirectly estimates repair activity.[85,87] In addition, the system is robust, sensitive, and quantitative. Unlike other systems, which measure DPC removal, this assay only detects complete repair events, i.e. it requires not only that the DPC lesion be removed but that the integrity of the duplex DNA be fully restored.[82] This is because abasic sites and nicks or breaks in the phosphodiester backbone block the assay as effectively as the original DPC lesion.[180]

While this report focuses on a particular type of DPC which was created by borohydride trapping of an enzyme reaction intermediate, we are currently developing approaches to study repair of DPCs involving other proteins and

lesions in which the protein linkage to the DNA occurs through the nucleoside base, rather than the ribose position. Using reductive amination, we have created protein and peptide crosslinks attached to the guanine or cytosine base of a DNA primer.[181] These oligonucleotides were purified to homogeneity and used to generate supercoiled plasmids containing DNA-protein and DNA-peptide crosslinks. While the efficiency of these reactions is somewhat reduced relative to that of the oxoguanine glycosylase crosslink approach described in detail above, they were nevertheless successful and permit us to examine the repair of these substrates in wild-type and nucleotide excision repair-deficient mammalian cell lines. We have also used the SSPE-qPCR assay to study the repair of oxoguanine lesions and a synthetic ribose-cholesterol conjugate, which was previously shown to be repaired *via* the cellular nucleotide excision repair machinery.[182] As **Figure 2.2** graphically depicts, repair of any lesion that blocks primer extension by Taq polymerase can, in principle, be measured using the SSPE-qPCR assay.

Current models of DPC repair suggest that larger DNA-protein crosslinks (>10 kDa) are subjected to proteolytic processing to smaller peptide lesion prior to removal.[183-185] Most likely candidates responsible for this proteolysis are the proteasome or a specific protease in human cells named Spartan.[6,93,94,97,101,176] Further investigations into the roles of these proteases can be conducted using the SSPE-qPCR assay. Proteasome inhibitors could be used to pretreat cells prior to transfection with DPC-containing substrates. Alternatively, Spartan

knockdown cell lines could be transfected with damaged plasmids to elucidate its role in proteolysis of larger DPCs.

Irrespective of the method used to create the crosslink or of the nature of the DNA lesion, it is worth stressing that the SSPE-qPCR methodology is critically dependent on the ability to generate substantial amounts of homogeneous DPC-plasmid substrate. Steps essential for this analysis include purification of covalently, closed-circular plasmid following primer extension to eliminate any nicked or linear plasmid molecules. These contaminants must be eliminated to ensure that any subsequent DPC repair observed is not due to nick-directed or double-strand break-directed repair processes. Failure to obtain sufficient quantities of supercoiled DNA following primer extension reactions may be overcome by varying the ratio of oligonucleotide to single-stranded DNA. Another important step for the SSPE-qPCR method, is the crosslinking efficiency of the protein to the plasmid. In this study, an efficient, enzymatic reaction was used to crosslink the oxoguanine glycosylase protein to an 8-oxo-guanine lesion. Sub-optimum crosslinking can be improved by varying the amount of protein added to the reaction.

While the results described in this report relied on lipofection to introduce DPC repair substrates into recipient cells, there is no reason, a priori, other transfections methods could not be employed. We have performed preliminary studies and observed that electroporation[39] can also be used. However, it is worth noting that in our experience, electroporation transfection efficiency is

reduced compared to lipofection, and we found it necessary to use carrier DNA (up to 5 μg) in addition to the 1.5 μg of DPC substrate to obtain repair data. Overall, the SSPE-qPCR method described above provides an innovative way to exclusively examine DPC repair on plasmid DNA and generate new insight into the DNA damage response.

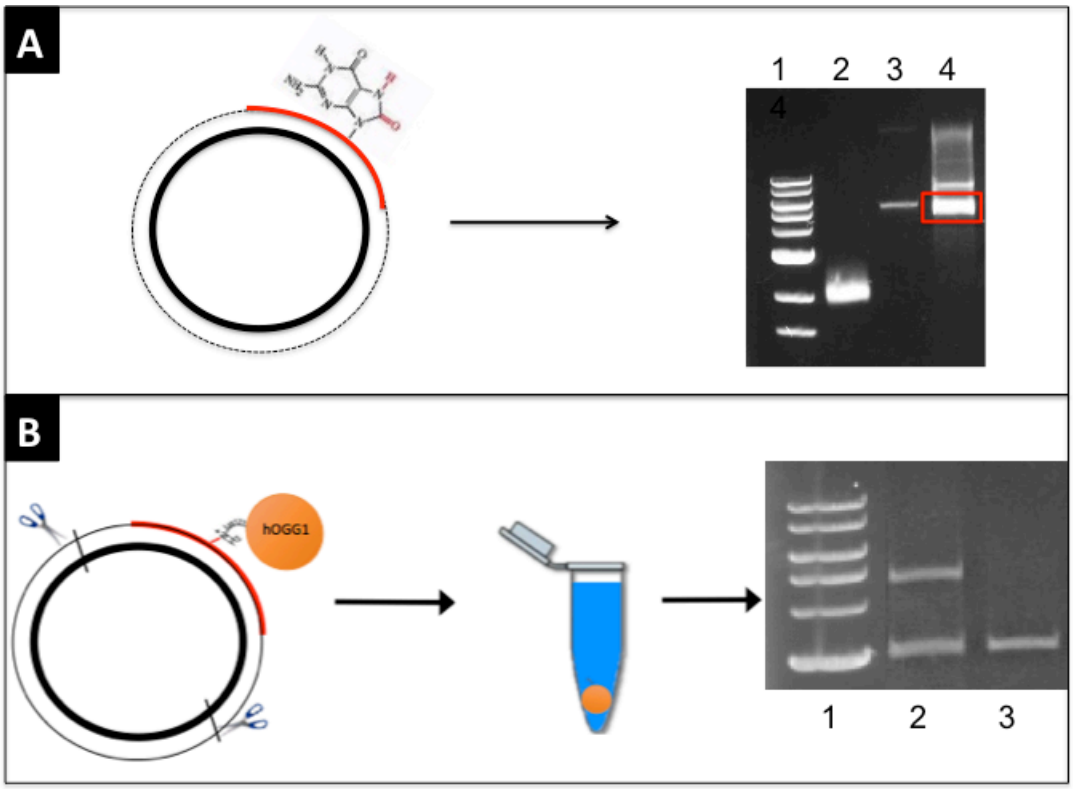

Figure 2.1. Generation of a DPC-containing plasmid. (A) An oligonucleotide containing an 8-oxo-guanine residue (red) is annealed to single-stranded DNA (bold black circle) and extended to create double-stranded plasmid (primer extension product indicated by dashed line). Following electrophoresis in ethidium bromide, the band corresponding to supercoiled DNA (red box) is excised from a low-melt agarose gel and digested with b-agarase. Lanes: (1) Molecular weight marker, (2) single-stranded DNA, (3) double-stranded DNA, (4) primer extended sample. **(B)** Oxoguanine glycosylase (abbreviated hOGG1, depicted as an orange circle) is crosslinked to the 8-oxo-guanine residue *via* sodium cyanoborohydride and the resulting DPC substrate digested to generate

a 2800 base pair free DNA fragment and a 4400 base pair fragment attached to the protein. SDS is added to the sample which is then divided into two portions, one of which is treated with KCl and centrifuged to sediment DPC-containing DNA (depicted as an orange pellet). The supernatant from this latter sample (depicted as blue fluid in centrifuge tube) and the sample not exposed to KCl are subjected to gel electrophoresis. Lanes: (1) Molecular weight marker, (2) –KCl, (3) +KCl.

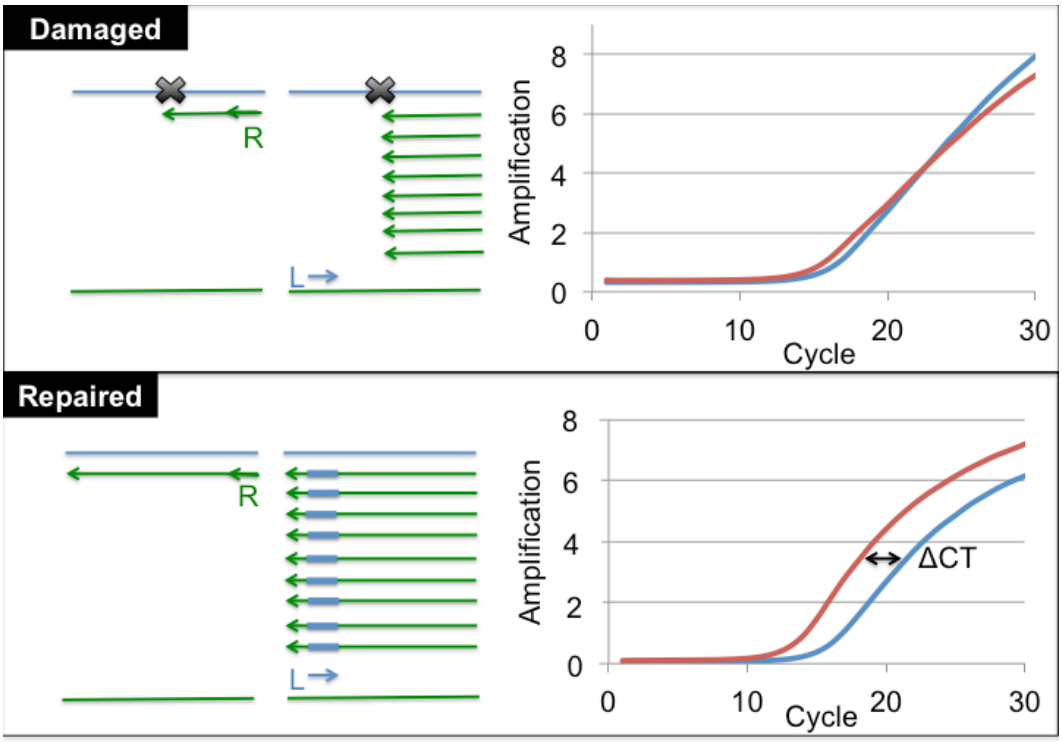

Figure 2.2: Quantification of damaged plasmid *via* strand-specific primer extension-qPCR (SSPE-qPCR). Plasmid DNA is denatured and a primer complementary to the damaged strand (R) is annealed and extended. This process is repeated for a total of 8 cycles. With a damaged substrate (top), Taq polymerase is blocked by the DPC lesion and will not produce full length product strands. In contrast, with a repaired substrate (bottom), Taq polymerase will produce full-length product strands containing the binding site for primer L. After 8 cycles, primer L is added and cycle threshold values determined using qPCR. Example amplification results for damaged and undamaged substrates are illustrated on the right with the red line representing DNA that underwent primer extension prior to qPCR and blue representing DNA that was not primer extended prior to qPCR.

Chapter 3

A quantitative PCR-based assay reveals that nucleotide excision repair plays a predominant role in the removal of DNA-protein crosslinks from plasmids transfected into mammalian cells

Lisa N. Chesner and Colin Campbell

Department of Pharmacology, University of Minnesota

Content adapted from published article: Chesner LN, Campbell C. A quantitative PCR-based assay reveals that nucleotide excision repair plays a predominant role in the removal of DNA-protein crosslinks from plasmids transfected into mammalian cells. *DNA Repair (Amst).* 2018 Feb; 62:18-27

I. PREFACE

DNA-protein crosslinks (DPCs) are complex DNA lesions that induce mutagenesis and cell death. DPCs are created by common antitumor drugs, reactive oxygen species, and endogenous aldehydes. Since these agents create other types of DNA damage in addition to DPCs, identification of the mechanisms of DPC repair is challenging. In this study, we created plasmid substrates containing site-specific DPC lesions, as well as plasmids harboring lesions that are selectively repaired by the base excision or nucleotide excision repair (NER) pathways. These substrates were transfected into mammalian cells and a quantitative real-time PCR assay employed to study their repair. This assay revealed that DPC lesions were rapidly repaired in wild-type human and Chinese hamster derived cells, as were plasmids harboring an oxoguanine residue (base excision repair substrate) or cholesterol lesion (NER substrate). Interestingly, the DPC substrate was repaired in human cells nearly three times as efficiently as in Chinese hamster cells (>75% vs ~25% repair at 8 h post-transfection), while there was no significant species-specific difference in the efficiency with which the cholesterol lesion was repaired (~60% repair). Experiments revealed that both human and hamster cells deficient in NER due to mutations in the xeroderma pigmentosum A or D genes were five to ten-fold less able to repair the cholesterol and DPC lesions than were wild-type control clones, and that both the global genome and transcription-coupled sub-pathways of NER were capable of repairing DPCs. In addition, analyses using this PCR-based assay revealed

that a 4 kDa peptide DNA crosslink was repaired nearly twice as efficiently as was a ~38 kDa DPC, suggesting that proteolytic degradation of crosslinked proteins occurs during DPC repair. These results highlight the utility of this PCR-based assay to study DNA repair and indicate that the NER machinery rapidly and efficiently repairs plasmid DPC lesions in mammalian cells.

II. INTRODUCTION

DNA-protein crosslinks (DPCs) are unusually bulky lesions formed upon covalent trapping of proteins on DNA strands [24]. These helix-distorting complexes are mutagenic, toxic, and are able to block essential cell processes such as transcription and replication [168,186]. Proteins of various sizes and functions can become crosslinked to DNA *via* multiple mechanisms [17,82]. For example, endogenous DPCs can be formed by the trapping of repair proteins recruited to sites of DNA damage or as a byproduct of lipid peroxidation of reactive oxygen species in the blood [15,171,187,188]. Exogenous agents such as ionizing radiation, UV light, cigarette smoke, and chemotherapeutics such as cisplatin also create DPCs [1,3,8,9,17,189,190]. Despite their common occurrence and cytotoxic effects, the exact mechanism(s) by which DPCs are repaired is still not well understood.

In order to gain insight into the repair mechanism of DNA-protein crosslinks, DPC-forming agents have been used to assess hypersensitivity in repair mutants [1]. Results from these experiments have provided evidence for the

roles of nucleotide excision repair (NER) and homologous recombination (HR) in DPC repair [61]. However, there are contradictory reports in the literature regarding the relative contributions of the two repair pathways. Specifically, genetic studies performed in *Escherichia coli* revealed that *uvrA* and *recA* mutants deficient in NER or HR were hypersensitive to the DPC-inducing agent formaldehyde [33,34]. However, only *recA* and not *uvrA* mutants were hypersensitive to DPCs induced by azacytidine [191,192]. In *Saccharomyces cerevisiae*, mutants deficient in NER, but not HR, were sensitive to formaldehyde [60,62]. Similarly, human cells from xeroderma pigmentosum patients possessing mutations in the NER pathway were sensitive to DPC-inducing agents [63,64].

Since all known DPC-forming agents induce other types of DNA damage, such as DNA monoadducts and DNA-DNA cross-links, it is difficult to conclude if sensitivity to these drugs is influenced by lesions other than DPCs. In an effort to overcome this potential limitation, investigators have directly examined the kinetics of DPC formation and removal from wild-type and repair-deficient clones following exposure to DNA damaging agents [193]. However, these studies have yielded contradictory results. For example, Quievryn *et al.* failed to detect differences in the kinetics of formaldehyde-induced DPC removal between NER-deficient human fibroblasts and control [194]. Conversely, DPCs induced by nornitrogen mustard accumulated at higher rates in human cells deficient in the NER gene *XPA* compared to HR-deficient or wild-type clones [82].

To more directly assess the involvement of NER in DPC repair, Minko *et al.* incubated DPC-containing oligonucleotides with UvrABC nucleases from *Escherichia coli* and saw slower incision rates of DNA containing a 16 kDa protein compared to smaller DNA-peptide crosslinks [183,184]. *In vitro* studies performed with human nucleases saw similar results where 4 and 12 amino acid peptide-crosslinks were recognized by the NER machinery but were unable to remove a 16 kDa protein-crosslink [185]. Nakano *et al.* later reported a size limit of 8-10 kDa for the excision of crosslinked proteins by NER in mammalian cells while Baker *et al*. saw NER-directed repair of a 38 kDa attached to plasmid DNA [87,92]. Currently, the role of NER in the repair of DPCs (specifically those consisting of proteins larger than 10 kDa) remains unclear. However, it is hypothesized that the decreased efficiency of NER to repair larger protein-crosslinks is caused by steric hindrance of damage recognition proteins and suggests that proteolytic degradation is necessary prior to repair. While it was originally proposed that the proteasome is responsible for proteolysis of full size DPCs, more recent studies have suggested that a different protease (Spartan in humans) is involved [6,93,94,97,101,176].

To clarify the role of NER in the repair of DPCs in mammalian cells, as well as to address more specific questions regarding how size and location influence DPC repair, we employed a PCR-based assay we term Strand-Specific Primer Extension-Quantitative Polymerase Chain Reaction (SSPE-qPCR). This assay is capable of quantifying the repair kinetics of a broad range of lesions

present on plasmid DNA transfected into repair deficient and corrected mammalian cells. This assay provides significant advantages over previously utilized approaches in that it is rapid, highly quantitative, and extremely flexible. Importantly, this method directly measures repair activity, in contrast to other plasmid-based strategies that rely on indirect measures such as host-cell reactivation of gene function. Results from our initial analyses provide new insight into the ability of the global genome and transcription-coupled NER pathways to repair DPCs in hamster and human cells.

III. MATERIAL AND METHODS

Materials

Chemicals and enzymes. Oligodeoxynucleotides (ODNs) containing 8-oxo-2'-deoxyguanosine (8-oxo-dG) or cholesterol modifications were obtained from Midland Certified Reagent (Midland, TX). All other ODNs were purchased from the University of Minnesota Genomic Center. Human oxoguanine glycosylase 1 (OGG1) was expressed and purified from BL21(DE3) bacteria (Thermo Fisher) using a pET-28a expression vector [13]. Single-stranded M13 vector and all enzymes were obtained from New England Biolabs (Beverly, MA) unless specified otherwise. Chemicals were purchased from Sigma Chemical (St. Louis, MO) unless indicated.

Cell lines. Chinese hamster lung fibroblast cell lines V79 (GM16136) and V-H1 (GM16141) were obtained from the Coriell Institute for Medical Research

(Camden, NJ). V79 are wild-type cells from which the V-H1 clones were derived following an ethylnitrosourea-induced mutagenesis screen [195-197]. V-H1 cells belong to nucleotide excision repair complementation group 2 and lack a functional *XPD* gene [198]. These cells are deficient in the *ERCC2* gene, which codes for the *XPD* protein involved in the helicase activity that unwinds duplex DNA during nucleotide excision repair [198]. Chinese hamster lung fibroblast cells were cultured in Ham's F-12 modified essential Eagle's media (Life Technologies, Grand Island, NY) supplemented with 9% fetal bovine serum (Atlanta Biologics, Atlanta, GA). Chinese hamster ovary CHO-K1 cells were a kind gift from Professor Harry Orr (University of Minnesota). Immortalized human dermal fibroblasts from xeroderma pigmentosum patients with inactivating mutations in the NER *XPD* gene (GM08207) or *XPA* gene (GM04312), as well as gene-corrected clones (GM15877 and GM15876, respectively) derived from these lines were obtained from the Coriell institute. Human and CHO-K1 cells were cultured in Dulbecco's modified Eagle's media (Life Technologies, Grand Island, NY) supplemented with 9% fetal bovine serum. All cells were maintained in a humidified atmosphere of 5% carbon dioxide, 95% air, at 37 °C.

Table 3.1. Oligodeoxynucleotides (ODNs) used is this study (5'→3').

ODN	Sequence	Use
M13-8oxo	AGGGTTTTCCA(8-oxo-dG)TCACGACGTT	Primer Extension
M13-cholesterol	CCGGGTACCGAGCTCGAATTC(cholesterol) GTAATCTTGGTCATAGCTG	Primer Extension
M13-RSV-Zeo-8oxo (template)	ACTGGTCAACTTGGCCAT(8-oxo-dG)TTGGCCTTGGAGGTCGACACC	Primer Extension
M13-RSV-Zeo-8oxo (coding)	CACCTCCAAGGCCAACAT(8-oxo-dG)GCCAAG TTGACCAGTGCCGTT	Primer Extension
M13 Primer R	CGGCTCGTATGTTGTGTG	qPCR of M13 plasmid
M13 Primer L	GCTGCAAGGCGATTAAGT	qPCR of M13 plasmid
RSV-Zeo 1	TATCCGAGATCCGAGGAA	Topo 2.1 PCR Cloning Kit
RSV-Zeo 2	TATGGATCGTCGAGACTC	Topo 2.1 PCR Cloning Kit
M13-Zeo R Primer	ACGCCATTTGACCATTCAAA	qPCR of M13-Zeo plasmid
M13-Zeo L Primer	CCGGTCGGTCCAGAACTC	qPCR of M13-Zeo plasmid
Primer C	GGCCAACATGGCCAA	Taq extension assay
Primer Z	GGTGTGCACCTCCAA	Taq extension assay
Zeo F1	CAAGTTGACCAGTGCCGTTC	RT PCR
Zeo R1	TGATGAACAGGGTCACGTCG	RT PCR
Abasic complement	GTCGACCTCCAA	Taq extension assay
Abasic	ACTGGTCAACTTGGCCAT(abasic)TTGGCC TTGGAGGTCGAC	Taq extension assay
Abasic correct	ACTGGTCAACTTGGCCATGTTGGCCTTGG AGGTCGAC	Taq extension assay

Methods

Taq polymerase extension assay. To confirm that Taq polymerase permanently stalls at abasic sites (and by extension, lesions attached to abasic sites) 200

pmol of the oligodeoxynucleotide M13-RSV-Zeo-8oxo (template) was annealed to 200 pmol of primer C **(Table 3.1)** in restriction enzyme buffer 2 (New England Biolabs) and water in a volume of 10 μL at 95°C for 5 minutes and slowly cooled to room temperature. The creation of a duplex is necessary because OGG1 protein will not react with single-stranded DNA. The duplex DNA was then incubated in the presence or absence of OGG1 (200 pmol) in buffer containing 100 mM NaCl, 1mM $MgCl_2$, and 20 mM Tris-HCl pH 7.0 at 37°C (final volume 15 μL) for 30 minutes. Samples incubated with OGG1 excise the 8-oxo-dG residue leaving an abasic site at its position. Each sample was divided in half and incubated in the presence or absence of primer Z (100 pmol, **Table 3.1**) with 10 mM dNTPs (Thermo Scientific), Taq reaction buffer (New England Biolabs), and Taq polymerase (20 units) in a final volume of 10 μL at 95°C for 5 minutes. Samples were then slow cooled to 75°C for 15 minutes, resolved on a NuPAGE 12% Bis-Tris Gel (Invitrogen) at 18V/cm at 55°C, and stained with ethidium bromide.

Construction of plasmid DNA repair substrates. Synthetic oligodeoxynucleotides (80 pmol) containing either cholesterol (NER positive control) or 8-oxo-dG modifications (M13-cholesterol or M13-8oxo, Table 1) were phosphorylated with T4 PNK (10 units) in ligase buffer (New England Biolabs) for 30 minutes at 37°C in a total volume of 50 μL. Phosphorylated oligonucleotides were then annealed to single-stranded M13 (8 pmol), extended with Taq polymerase (100 units), Taq

reaction buffer (New England Biolabs), 100 mM ATP (Teknova), 10 mM dNTPs (Thermo Scientific), restriction enzyme buffer 2 (New England Biolabs), and 8 μg bovine serum albumin for 15 minutes at 75°C in 260 μL. The temperature was then lowered to 37°C at which point T4 polymerase (60 units) and T4 ligase (8000 units) were added and the reaction incubated at 37°C overnight in 375 μL **(Figure 3.2).** Extension products were resolved on a 0.8% low melting temperature agarose gel. Supercoiled DNA was excised with a razor blade, digested with β-agarase (10 units) according to manufacturer's protocol, purified by phenol: chloroform extraction and ethanol precipitation, and resuspended in water. DNA containing an 8-oxo-dG residue (0.36 pmol) was crosslinked to OGG1 (36 pmol) in buffer containing 100 mM NaCl, 1 mM $MgCl_2$, 20 mM Tris-HCl pH 7.0, and 10 mM sodium cyanoborohydride at 37°C for 30 minutes [177,199]. During this reaction, the 249K active residue attacks the C1 position of the 8-oxo-dG lesion, expelling the base to create an abasic site. Addition of sodium cyanoborohydride reduces the intermediate Schiff base formed, trapping the protein to the ribose **(Figure 3.4).** To study of the effect of protein size on DPC repair efficiency, DPC substrates created as described above were exposed to 0.5 μg of trypsin (Promega) at 37°C in 50 mM Tris-HCl pH 8 overnight prior to transfection. Molecular weight of the digestion product was confirmed by crosslinking 500 pmol (1μL) of OGG1 protein to 500 pmol of duplex oligo containing an 8-oxo-dG modification using the same conditions stated above. This material was subsequently treated with 5 μg trypsin (10 μL) in 50 mM Tris-

HCl pH 8 buffer (20 μL) overnight at 37°C, followed by addition of 10 U DNASE I (5 μL) in DNASE I buffer (15μL) at 37°C for 30 minutes. This material was subsequently resolved on a 16% Tris-Tricine Gel (Bio-Rad) and stained with simply blue (Invitrogen).

KCl/SDS precipitation of DNA-protein crosslinks. To confirm the presence of the OGG1 protein crosslink, lesion-containing M13 plasmids (prepared as described above) were digested with *Bsp*DI for 1 hour at 37°C to generate two restriction fragments, one containing the DPC (4.4 kb) and a second, protein-free fragment (2.8 kb). The digest was treated with SDS at a final concentration of 0.5% and incubated at 65°C for 10 minutes to facilitate protein binding. The samples were then divided in two, and KCl (final concentration 100 mM) was added to one sample and omitted from the other. The reactions were incubated on ice for 5 minutes followed by centrifugation at 12K x G for 5 minutes at 4°C [66]. The supernatant from both samples was resolved by agarose gel electrophoresis and stained with ethidium bromide. Crosslinking efficiency was determined by scanning densitometry using ImageJ to determine the amount of plasmid DNA recovered from solution following KCl/SDS precipitation, as depicted in **Figure 3.5.**

Cloning of a transcriptional unit into M13mp18. Two pg of plasmid psF-CMV-RSV-Zeo Asc1 (Sigma) was amplified with RSV-ZEO 1 and 2 primers (1μM,

Table 1) using Pfu Master Mix (G-Biosciences). PCR conditions were as follows: pre-treatment at 94°C for 3 minutes followed by 25 cycles at 94°C for 30 seconds, 55°C for 30 seconds, and 72°C for 1 minute. The 925 bp PCR product containing the RSV promoter and zeocin gene (RSV-Zeo) was cloned using a Topo 2.1 PCR Kit (Thermo) and transformed into Top 10 F' bacteria (Thermo). Clones harboring the PCR product were isolated and the insert recovered by digestion with *Eco*RI followed by gel purification and ligation into pLC118. (The plasmid pLC118 was created by cloning the neomycin phosphotransferase gene from pSV2neo [200] into a *Eco*RI-linearized M13mp18. One microliter of the ligation mixture was transformed into NEB Turbo electrocompetent bacteria (New England Biolabs), and individual clones harboring recombinant M13 molecules containing the RSV-Zeo insert were screened by restriction digestion analysis of double-stranded virion DNA to determine orientation. Single-stranded virion DNA was subsequently recovered from cultures harboring the insert in the two different orientations (referred to, respectively, as pLC119 and pLC120) and primer extension reactions performed as described above. M13-RSV-Zeo-8oxo template or M13-RSV-Zeo-8oxo coding primers **(Table 3.1)** were used to generate double-stranded plasmid substrates in which the 8-oxo-dG residue is present on, respectively, the template or coding strands of the RSV-Zeo transcriptional unit **(Figure S3.1).** Transcription of these plasmids following transfection into wild-type V79 cells was confirmed *via* quantitative reverse transcriptase PCR using SuperScript VILO (Invitrogen) according to

manufacturer's instructions and primers Zeo F1 and Zeo R1 **(Table 3.1)** for amplification [201].

Purification of single-stranded DNA. Approximately 10 ng of double-stranded pLC119 or pLC120 was electroporated into NEB Turbo bacteria according to manufacturer instructions and shaken in 1 mL Luria-Bertani broth (LB) for 1 hour at 37°C. Either 50 or 100 µL of culture broth was added to 100 µL of an overnight culture of non-transfected bacteria and 3 mL of top agar containing 5 mM $MgCl_2$. This solution was mixed, poured onto an LB plate, and incubated at 37°C overnight. Plaques formed were picked using a Pasteur pipette and incubated in 1 mL of LB for 3 hours at room temperature followed by 4°C overnight. The next day, 100 µL of an overnight culture of NEB Turbo bacteria was diluted into 5 mL of LB containing 5 mM $MgCl_2$ and shaken for 2 hours at 37°C. The 5 mL culture was then diluted into 45 mL of LB containing 5 mM $MgCl_2$ and divided into 1 mL aliquots. Next, 100 µL of diluted plaques were added to each aliquot and shaken at 37°C for 5 hours [202]. Cultures were then spun at 12K x G in a table-top centrifuge for 5 minutes at room temperature [203]. The supernatants were collected and single-stranded DNA purified using a QiaPrep Spin M13 kit (Qiagen).

Transfection. Mammalian cells were plated at 0.5 x 10^6 cells/well in a 6-well plate the night prior to transfection. For a one well transfection, 15 µL (1.2 pmol) of

purified, DNA repair substrates prepared as described above was incubated with 6 µL of lipofectamine (Invitrogen) and 300 µL of serum-free culture media for 5 minutes at room temperature. (Note that 1 µL of the DNA substrate is reserved as non-transfection (i.e. 0 hour time point) controls. This material is diluted in 500 µL of water and subsequently included in the SSPE-qPCR assay described below.) 250 µL of DNA complexes were added to the well and allowed to recover for either 1.5, 3, 5, 7, or 8 hours. For multiple well transfections, the above conditions were doubled or tripled as needed. Following incubation, cell culture media was removed and 1 mL of 0.6% SDS/0.01 M EDTA was added to each well for 10-15 minutes at room temperature. Lysed cells were scraped with a rubber policeman and transferred to a 1.5 mL centrifuge tube. Sodium chloride was added to a final concentration of 1 M, inverted gently 5 times, and incubated at 4°C overnight [178]. The next day, samples were spun at full speed in a table top centrifuge at 4°C for 30 minutes. The supernatant was ethanol precipitated, resuspended in 100 µL water and stored at -20°C until SSPE-qPCR.

Strand-specific primer extension-quantitative polymerase chain reaction (SSPE-qPCR) repair assay. Low molecular weight DNA recovered from transfected cells (1 µL) as well as non-transfected DNA samples (0 hour controls) were mixed with a PCR primer (1µM) complementary to the damaged strand of the plasmid (M13 Primer R, Table 1, **Figure 3.1**) in SYBR green master mix buffer (Invitrogen). Following a 10-minute melting step at 90°C, the DNA was melted at 90°C for 15

seconds and then reduced to 65°C for 1 minute to permit primer annealing/extension. This step was repeated an additional seven times, at which point a primer complementary to the undamaged strand of the plasmid (M13 Primer L, Table 1, Figure 3.1) was added (1μM). Cycle threshold (Ct) values were then measured *via* quantitative real-time PCR on an Applied Biosystems StepOnePlus Real Time PCR System using the reaction conditions described above. In parallel, a qPCR experiment analogous to that above was performed in which the eight rounds of primer extension were omitted. The Ct values from the latter experiment were subtracted from that of the former to calculate the delta Ct value $\Delta Ct = [Ct] - [Ct_{\text{primer extension}}]$. Because the presence of an abasic site, cholesterol, or DPC lesion blocks primer extension, this delta Ct value can be used to calculate the percent of lesion repair using the formula: percent DNA repair = $(2^{\Delta Ct}/2^3) \times 100$ [179,201]. The percent repair calculated at each time point using this method is then subtracted from the 'apparent percent repair value' calculated using the 0 hour time point (i.e. non-transfected DNA repair substrate sample) to correct for PCR background noise induced by the strand-specific primer extension.

Measurement of base excision repair (BER) activity in wild-type and NER-deficient cell lines. A plasmid containing an 8-oxo-dG modification was transfected into Chinese hamster V79 and V-H1 cell lines and low molecular weight DNA recovered at 1.5 and 3 hours post-transfection as described above.

This material was then treated with 80 pmol of OGG1 enzyme for 30 minutes at 37°C. Under these conditions, the OGG1 enzyme quantitatively excises any unrepaired 8-oxo-dG residues from the plasmid, thereby creating an abasic site that blocks primer extension by Taq polymerase. It is thus possible to use the strand-specific primer extension-qPCR assay described above to calculate the respective levels of BER activity present in wild-type and NER-deficient cell lines.

Measurement of cisplatin-induced DNA-protein crosslinks in Chinese hamster cell lines. Wild-type V79 and NER-deficient V-H1 Chinese hamster cells were grown to confluence on 10 cm dishes (2 per cell line). One dish each per cell line was maintained in serum-free media plus or minus 100 μM cisplatin for one hour at 37°C. Cells were then washed twice with PBS and re-suspended at a density of $1x10^7$ cells/mL [66]. Protein-linked DNA was isolated using 100 μL of cells lysed with 0.5 mL 2% SDS, 1mM PMSF, and 20 mM Tris-HCl pH 7.5 and frozen at -80°C. Cells were then thawed at room temperature, vortexed for 10 seconds, and incubated at 65°C for 10 minutes. Next, 0.5 mL of 200 mM KCl in 20 mM Tris-HCl pH 7.5 was added and the material passed through a 1 mL pipet tip five times. Samples were then put on ice for 5 minutes, spun at 3K x G for 5 minutes at 4°C, and the pellet resuspended in 1 mL of 100 mM KCl in 20 mM Tris-HCl pH 7.5 by pipetting 5 times to evenly disperse recovered material. Samples were heated to 65°C for 10 minutes, chilled on ice for 5 minutes, and spun at 4°C for 5 minutes at 3K x G. Resuspension of the pellet in 100 mM KCl in 20 mM Tris-HCl,

heating, chilling, and spinning were repeated twice more before resuspending the final pellet in 1 mL of 100 mM KCl, 10 mM EDTA, 20 mM Tris-HCl pH 7.5 and proteinase K (final concentration 0.2 mg/mL). Samples were incubated at 50°C for 3 hours after which 100 μg of bovine serum albumin was added, chilled on ice, and spun at 10K x G for 10 minutes at 4°C. The supernatant was collected and mixed with 1 mL of freshly prepared 200 ng/mL Hoechst dye 33258 reagent (ChemCruz) in 20 mM Tris-HCl pH 7.5, vortexed, and incubated for 30 minutes in the dark at room temperature. Total DNA was isolated by lysing 100 μL of cells in 1 mL of 2M NaCl in 20 mM Tris-HCl pH 7.5 and mixed with the fluorescent agent as stated above. Fluorometer measurements of total DNA and protein-linked DNA were obtained using a Fluoromax 4 Spectrofluorometer (Horiba) at room temperature with 360 excitation and 450 emission filters. Protein-linked DNA values were divided by total DNA to obtain percent of protein-crosslinked DNA.

IV. RESULTS

Taq polymerase extension is blocked by abasic sites.

The SSPE-qPCR assay utilized in this study is dependent on the ability of the lesions analyzed to permanently stall Taq polymerase extension. To confirm this, we performed two parallel primer extension reactions, one using a 40-mer oligonucleotide (M13-RSV-Zeo-8oxo (template), see **Table 3.1**) containing an 8-oxoguanine residue at position 19, and the other harboring an AP site created by OGG1 at this same position (see Methods for details). It has been reported that

Taq polymerase is able to efficiently read-through an 8-oxoguanine residue but is blocked by abasic sites [180]. We thus anticipated that a primer annealed to the 8-oxoguanine-containing strand would be extended by Taq polymerase, producing a 40-nucleotide product, while a primer annealed to the AP-containing oligonucleotide would not be extended to produce a full-length product. The densitometry results presented in **Figure 3.2** (calculated using ImageJ) confirm this prediction, showing the presence of a full-length primer extension product when the 8-oxoguanine lesion-containing substrate (8oxo) was extended with Taq polymerase in the presence of a complementary primer. In contrast, no product was produced when the AP-containing substrate (AP, **Figure 3.2**) was extended with Taq polymerase and a complementary primer. We also observed a ~ 21 nucleotide product (data not shown), as would be expected were the Taq polymerase stalled at the abasic site. It is noteworthy that creation of an AP site using OGG1 can also generate a single-strand break via beta-elimination by OGG1 (43). To confirm that Taq polymerase is blocked at abasic sites in the absence of single-strand breaks, the above experiment was repeated using an oligonucleotide ordered with an abasic modification (abasic, **Table 3.1**) or no lesion (abasic corrected, **Table 3.1**) in the presence or absence of a complementary primer (abasic complement, **Table 3.1**). These experiments confirmed an increase in full-length product during extension of an unmodified oligonucleotide but not with an abasic-containing substrate. Additionally, an 18-nucleotide product corresponding to the site of the abasic lesion was observed

during extension of the damaged substrate, indicating halting of the Taq polymerase at the lesion, but not in the undamaged oligonucleotide extension (**Figure S3.2**).

Repair of 8-oxo-dG in wild-type and NER-deficient cells.

While our ultimate objective was to use the SSPE-qPCR assay to compare the relative efficiency with which NER proficient and NER-deficient clones repaired a DPC-containing plasmid substrate, we first performed two series of experiments to confirm: 1. That NER proficient and NER deficient clones would repair plasmids harboring a base excision repair substrate with equivalent efficiencies, and 2. That a plasmid harboring a lesion *known* to be selectively repaired by the NER pathway would be significantly more efficiently repaired in NER proficient cells than in isogenic clones deficient in NER.
As a first step, we transfected covalently closed circular plasmids harboring a site-specific 8-oxo-dG modification (see methods for details of construction and purification) into wild-type (V79) and NER-deficient (V-H1) Chinese hamster cell lines and, following incubation periods of 1, 1.5 or 3 hours, purified low molecular weight DNA from the cells. This material, as well as non-transfected DNA was treated with OGG1, was analyzed using SSPE-qPCR, as described in the Methods section. As illustrated in **Figure 3.3**, both wild-type and NER-deficient cells showed rapid and efficient repair of 8-oxo-dG lesions indicating that there is no appreciable difference in the relative BER activity in V79 and V-H1 clones. (It

is critical to note that, as described in the Methods section, the percent repair calculated at 1, 1.5 and 3 hours post-transfection was corrected to subtract 'apparent repair' observed in the '0 hour', i.e. no-transfection control.) This result is consistent with the interpretation that equivalent amounts of transfected DNA gain access to the cellular DNA repair machinery in the two cell lines. We next pursued a second series of experiments to test the hypothesis that NER-deficient clones would repair a plasmid substrate harboring a known NER substrate with reduced efficiently than would their isogenic wild-type counterparts.

Repair of cholesterol adducts in wild-type and NER-deficient cells.

A plasmid containing a site-specific cholesterol-ribose lesion was prepared and purified as described in the methods. It has previously been shown that this lesion is subject to NER [182]. This substrate was transfected into V79 (NER proficient) and V-H1 (NER deficient) cells. Low molecular weight DNA was recovered eight-hours post-transfection and subjected to the SSPE-qPCR assay to calculate DNA repair activity as described above. As depicted in **Figure 3.4**, the efficiency of repair of the cholesterol-containing plasmids in NER-deficient V-H1 cells was nearly fifteen-fold lower (4% vs 57%) than that detected in the NER proficient V79 cells. To confirm that this difference was indeed due to a defect in NER, an identical experiment was performed in human cell lines deficient (XPD) or proficient (XPDcorr) in NER. Results from this experiment indicated that repair of the cholesterol-containing plasmid in wild-type human cells was six-fold more

efficient than that detected in the isogenic NER-deficient clone (63% vs 11%, **Figure 3.4**). (As in the experiment above, repair efficiency values have been corrected by subtracting the background seen in the 0 hour, no transfection control sample.) These results confirmed the expectation that NER-deficient clones would show significantly decreased repair of a cholesterol moiety crosslinked to plasmid DNA, and that our SSPE-qPCR assay is capable of detecting differences in the repair of adducts processed by the NER pathway.

Crosslinking OGG1 to 8-oxo-dG-containing plasmid DNA substrates.

As was outlined in the Introduction, proteins become crosslinked to DNA *via* multiple mechanisms. To address specific questions regarding DPC repair on plasmid DNA, an enzymatic reaction was chosen to crosslink the repair protein OGG1 to a deoxyribosyl residue. This biologically relevant lesion represents the main source of endogenous DPCs of apurinic/apyrimidinic (AP) site within nucleosome core particles [12]. To quantify the crosslinking efficiency of these substrates, plasmids containing a site-specific OGG1-DNA crosslink were subjected to KCl/SDS precipitation as described in the Methods section. As the results in **Figure 3.5** illustrate, the 4.4 kb fragment was quantitatively removed from the sample in which KCl was added while there is no evident reduction in the amount of the 2.8 kb fragment in this sample, compared to the untreated control. This result confirms that the crosslinking reaction is highly efficient, with

nearly 100% of the plasmid molecules containing a site-specific DNA-protein crosslink.

Repair of OGG1 crosslinked to plasmid DNA in Chinese hamster and human clones.

To determine whether the M13 plasmid containing a covalent OGG1 crosslink is subject to repair, DPC-containing plasmids were transfected into wild-type V79 Chinese hamster cells. Low molecular weight DNA was recovered 3, 5, 7 and 8-hours post-transfection as described in Methods. SSPE-qPCR assays on this material as well as on a 0 hour, no transfection control, sample was used to calculate percent DNA repair as outlined in the Methods section. These results revealed essentially linear repair kinetics reaching 28% repair at the final time point (**Figure 3.6**, left panel), indicating that V79 cells are capable of repairing OGG1 crosslinked to a non-replicating plasmid DNA molecule. We performed similar experiments in a second Chinese hamster-derived cell line (CHO-K1), as well as in two human wild-type cell lines. In each instance, these clones were capable of repairing the plasmid DPC lesion (**Figure 3.6**, right panel). Interestingly, DPC repair efficiency in each of the hamster clones was in the range of ~20-25%, whereas the corresponding repair efficiency in two human cell lines derived from unrelated donors was significantly greater (>70%). While there was no significant difference in the repair levels between species, the level of DPC repair detected in human cells was significantly greater than that detected

in the Chinese hamster-derived clones. Interestingly, despite this species-specific difference in DPC repair activity there was no significant difference in the efficiency with which human and hamster cells repaired the cholesterol lesion (63% vs 57%, **Figure 3.4**).

Reduced DPC repair in Chinese hamster and human clones deficient in NER.

To test the hypothesis that DPCs are repaired by the NER machinery, we transfected the DPC-containing plasmid into isogenic NER-deficient and NER-proficient Chinese hamster and human clones, and used the methodology outlined above to quantitatively measure cellular repair activity. Consistent with our prediction, DPC repair efficiency was dramatically lower in NER-deficient cells compared to their isogenic NER-proficient counterparts (**Table 3.2**). Chinese hamster V-H1 cells (XPD deficient) repaired the DPC nine-fold less efficiently than did their isogenic, wild-type counterpart V79 (3% vs 27%). Similarly, XPD deficient human cells repaired the DPC nearly four-fold less efficiently than did their gene-corrected counterpart (20% vs 73%). We extended this analysis to look at the effect of inactivation of another NER gene. As **Table 3.2** illustrates, inactivation of the human XPA gene was associated with a five-fold reduction in DPC repair efficiency (16% vs 78%). In all instances the differences in DPC repair activity observed between NER-deficient and NER-proficient clones were statistically significant. These results indicate that in

mammalian cells, the NER pathway is capable of rapidly and efficiently repairing plasmid DPC substrates.

Table 3.2. OGG1-DNA crosslink repair in NER-deficient cells. *Values depict mean percent repair, ± SEM, N=3.

Percent Repair* (mutated)	Percent Repair* (control)	Fold Reduction (vs control)
V-H1 (3 ± 1)	V79 (27 ± 2)	9
XPD (20 ± 7)	XPD Corr (73 ± 5)	3.7
XPA (16 ± 5)	XPA Corr (78 ± 10)	4.9

Transcription-coupled repair of OGG1 crosslinked to a plasmid in Chinese hamster cells.

The NER pathway is comprised of two distinct sub-pathways, respectively referred to as the transcription-coupled (TC) and global genome (GG) pathways [204]. The DPC substrate studied in the experiments presented above was localized within a portion of the plasmid that was transcriptionally silent. Consequently, we conclude that the repair events we detected were catalyzed by the global genome NER pathway. To determine whether TC-NER is also capable of repairing DPCs, molecular cloning was employed to generate plasmids harboring an 8-oxo-dG-residue localized within a minigene encoding the bacterial zeocin-resistance gene driven by the RSV promoter. Because of the way these clones (pLC119/pLC120) were generated, the 8-oxo-dG residues were present,

respectively, on the coding, or template strands of the DNA (Details of the creation of these clones, as well as how the activity of the RSV/zeocin transcription unit in Chinese hamster cells is described in the Methods section). We subsequently crosslinked recombinant OGG1 protein to the 8-oxo-dG residues in the pLC119 and pLC120 plasmids via the cyanoborohydride-trapping technique outlined above to generate plasmid substrates harboring a DPC with either the template or coding strand of the RSV/zeocin transcriptional unit. To confirm that the crosslinking efficiency of OGG1 was similar in both plasmids, KCl/SDS precipitation was performed on DPCs crosslinked to the template or coding strand. The soluble material remaining was resolved by agarose gel electrophoresis (see Methods for details), and scanning densitometry performed using ImageJ software. This analysis revealed that the crosslinking efficiency on the two clones was 94% and 95%, respectively (data not shown). The two plasmid DPC substrates were subsequently transfected into wild-type (V79) and NER-deficient (V-H1) Chinese hamster cell lines and their respective repair efficiencies determined using the strategy outlined above. Based on results from experiments investigating the repair of actively transcribing loci within mammalian cells exposed to UV radiation, we predicted that DPC lesions present on the template strand would be repaired more efficiently that would lesions present on the coding strand [205]. The results depicted in **Figure 3.7** are consistent with this expectation, showing that a DPC present on the template strand was repaired approximately 2.5-fold more efficiently than was an identical

DPC lesion present on the coding strand. The data further illustrate that for both lesions, repair occurs significantly less efficiently in the NER-deficient V-H1 background than in its wild-type counterpart.

A 4 kDa DNA-peptide crosslink is repaired more efficiency than a 38 kDa DPC.

Results from our lab and others confirm that several agents are able to crosslink proteins of dramatically different sizes to DNA, both *in vitro* as well as in intact cells [4,16,206]. It has been suggested that the size of the protein crosslink may influence the pathway through which a DPC lesion is repaired [61]. We thus sought to examine whether a substantially smaller DPC substrate would also be subject to NER-mediated removal. To achieve this objective, OGG1-crosslinked plasmid DNA substrates were exhaustively digested with trypsin (see Methods) to generate a substrate in which a 39-amino acid residual (~4.9 kDa) peptide fragment remained attached to the DNA (**Figure S3.3).** This peptide-DNA crosslink substrate was transfected into Chinese hamster V79 and V-H1 cells and repair efficiency analyzed at three and eight hours post-transfection using the SSPE-qPCR assay, as outlined above. The results in **Figure 3.8** indicate that repair of this DNA peptide substrate was significantly more efficient in the NER-proficient V79 cells than in their isogenic NER-deficient V-H1 counterparts. Interestingly, the DNA peptide (39 amino acid residue) crosslink was repaired

approximately twice as efficiently as was the full length OGG1 DNA-protein (345 amino acid residue) crosslink (43% **Figure 3.8** vs 27% **Figure 3.6**).

Repair of cisplatin-induced chromosomal DPCs in wild-type and NER-deficient Chinese hamster cells.

The results presented above convincingly demonstrate that both the global genome and transcription-coupled NER pathways are able to efficiently repair a DPC comprised of the OGG1 protein (or a proteolytic fragment derived therefrom) covalently trapped onto a deoxyribosyl residue of a plasmid DNA molecule. However, it is conceivable that similar substrates crosslinked to genomic DNA may be subject to different DNA repair pathways, or that the nature of the chemical bond linking protein to DNA can influence the mechanism(s) through which DPCs are repaired. To confirm that results obtained using the SSPE-qPCR assay generally reflect the ability of the NER machinery to repair DPCs present on chromosomal DNA, we quantitated the level of accumulated DNA-protein crosslinks present in wild-type and NER-deficient cells following exposure to cisplatin. We hypothesized that if NER plays a significant role in repair of chromosomal cisplatin-induced lesions, levels of DPCs present following a one-hour exposure to 100 μM cisplatin would be elevated in V-H1 cells, compared to V79 cells. The results in **Figure 3.9** illustrate an approximate 3.6-fold higher level of DPCs in cisplatin-treated V-H1 cells compared to their wild-type, isogenic counterpart, consistent with the interpretation that the NER

pathway plays a significant role in the repair of drug-induced chromosomal DPCs.

V. DISCUSSION

In this report, we describe the development of a DNA repair assay we named strand-specific primer extension-quantitative PCR (SSPE-qPCR) and illustrate its utility in studying the repair of lesioned plasmids transfected into wild-type and NER-deficient human and Chinese hamster-derived cell lines. The versatility of this assay permits one to generate multiple distinct DNA repair substrates and subsequently measure the respective efficiencies with which they are repaired in different genetic backgrounds. In this way, we were able to show that both human and Chinese hamster-derived clones are able to efficiently repair episomal plasmids harboring a DPC, and that in both species this process was primarily dependent on the NER machinery. We presented evidence that both the GG and TC sub-pathways of NER can contribute to mammalian DPC repair. Our results also indicated that a DNA-crosslinked 39 amino acid polypeptide was repaired significantly more efficiently than was a 345 amino acid protein crosslink. While in this instance, our primary focus was on DNA protein crosslink repair, our results illustrate that with appropriate modifications this assay would be useful in the study of any number of DNA lesions.

This study was undertaken in an attempt to resolve a controversy in the literature regarding the role of nucleotide excision repair in the removal of DNA-

protein crosslinks. Baker *et al.* (31) detected higher levels of host cell reactivation activity of a DPC containing plasmid transfected into NER-proficient cells compared to that detected in a NER-deficient clone. This group presented additional information leading them to conclude that larger protein crosslinks were proteolytically degraded to smaller peptide crosslink lesions that were subsequently repaired in an NER-dependent manner. In contrast, Nakano *et al*. (30) published results supporting a model in which the mammalian NER pathway was only capable of repairing DPCs smaller than approximately 10 kDa. In an effort to resolve this apparent paradox, we developed the SSPE-qPCR assay and used it to compare the relative efficiency with which NER-deficient and NER-proficient isogenic cell line pairs repaired a synthetic DPC substrate. Critically, as part of our experimental design, we also compared the relative efficiency with which these same cell line pairs repaired plasmid substrate harboring an 8-oxo-dG residue or a site-specific cholesterol moiety. While the former lesion is repaired by the base excision repair machinery, the latter lesion is known to be subject to NER repair. We were thus able to use these latter repair substrates as, in effect, negative and positive controls for the SSPE-qPCR assay. Were the assay faithfully monitoring cellular DNA repair function, there should be no difference in 8-oxo-dG repair activity between the NER-deficient and NER-proficient clones, however, these latter cells should display significantly greater repair efficiency directed towards the cholesterol substrate. Results presented above confirmed these predictions. Thus, our subsequent finding that repair of a

DPC substrate was significantly reduced in the NER-deficient V-H1 cells, compared to their wild-type isogenic counterpart V79 is most consistent with the interpretation that the primary mechanism of repair of this substrate is NER. While our assay cannot definitively rule out the possibility that differential kinetics of plasmid nuclear uptake or transfection efficiency influence DPC repair efficiency, these potential explanations are inconsistent with our finding that there was no statistically significant difference in the cycle threshold values obtained from experiments in which plasmid DNA harboring 8oxoG or DPC lesions were transfected into WT and NER-deficient cell lines. Additional support for the interpretation that plasmid DPC repair activity in mammalian cells is primarily due to NER was obtained when we showed that human clones deficient in the XPA or XPD genes also showed greatly diminished efficiency of repair of the DPC substrate, compared to their isogenic wild-type counterparts.

Another advantage to using the SSPE-qPCR assay to study the repair of DNA substrates, is that parameters such as sequence context can be easily manipulated to assess their influence on repair. We demonstrated this by crosslinking a DPC to either the template or coding region of a transcriptional unit and measuring differences in repair efficiency using the SSPE-qPCR assay. Results from this experiment revealed that DPCs crosslinked to the template strand were repaired significantly higher than those attached to the coding strand and that in both cases, repair was significantly decreased in NER-deficient clones. Based on these observations we conclude that the TC-NER pathway is

able to repair DPCs. It is notable that the repair efficiency of the template strand-containing DPC in this sequence context (32%) was not appreciably different from the ~28% repair efficiency observed for a substrate present in a locus that does not support transcription (see **Figures 3.6 and 3.7**). Thus, it appears that additional factors besides transcription can influence DPC repair efficiency. For example, it is conceivable that additional factors, such as sequence context, %GC composition, etc., could potentially influence the efficiency of DPC repair. In addition to investigating these possibilities, it will be of interest to examine the effect on DPC repair of replication by generating a DPC on a plasmid containing an origin of replication.

Although our repair data refute the hypothesis that NER is incapable of repairing lesions larger than 10 kDa, we wanted to further investigate whether a DNA-peptide crosslink (~4 kDa) would be more efficiently repaired than a DPC (38 kDa) using the SSPE-qPCR assay. Results presented above confirmed that the smaller, DNA-peptide crosslink was repaired twice as efficiently as the OGG1 crosslink in wild-type cells and that repair of either of these lesions was also dependent on the NER pathway. This data is consistent with the hypothesis that repair of DPC lesions requires one or more processing steps, and that a larger protein substrate requires more processing than does a smaller, peptide-crosslink substrate. Several publications have shown that the yeast WSS1 and its human homolog Spartan are DNA-dependent proteases that play critical roles in DPC repair [6,93,94]. Currently Spartan's role in DNA damage tolerance and DPC

repair is not fully understood but it's thought to be replication-coupled [96,98,207]. It has been shown that Spartan-deficient worms are hypersensitive to DPC-inducing agents, and that patients with Ruijs-Aalfs syndrome possessing germline mutations in the Spartan gene develop early onset hepatocellular carcinoma, as do mice hemizygous for the Spartan gene [97,98,208]. It is conceivable that this cancer predisposition phenotype reflects a defect in repair of endogenously produced DPCs. Although our data are consistent with the hypothesis that non-replicating plasmids are also subject to proteolytic processing, additional experiments using the SSPE-qPCR assay will be required to rigorously test this. It will also be important to determine whether, as others have proposed (Baker *et al.*), the proteasome is capable of processing proteins crosslinked to DNA.

It is notable that results generated using the SSPE-qPCR assay uncovered a species-specific difference in DPC repair efficiency. While the overall repair efficiency of crosslinked OGG1 in two human cell lines obtained from unrelated donors exceeded 70%, repair efficiency of this substrate in two different Chinese hamster-derived clones was significantly lower (~20%). As the data in **Figure 3.4** illustrates, there is essentially no difference in the efficiency with which the cholesterol lesion is repaired in human versus Chinese hamster-derived cells. Thus, the species-specific difference in DPC repair efficiency is not due, *per se*, to reduced levels of NER activity in hamster cells. Based on data implicating the involvement of proteolysis in DPC repair, it is tempting to

speculate that human cells possess a more active protease to generate smaller adducts that can be more easily excised by the NER machinery. Currently, experiments are underway to employ the SSPE-qPCR assay to determine the precise cause of this DPC repair deficit in Chinese hamster clones and determine whether it reflects a trend of reduced DPC repair activity in the cells of other short-lived mammals.

Finally, we tested the hypothesis that chromosomal DPC lesions formed following cisplatin treatment are subject to repair *via* the NER machinery. We determined that NER-deficient cells harbored significantly higher levels of cisplatin-induced DPCs than did isogenic wild-type cells immediately following a one hour incubation with 100μM cisplatin. We are currently using the SSPE-qPCR assay to assess the role of additional repair pathways, such as homologous recombination as a potential mechanism through which mammalian cells repair DPCs.

VI. CONCLUSIONS

The SSPE-qPCR assay detailed above demonstrates a new way to quantitatively assess the repair mechanisms involved in DPC repair on plasmid substrates. This method is easy, sensitive, and capable of directly quantifying DPC repair at time points as early as 2 hours post-transfection. Using this assay, parameters such as DPC size, chemical crosslink, and DNA sequence context can be independently assessed to gain insight into the efficiency with which the

plasmid DPC is repaired. Initial studies in our lab using the SSPE-qPCR assay have demonstrated that DPC lesions on transcribing and non-transcribing plasmids are repaired by a mechanism that is dependent on the nucleotide excision repair pathway and that DNA-peptide crosslinks are repaired at a higher efficiency than larger, DNA-protein crosslinks.

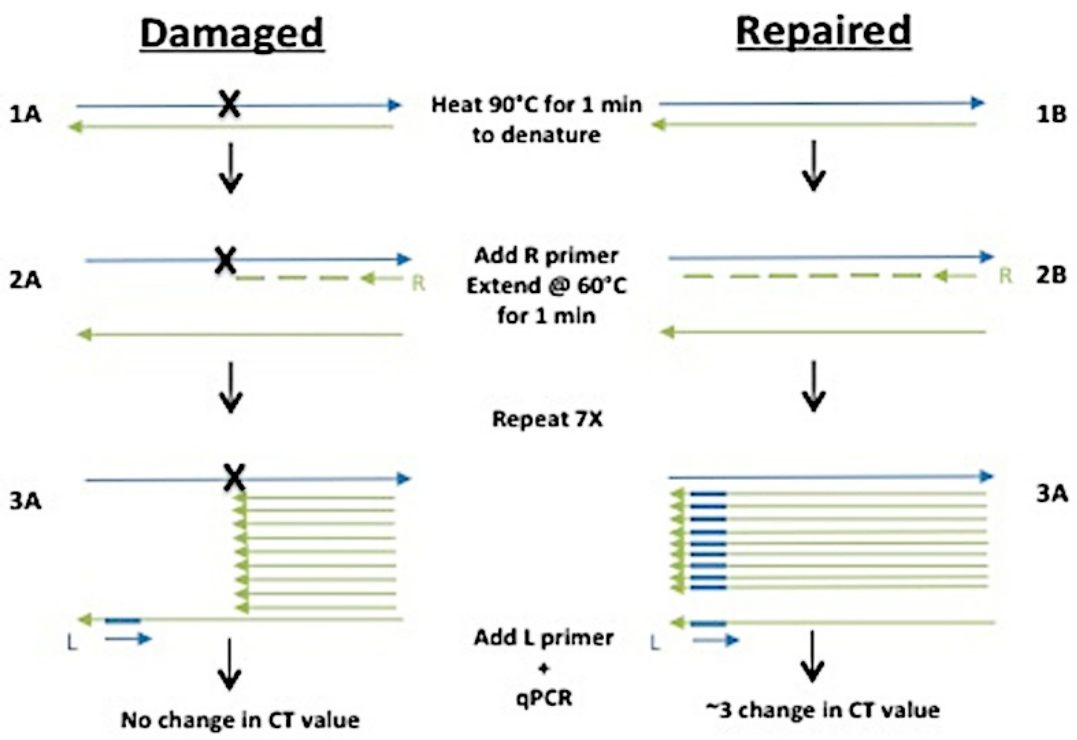

Figure 3.1: Quantification of damaged plasmid *via* strand-specific primer extension/qPCR (SSPE-qPCR). Repair of damaged plasmids is quantified using SSPE-qPCR: (1) Plasmid DNA is denatured, (2) a primer extension reaction is performed using primer R, (3) the denaturation/primer extension step is repeated and additional 7 cycles. After 8 cycles, primer L is added and Ct values determined using qPCR. The presence of an abasic site, cholesterol, or DPC (A) will cause Taq polymerase to stall, resulting in no full-length product strands. In contrast, when repair has occurred (B), Taq polymerase will produce full-length product strands containing the binding site for primer L.

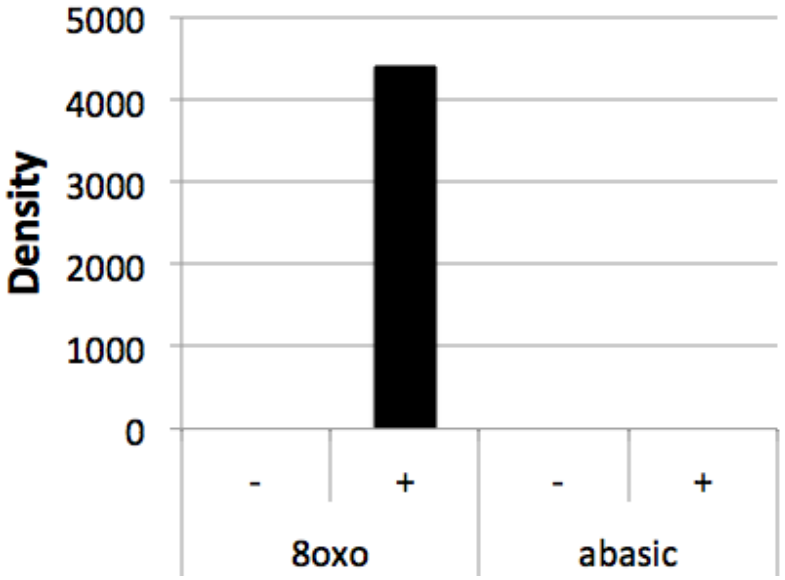

Figure 3.2: An AP site blocks Taq-mediated primer extension. Taq polymerase extension reactions were performed as described in the text on 40-mer oligonucleotides containing either an 8-oxo dG residue (8oxo) or an AP site (AP), see methods section for details, in the absence (-) or presence (+) of complementary primer Z (15-mer, see methods). The products were resolved by electrophoresis, stained with ethidium bromide and subject to scanning densitometry. The relative amount of full-length product (40 nt) was quantitated using image J and plotted on the y axis (arbitrary units).

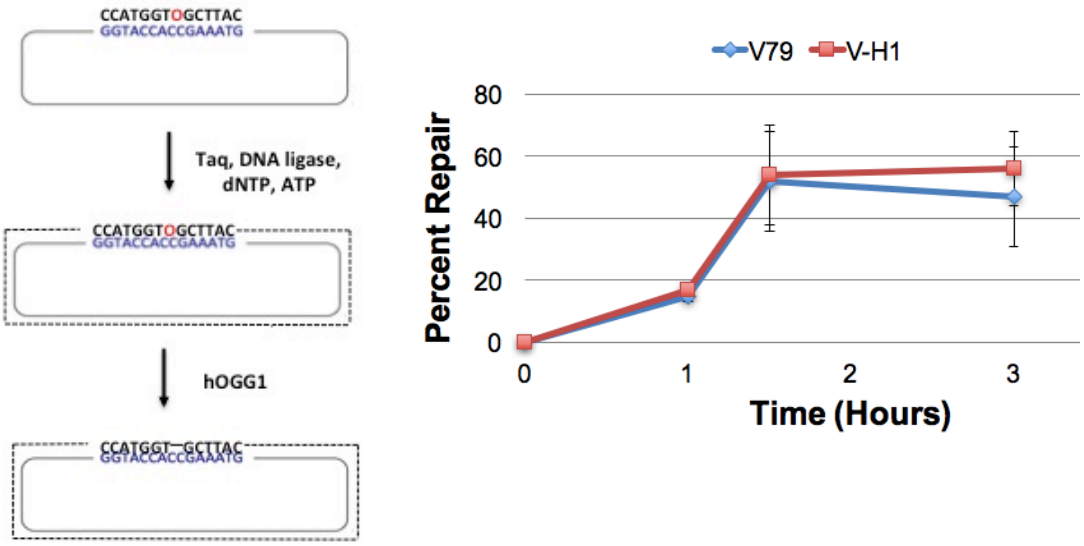

Figure 3.3: 8-oxo-dG repair efficiency is similar in wild-type and NER-deficient Chinese hamster clones. An oligonucleotide containing an 8-oxo-dG modification (O, in red) is annealed to single-stranded M13 and a primer extension reaction performed as described in the Methods. Covalently closed circular double-stranded DNA is gel-purified, and transfected into wild-type V79 (blue) and NER-deficient V-H1 (red) Chinese hamster cells *via* lipofection. Low molecular weight DNA was recovered 1, 1.5 and 3-hours post-transfection and treated with OGG1 to convert unrepaired 8-oxo-dG residues to abasic sites. DNA repair assays were then performed as described in the legend to Figure 1. Values depict mean percent repair, ± SEM, N=3.

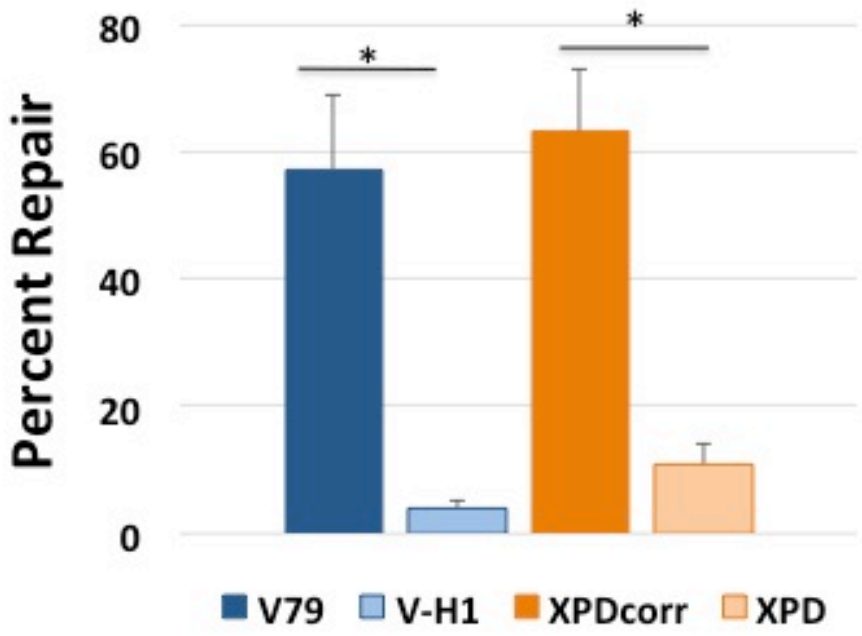

Figure 3.4: Cholesterol-DNA adducts are repaired with reduced efficiency in NER-deficient cells. Plasmid DNA containing a cholesterol adduct was transfected into Chinese hamster (blue) and human (orange) cells lines proficient (dark bars) or deficient (light bars) in NER *via* lipofection and low molecular weight DNA recovered after 8 hours. DNA repair assays were performed as described above. Values depict mean percent repair, ± SEM, N=4, *P < 0.05.

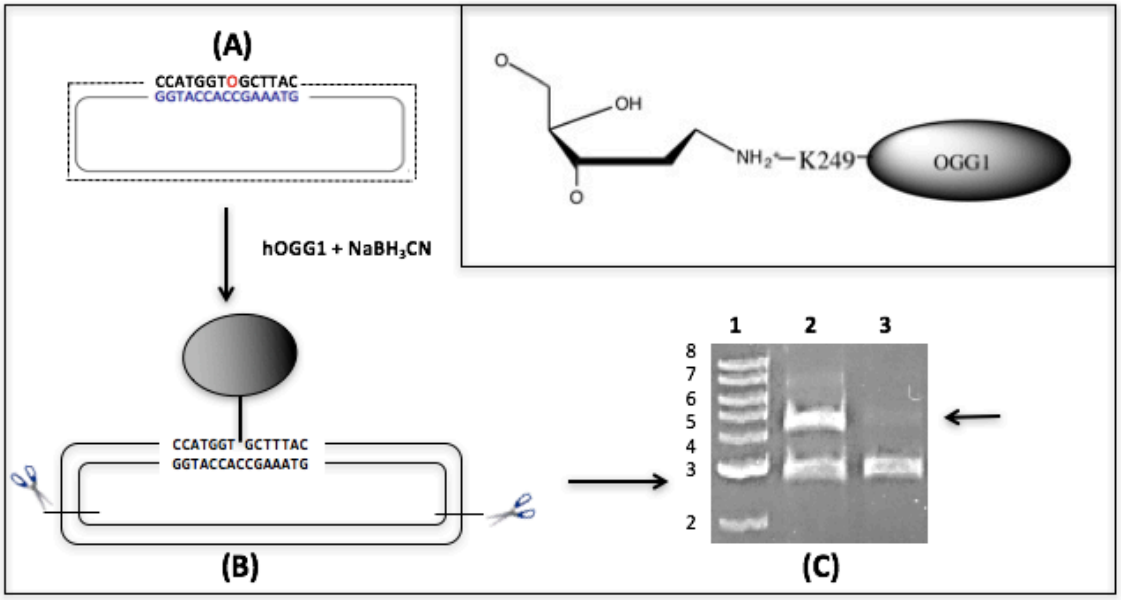

Figure 3.5. Creation of an OGG1-plasmid DNA crosslink substrate. (A) Plasmid DNA containing an 8-oxo-dG residue (O, in red) was reacted with OGG1 in the presence of sodium cyanoborohydride to create a covalent bond between lysine residue 249 and a deoxyribosyl moiety on the plasmid (see Methods for details, chemical structure depicted in inset). **(B)** This product was cut with restriction enzymes to generate two fragments: a 2800 bp protein-free DNA fragment and a 4400bp fragment crosslinked to OGG1. **(C)** The restriction digested material was resolved by agarose gel electrophoresis prior to (lane 2) or following (lane 3) precipitation in the presence of K-SDS (see Methods), and stained with ethidium bromide. The arrow illustrates the selective loss of the OGG1-crosslinked DNA fragment following K-SDS precipitation. Lane 1; molecular weight marker in kilobase pairs.

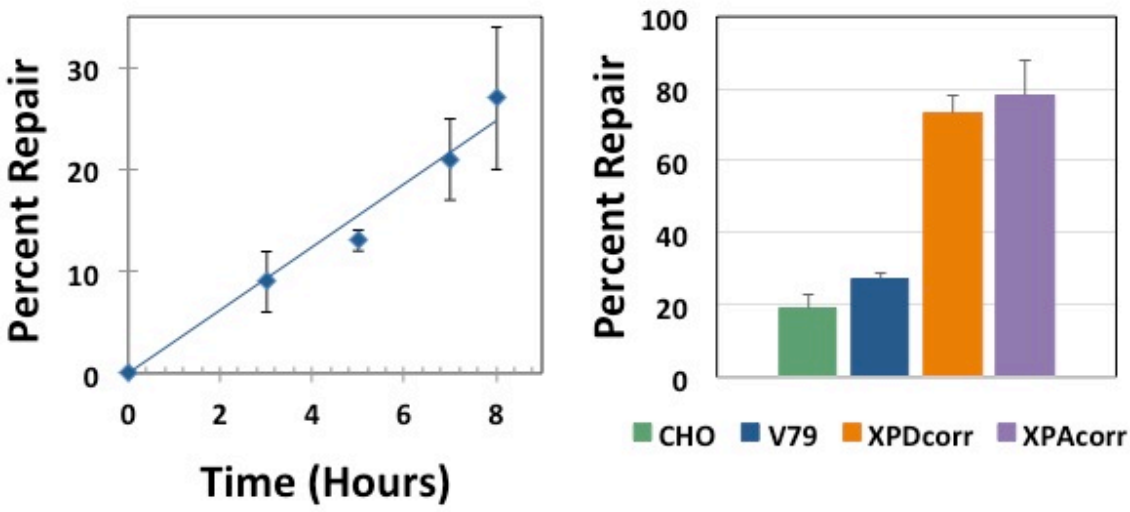

Figure 3.6: OGG1-DNA crosslink repair in wild-type cells. **Left**: Plasmid crosslinked to OGG1 was transfected into V79 cells *via* lipofection, low molecular weight DNA recovered 3, 5, 7, and 8 hours post-transfection, and repair assays performed as described above. The graph depicts mean percent repair, ± SEM, N=3. **Right:** Plasmid DNA containing an OGG1 crosslink was transfected into: Chinese hamster ovary (CHO-K1, green), Chinese hamster lung fibroblast (V79, blue), and human (XPDcorr, orange and XPAcorr, purple) cells, low molecular weight DNA recovered 8 hours post-transfection and repair assays performed as described above. Values depict mean percent repair, ± SEM, N=4.

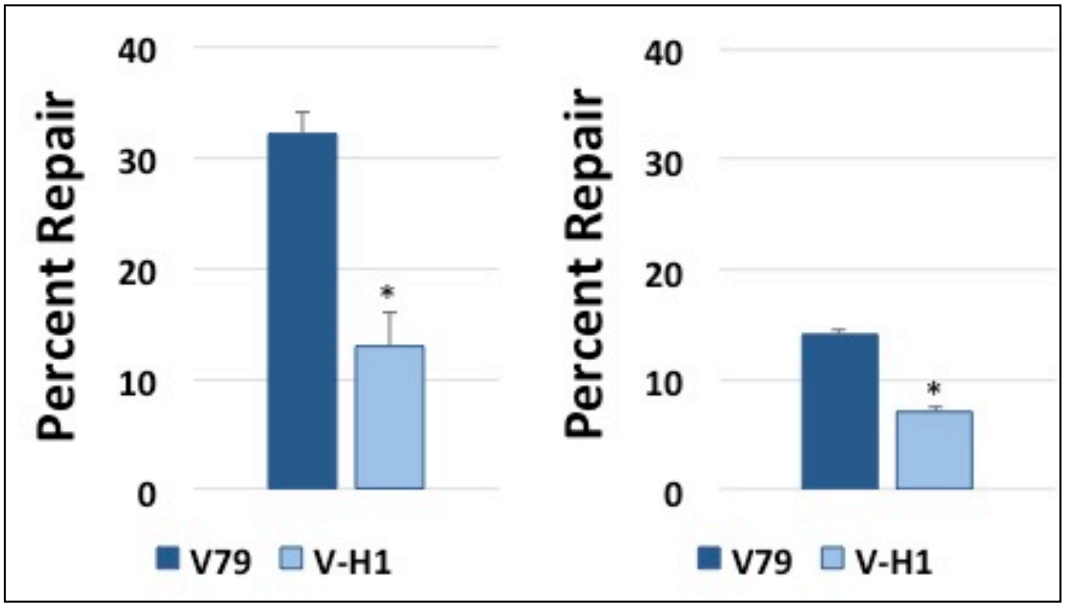

Figure 3.7: OGG1-DNA crosslinks are repaired more efficiently when present on a template strand than when present on a coding strand. Plasmid pLC119/pLC120 DNA substrates containing an OGG1 crosslink present on the template strand (**left**), or coding strand (**right**) of a transcriptional unit (construction described in Methods) were transfected into wild-type (V79, dark bars) and NER-deficient (V-H1, light bars) cells, and repair assays performed as described above. The graph depicts mean percent repair, ± SEM, N=3, *P < 0.05.

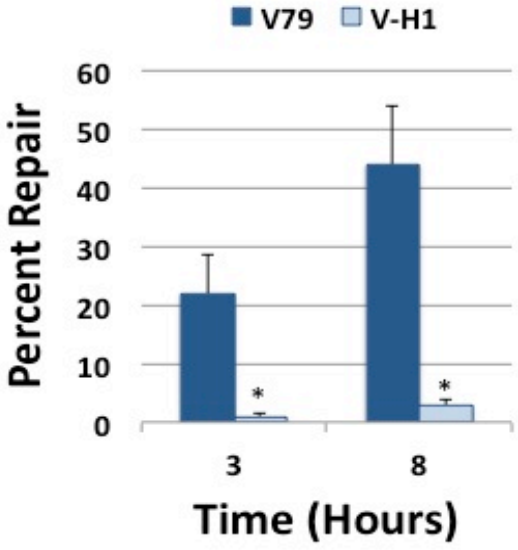

Figure 3.8: A DNA-peptide crosslink is repaired with reduced efficiency in NER-deficient Chinese hamster cells. Plasmid DNA containing a DNA-peptide crosslink (prepared as described in the Methods) was transfected into wild-type (V79, dark bars) or NER deficient (V-H1, light bars) Chinese hamster cells *via* lipofection, low molecular weight DNA recovered at 3 and 8 hours post-transfection, and repair assays performed as described above. The graph depicts mean percent repair, ± SEM, N=4, *P < 0.05.

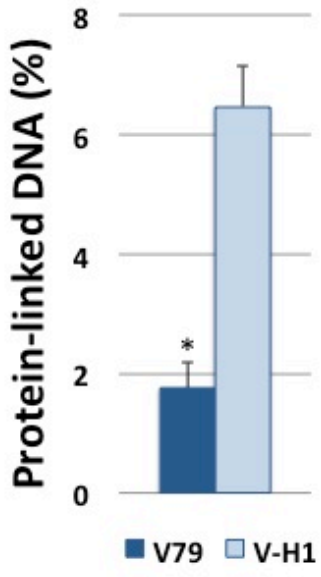

Figure 3.9: Cisplatin-induced DNA-protein crosslinks accumulate at elevated levels in NER-deficient Chinese hamster cells. Wild type (V79, dark bar) and NER-deficient (V-H1, light bar) Chinese hamster cells were exposed to 100 μM cisplatin for one hour in serum-free media, and levels of chromosomal DPCs determined. The graph depicts mean percent of protein-crosslinked DNA (calculated as described in the Methods), ± SEM, N=3, *P < 0.05.

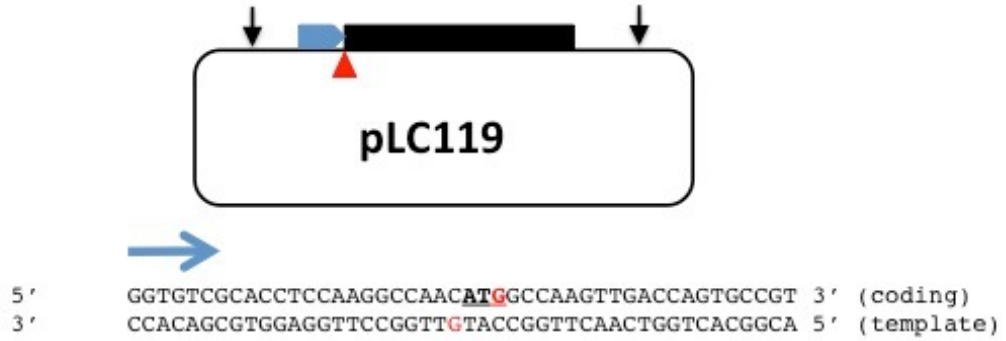

Supplemental Figure 3.1: Schematic of plasmid pLC119. The upper panel depicts plasmid pLC119, which was created by cloning a minigene comprised of the RSV promoter (blue box) and the coding region of the zeocin gene (black box) into pLC118 (see Methods for details). Black arrows indicate the *Eco*RI cloning sites and the red triangle indicates the location of the 8-oxo-guanine on the coding (pLC120) or template (pLC119) strands of the plasmid. The lower panel provides the sequence of attachment sites on the coding or template strands, with the blue arrow indicating the direction of transcription, the ATG site highlighted in bold, and the respective 8-oxo-guanine residues indicated in red.

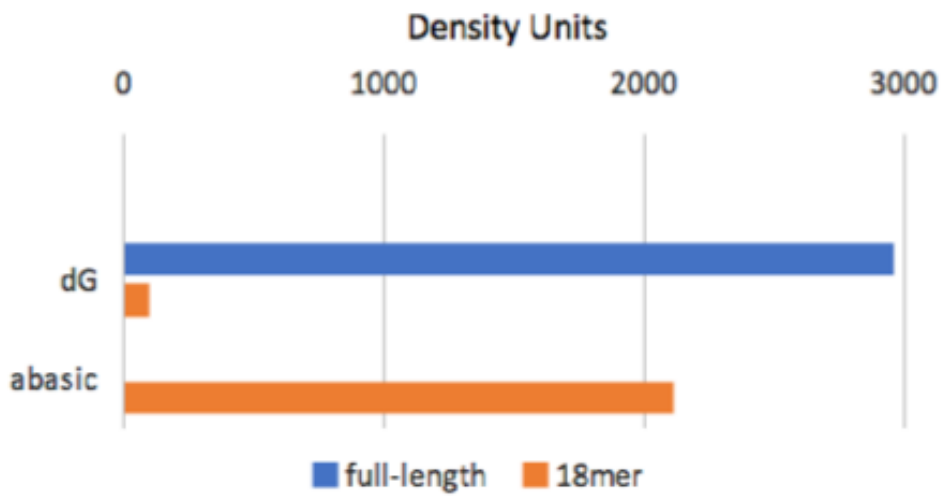

Supplemental Figure 3.2: An abasic site blocks Taq-mediated primer extension. Taq polymerase extension reactions were performed on 37-mer oligonucleotides containing either a deoxyguanine residue (dG) or an abasic site (abasic) annealed to a 12-mer complementary oligonucleotide. The primer extension reaction products were resolved by electrophoresis, stained with ethidium bromide and subject to scanning densitometry. The relative amount of full-length product (blue bars) and 18-mer product (orange bar, anticipated length of a primer extension terminated at the abasic site) was quantitated using image J (depicted with arbitrary 'density' units.

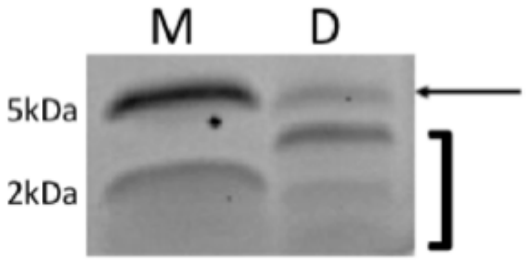

Supplemental Figure 3.3: Trypsin digestion of a DNA-OGG1 crosslink. OGG1 was crosslinked to duplex oligonucleotide, incubated overnight with trypsin, followed by a 30 minute treatment with DNASE 1, and resolved on a 16% Tris-Tricine gel, and stained with simply blue (see methods). Arrow refers to the 39mer peptide (~4.9 kDa) proteolysis product, corresponding to the OGG1 tryptic fragment that was crosslinked to DNA. Lanes: (M) Molecular weight markers (kDa) (D) OGG1 digest. Bracket indicates presence of additional OGG1 proteolysis fragments.

Chapter Four:

Homologous recombination of plasmids containing DNA-protein crosslinks in mammalian cells and mitochondria

Lisa N. Chesner[1], Maram Essawy[1*], Shaofei Ji[2#], Natalia Tretyakova[2], and Colin Campbell[1]

[1]Department of Pharmacology, University of Minnesota

[2]Department of Medicinal Chemistry, University of Minnesota

[*]ME was responsible for performing cytochrome c oxidase and BCA mitochondrial assays.

[#]SJ created oligonucleotides containing OGG1 and 11mer peptide crosslinks.

I. PREFACE

DNA-protein crosslinks (DPCs) are toxic lesions formed on nuclear and mitochondrial DNA. However, details of their repair mechanisms have yet to be fully elucidated. The work described below presents direct evidence for the role of homologous recombination (HR) in the repair of DPC-containing plasmids transfected into the nucleus and mitochondria of mammalian cells. Using a new strand-specific primer extension-qPCR assay, we have made the following observations. 1.) In the absence of the nucleotide excision repair pathway (NER), DPC-containing plasmids were repaired in the nucleus and mitochondria via HR. When compared to repair in the absence of a donor, DPC repair in the presence of a homologous donor increased two-fold in NER-deficient hamster cells (22% vs 11%) and five-fold in NER-deficient human cells (73% vs 14%). DPC-containing plasmids were not repaired in mitochondria unless a homologous donor plasmid was co-electroporated with the damaged substrate. This repair exhibited linear kinetics over time and increased two-fold when the DPC substrate harbored an adjacent DNA double-strand break. 2.) The RAD51 protein but not the RAD51D paralog is required for HR repair of DPC-containing plasmids in the nucleus and mitochondria. Pre-treatment of human cells with the RAD51 inhibitor B02 showed significantly decreased repair of DPC-containing plasmids in the nucleus (15% vs 59%) and mitochondria (0% vs 9%) while RAD51D knockout cells showed no difference in repair compared to wild-type. 3.) HR is not involved in the repair of smaller DNA-peptide crosslinks in the nucleus.

Inhibition of the RAD51 protein in human cells had no effect on the repair of a 4 kDa peptide crosslinked to plasmid DNA (28% vs 33%). 4.) The mitochondrial genome can be used as a donor for repairing homologous DPC-containing plasmids. DPCs crosslinked to a plasmid containing a 475bp insert homologous to the human mitochondrial genome were repaired when electroporated into mitochondria without a donor plasmid. Overall, this data extends previous observations of HR and NER in the repair of DPCs in the nucleus and provides new insight into DPC repair mechanisms in mammalian mitochondria.

II. INTRODUCTION

As explained in Chapter 1, DNA-protein crosslinks (DPCs) are toxic lesions formed by a variety of DNA-damaging agents[1,15,24]. These lesions are challenging to study due to their heterogeneous nature and induction with other types of DNA damage[3,8]. Several methods have been used to study their repair, including a new strand-specific primer extensions-quantitative polymerase chain reaction (SSPE-qPCR) assay described in Chapter 2[90]. Initial results using this SSPE-qPCR assay, confirmed a role for both the global genomic and transcription-coupled nucleotide excision repair (NER) pathway in the repair of DPC-containing plasmids transfected into mammalian cells[91]. However, other DNA repair pathways, such as homologous recombination (HR) and proteolysis, have been suggested to play a role in DPC repair[61,92,93,101]. To assess the role of HR, we co-transfected DPC-containing plasmids with an undamaged,

homologous donor into mammalian cells and calculated their repair using SSPE-qPCR. We also used this assay to measure differences in DPC repair in cells deficient in the protease Spartan and cells treated with the proteasome inhibitor lactacystin.

Mitochondrial DNA is also exposed to DNA-damaging agents and forms DPCs[209]. However, it is unknown how DPCs are repaired in the mitochondria. To gain insight into the mechanisms involved in mitochondrial DPC repair, we electroporated DPC-containing plasmids with and without a homologous donor into purified mitochondria and quantified repair using the SSPE-qPCR assay. Overall, results from these experiments provide strong evidence for the role of homologous recombination in the repair of DPCs in the nucleus and mitochondria.

III. MATERIALS AND METHODS

Materials

Chemicals and enzymes. Chemicals were purchased from Sigma Chemical (St. Louis, MO) unless otherwise indicated. Materials and enzymes needed for creation of 8-oxo-guanine and OGG1-containing plasmids and the SSPE-qPCR assay are the same used in Chesner and Campbell, *DNA Repair*, 2018.

Table 4.1. Oligodeoxynucleotides (ODNs) used is this study (5'→3').

ODN	Sequence	Use
7DG/5FC crosslinks	AGGGTTTTCCAGTCACGACGTT	Primer extension
EcoRI	CCGGGTACCGAGCTC(8oxodG)AATTCGTAATCT TGGTCATAGCTG	Primer extension
M13-mito	AGCCACCCCTCACCCACTA(8oxodG)GAT	Primer extension
M13-mito reverse	GGGATCTCATGCTGGAGTTC	SSPE-qPCR
M13-mito forward	AAGGGTGGGTAGGTTTGTTG	SSPE-qPCR

Cell lines. The human fibrosarcoma cell line HT1080 (CCL-121) were purchased from the American Type Culture Collection and human embryonic kidney cells expressing the large-T antigen (HEK293T) were a kind gift from Dr. Ashis Basu (University of Connecticut). Immortalized human dermal fibroblasts from xeroderma pigmentosum patients with inactivating mutations in the NER *XPD* gene (GM08207) were obtained from the Coriell institute. Human cells were cultured in Dulbecco's modified Eagle's media (Life Technologies, Grand Island, NY) supplemented with 9% fetal bovine serum. Chinese hamster AA8 knockout 51D1 cells were a kind gift from Professor Claudia Wiese (Colorado State University) in which the RAD51D gene was knocked out using a gene-targeting vector[210]. RAD51D is a paralog of RAD51 which contributes to the homologous recombination pathway in vertebrates[211]. These cells were cultured in alpha minimal essential medium (Life Technologies, Grand Island, NY). Chinese hamster lung fibroblast cell line V79 (GM16136) and V-H1 (GM16141) were obtained from the Coriell Institute for Medical Research (Camden, NJ) and

cultured in Ham's F-12 modified essential Eagle's media (Life Technologies, Grand Island, NY) supplemented with 9% fetal bovine serum (Atlanta Biologics, Atlanta, GA). V79 are wild-type cells from which the V-H1 clones were derived following an ethylnitrosourea-induced mutagenesis screen[198]. V-H1 cells belong to nucleotide excision repair complementation group 2 and lack a functional *XPD* gene. All cells were maintained in a humidified atmosphere of 5% carbon dioxide, 95% air, at 37°C.

Methods

Creation of DPC-containing substrates. DPC-containing oligonucleotides crosslinked via 7-deaza-guanine and 5-formyl-cytosine were created by Shaofei Ji (University of Minnesota) using reductive amination and oxime ligation[181,212]. These substrates were then annealed to single-stranded M13, extended, and purified as previously described[91]. All other damaged substrates were created according to Chesner and Campbell, *DNA Repair*, 2018.

Transfection of DPC-containing plasmids into cultured cells. DPC-containing plasmids were transfected into mammalian cells lines, recovered, and subjected to SSPE-qPCR as previously described[91]. Experiments involving the cotransfection of a homologous donor used 300 ng (3μL) of M13mp18 (New England Biolabs) for every 1.5 μg (15μL) of DPC-containing plasmid.

Cell treatment with the proteasome inhibitor lactacystin. Transfection of plasmids containing an 8-oxo-guanine residue, cholesterol lesion, or OGG1 crosslink were performed as previously described following treatment with the proteasome inhibitor lactacystin (10μM) for 3 hours at 37°C[91,194].

Treatment with B02 inhibitor. For experiments assessing DPC repair in the nucleus, prior to transfection, XPD cells were treated with 5μM of the RAD51 inhibitor B02 (Sigma) for 1 hour at 37°C[213]. For experiments assessing DPC repair in mitochondria, HEK293T cells were treated with 5μM of the RAD51 inhibitor B02 (Sigma) for 1 hour prior to mitochondria purification.

Purification of nuclei. Note: cells and reagents were kept cold or on ice at all times during purification. Eight 15cm dishes of wild-type Chinese hamster fibroblasts (V79) were grown to confluency, scraped with a rubber policeman into a 15mL conical tube, and spun down in a table-top centrifuge for 5 minutes at 1000 X G. Cells were washed twice with 5mL of 1X PBS and resuspended in 2mL of Buffer A (10mM Tris-HCl pH 7.4, 10mM $MgCl_2$, 10mM KCl, and 1mM DTT). Resuspended cells were then incubated on ice for 10-15 minutes and broken with 20 strokes of a dounce homogenizer and 'loose' pestle[214]. Broken cells were spun in a table-top microcentrifuge at 1150 x G for 8 minutes at 4°C and washed with 0.5mL of NIB-250 Buffer (15mM Tris-HCl pH 7.5, 60mM KCl, 15mM NaCl, 5mM $MgCl_2$, 1mM $CaCl_2$, 250mM sucrose, and 1mM DTT)[215]. The

resuspended pellet was then spun using the same conditions described above. The final nuclei pellet was resuspended in 800μL NIB-250 Buffer, divided in half, and mixed with 100ng of 8-oxo-guanine or DPC-containing plasmid. Samples were then transferred to a chilled, 4mm gap cuvette (Fisher Scientific, Waltham, MA) and electroporated using a ECM 630 Electro Cell Manipulator (BTX, Molliston, MA) at a field strength of 300V/cm, resistance of 25Ω, and 950μF capacitance. Following electroporation, samples were transferred to a microcentrifuge tube, spun down using the same conditions as above, and resuspended in 400μL Incubation Buffer (40mM Tris-HCl pH 7.4, 25mM NaCl, 5mM $MgCl_2$, 10% glycerol, 1mM pyruvate, 1mM ATP (Teknova), 1 mg/mL BSA (New England Biolabs), and 10μM dNTPs (Thermo Scientific))[216]. Nuclei were incubated in a 37°C water bath for 2 hours and lysed with 0.6% SDS/0.01M EDTA (final concentration) at room temperature for 12 minutes. Chromosomal DNA was then precipitated by adding NaCl to a 1M final concentration and incubated at 4°C overnight. The next day, samples were spun in a table-top microcentrifuge at 21130 X G for 30 minutes at 4°C. The supernatant was ethanol precipitated overnight at -20°C and resuspended in 50μL of water[66]. One microliter of this sample was used to calculate percent repair using SSPE-qPCR as previously described[90].

Mitochondria purification. Note: cells and reagents were kept cold or on ice at all times during purification. Hamster V79 or human HEK293T cells were grown to

confluency in four 15cm dishes and mitochondria purified as described in Yoon and Koob et al., *NAR*, 2003[216]. Cells were scraped into conical tubes and washed twice with 5mL of buffer containing 1mM Tris-HCl pH 7.0, 0.13M NaCl, 5mM KCl, and 7.5mM $MgCl_2$ in a table-top centrifuge at 1000 X G for 5 minutes at room temperature. The cell pellet was resuspended in half the cell volume with 0.1X incubation buffer (IB buffer) consisting of 4mM Tris-HCl pH 7.4, 2.5mM NaCl, and 0.5mM $MgCl_2$ and broken with 10 strokes of a dounce homogenizer. One-ninth the volume of the original cell pellet was then added of 10X IB buffer (400mM Tris-HCl pH 7.4, 250mM NaCl, and 50mM $MgCl_2$) to reach a final concentration of roughly 1X. This sample was then transferred to a microcentrifuge tube and spun in a table-top microcentrifuge at 376 x G for 5 minutes at 4°C. The supernatant was then transferred to a new tube and spun again to completely rid the sample of any unbroken cells and nuclei. To purify mitochondria, the supernatant was spun in a table-top microcentrifuge at 21130 X G for 10 minutes at 4°C. The mitochondria were then washed with 0.5mL of 1X IB buffer (40mM Tris-HCl pH 7.4, 25mM NaCl, and 5mM $MgCl_2$) and spun again using the same conditions stated above. Purified mitochondria were then resuspended in the respective buffer for the cytochrome c oxidase assay, bicinchoninic acid assay, or electroporation assay listed below.

Cytochrome c Oxidase Assay. One-hundred and forty micrograms of purified mitochondria (described above) from HEK293T cells was resuspended in 200μL

of 1X IB buffer (40mM Tris-HCl pH 7.4, 25mM NaCl, and 5mM $MgCl_2$) and split into two samples of 100μL each. These samples were then spun in a table-top microcentrifuge at 21130 X G for 10 minutes at 4°C. One sample was resuspended in 100μL of a lysis buffer containing 10mM Tris-HCl pH 7.4, 10mM $MgCl_2$, and 10mM KCl and the other in 100μL of 1X IB buffer. Both samples were incubated on ice for 1 hour. After the incubation period, 40μL of each sample was set aside to use for a bicinchoninic acid assay (see below). Fifty microliters of the remaining sample were resuspended in lysis buffer and used to confirm cytochrome c oxidase activity according the manufacturer's protocol (CYTOCOX1, Sigma-Aldrich). Thirty-three microliters of the remaining sample resuspended in 1X IB buffer was used to measure the outer membrane integrity of the mitochondria (CYTOCOX1, Sigma-Aldrich). Results from these experiments showed that 72% of purified mitochondria had intact outer membranes (N=3).

Bicinchoninic acid assay (BCA). Following resuspension in lysis buffer (see above), 40μL of the sample was diluted with another 40μL of lysis buffer. In contrast, samples saved in 1X IB buffer were spun in a table-top microcentrifuge at 21130 X G for 10 minutes at 4°C and resuspended in 80μL of water. Diluted albumin (BSA) standards were then prepared in lysis buffer or water according to the manufacturer's protocol (23225, Thermo Scientific) and 25μL of each diluted standard was added to a 96-well plate (3595, Costar) along with 25μL of each

sample in either lysis solution or water (loaded in triplicate). The protein concentration was determined according to the manufacturer's protocol (23225, Thermo Scientific).

Electroporation of purified mitochondria. The final mitochondria pellet was resuspended in 50μL 0.33M sucrose/10% glycerol and mixed with 100ng of an 8-oxo-guanine or DPC-containing plasmid (15μL) (see Chesner and Campbell, *DNA Repair*, 2018 for details). For co-electroporation experiments, 100ng of damaged DNA was mixed with 25ng (1μL) of undamaged M13mp18 (New England Biolabs, Beverly, MA) or 25ng (1μL) of pQe30 (Addgene). Note: 1μL of the DNA mixture was saved and diluted in 500μL of water to be used as a 'time 0' sample for SSPE-qPCR (see section below). Samples were then transferred to a chilled, 1mm gap cuvette (Fisher Scientific, Waltham, MA) and electroporated using a ECM 630 Electro Cell Manipulator (BTX, Molliston, MA) at a field strength of 1000V/cm, resistance of 400Ω, and 25μF capacitance. Following electroporation, cuvettes were rinsed with 100μL of 1X IB buffer + 10% glycerol (40mM Tris-HCl pH 7.4, 25mM NaCl, 5mM $MgCl_2$, and 10% glycerol). An additional 900μL of 1X IB buffer + 10% glycerol was then added, mixed, and spun in a table-top microcentrifuge at 21130 X G for 10 minutes at 4°C. The supernatant was then discarded and the pellet washed three times with 200μL of 1X IB buffer + 10% glycerol and spun at the same conditions described above. After the washes, the final pellet was reususpended in 50μL of a solution

containing 40mM Tris-HCl pH 7.4, 25mM NaCl, 5mM $MgCl_2$, 10% glycerol, 1mM pyruvate, 1mM ATP (Teknova), 1 mg/mL BSA (New England Biolabs), and 10μM dNTPs (Thermo Scientific) and incubated in a 37°C water bath for 1, 2, or 4 hours. Following incubation, samples were pelleted in a table-top microcentrifuge at 21130 X G for 10 minutes at 4°C. The supernatant was discarded and the pellet washed twice with 200μL of 1X IB buffer + 10% glycerol and spun at the same conditions described above[216].

To assess their integrity, mitochondria were resuspended in 200μL DNase buffer containing 66 units DNase (New England Biolabs), 10% glycerol, 10mM Tris-HCl pH 8, and 1mM $MgCl_2$ and incubated in a 37°C water bath for 30 minutes. Following incubation, samples were pelleted in a table-top microcentrifuge at 21130 X G for 10 minutes at 4°C. The supernatant was discarded and the pellet washed twice with 200μL of a washing buffer containing 10% glycerol, 10mM Tris-HCl pH 7.4, and 1mM EDTA and spun at the same conditions described above[216]. Experiments conducted with or without DNase showed no difference in repair of plasmids containing an 8-oxo-guanine modification (19% vs 20% repair). Thus, confirming that following electroporation, mitochondrial membranes were not “leaky” and any DNA that did not enter the mitochondria was eliminated during subsequent washing steps.

For all other experiments not utilizing DNase, mitochondria were resuspended in 300μL lysis buffer (0.5% SDS, 10mM Trish-HCl pH 7.4, 150mM NaCl, 1mM EDTA, and 100μg proteinase K (New England Biolabs)) and incubated in a 37°C water bath for 15 minutes. Samples were then mixed with 300μL of a 50:50 phenol:chloroform mixture. To create the 50:50 phenol:chloroform mixture, equal volumes of buffer-saturated phenol (Invitrogen) and chloroform (Acros) were mixed and spun in a table-top centrifuge at 1000 X G for 5 minutes at room temperature. The bottom layer of the mixture was then added to the sample, mixed, and spun in a table-top microcentrifuge at 21130 X G for 5 minutes at room temperature. The top layer was then transferred to a new microcentrifuge tube and ethanol precipitated using 18μL of 5M ammonium acetate (final concentration 0.3M), 12μL glycogen (Invitrogen, 60μg), 700μL of 100% ethanol, and precipitated at -20°C overnight[216].

Quantification of mitochondrial DPC repair. Precipitated samples were pelleted in a table-top microcentrifuge at 21130 X G for 10 minutes at 4°C, allowed to dry, and resuspended in 30μL of water. For experiments assessing the repair of the 8-oxo-guanine lesion, 15μL of sample was mixed with OGG1 (2pmol) in a buffer containing 100mM NaCl, 1mM $MgCl_2$, 20mM Tris-HCl pH 7.0, and water to reach a final volume of 30μL and incubated in a 37°C water bath for 30 minutes. One microliter of resuspended or OGG1-treated samples as well as ‘time 0’ samples

were then used to quantify repair using SSPE-qPCR (see Chesner and Campbell, *DNA Repair*, 2018 for details).

KCl/SDS precipitation of recovered DNA from mitochondria. Following resuspension of recovered DNA from mitochondria, water was added to reach a final volume of 40μL and then divided in two. One microliter of 10% SDS (final concentration 0.5%) was then added to one tube and omitted from the other and incubated at 65°C for 10 minutes in a heating block. Two microliters of 1M KCl (100mM final concentration) was then added to the sample containing SDS and omitted from the other. These samples were incubated on ice for 5 minutes and then spun in a table-top microcentrifuge at 21130 X G for 10 minutes at 4°C to precipitate any protein-bound DNA[66]. The supernatant (containing DNA not bound to protein) was then run on a 1% agarose gel at 60V for 2 hours, stained with ethidium bromide (0.5μg/mL) for 30 minutes, and destained in water for 30 minutes. Gels were imaged for 0.3 seconds on a Thermo Scientific myECL Imager and DNA bands quantified using ImageJ. ImageJ creates density histograms of each DNA band in order quantitate the amount of DNA present. Values generated by the program (arbitrary units) are then subtracted to obtain differences in intensity between samples treated with and without KCl/SDS **(Figure 4.7).** These differences were averaged from three different experiments in which DPC-containing plasmids were electroporated with a homologous or non-homologous donor and analyzed using a student t-test to assess

significance. Using this method, a greater difference in intensity between samples treated with and without KCl/SDS is associated with lower DPC repair. This is because unrepaired samples still crosslinked to protein will be precipitated by the KCl/SDS treatment resulting in a greater loss of DNA from the supernatant compared to repaired DNA (no longer containing a DPC) which will remain in solution.

KCl/SDS precipitation of mitochondrial DNA treated with cisplatin. Twenty 15cm dishes of HT1080 cells were grown to confluency. Five mL of a 5mM cisplatin stock was mixed with serum-free media in a total volume of 250mL. Growth media was then removed and replaced with 25mL of serum-free media with or without drug and incubated at 37°C for 3 hours. Following incubation, cells were washed with 5mL of 1X PBS, scrapped into conical tubes, and spun in a table-top centrifuge at 1000 X G for 5 minutes at room temperature. Cell pellets were then resuspended in 4mL isolation buffer (0.3M mannitol, 0.1% BSA, 0.2mM EDTA, and 10mM HEPES adjusted to a final pH of 7.4) and lysed in a glass dounce homogenizer (357542, Wheaton) for 5 strokes with the loose pestle and 5 strokes with the tight pestle. Samples were then divided into 1.5mL microcentrifuge tubes and spun at 1000 X G in a table-top microcentrifuge for 10 minutes at 4°C. The supernatant was transferred to a new tube and spun in a table-top microcentrifuge at 14000 x G for 15 minutes at 4°C to pellet the mitochondria[217]. Mitochondrial DNA was purified using alkaline lysis with SDS

and resuspended in 40μL TE (pH 8.0) containing 20μg/mL RNase A[203]. Each sample was then divided in half and subjected to KCl/SDS precipitation and quantification as described above.

Cloning of a 475bp human mitochondrial insert into M13mp18. A portion of the human mitochondrial genome was cloned into the plasmid backbone of pUCIDT-AMP (University of Minnesota's Genomic Center) and digested with *Kpn*1 and *Sac*1 for 2 hours in a 37°C water bath to excise a 475bp fragment. In parallel, a modified M13mp18 plasmid containing a kanamycin resistance gene (see Chesner and Campbell, *DNA Repair*, 2018 for details) was linearized using the same conditions and run on a 0.8% low-melt agarose gel. Digestion products were excised with a razor blade and ligated at a 1:5 vector to insert ratio overnight at 16°C. The next day, 1μL of the ligation mixture was transformed into NEB Turbo electrocompetent bacteria (New England Biolabs) and plated on LB agar plates with kanamycin (50μg/mL). Individual clones containing the mitochondrial insert were screened by restriction digest of double-stranded DNA. Single-stranded virion DNA was subsequently purified, primer extended with an 8-oxo-guanine-containing oligonucleotide **(Table 4.1),** and crosslinked as described in Chesner and Campbell, *DNA Repair*, 2018. Crosslinked plasmids containing the human mitochondrial insert (M13-Kan-Mito) were electroporated into purified mitochondria from the HEK293T cells, as described above, without a donor plasmid and repair quantified after 2 hours using SSPE-qPCR.

IV. RESULTS

DPC-containing plasmids are repaired by the NER pathway.

One of the advantages of the SSPE-qPCR assay is its ability to assess the repair of a variety of lesions on plasmid DNA. We first assessed the repair of DPC-containing plasmids using SSPE-qPCR by trapping the repair protein human oxoguanine glycosylase (OGG1) to the deoxyribose backbone and saw significantly decreased repair in NER-deficient cells (27% vs 3%, **Table 3.2**). We next wanted to test the hypothesis that lesions attached to the DNA base are also repaired by the NER pathway. To do this, the OGG1 protein was crosslinked to a guanine or cytosine base on an oligonucleotide complementary to M13mp18 (see Methods for details). This DPC-containing oligonucleotide was then phosphorylated, annealed, extended, and purified as previously described[91]. Following transfection into wild-type (V79) and NER-deficient (V-H1) Chinese hamster fibroblasts, DPC-containing plasmids attached to the guanine base were 34% repaired by 8 hours in V79 cells compared to 10% in V-H1 cells. Interestingly, DPCs attached to cytosine were not as efficiently repaired in neither V79 cells (10%) nor V-H1 cells (5%), suggesting that chemical linkage can influence repair of DPCs **(Figure 4.1).**

Previously, we reported that smaller DNA-peptide crosslinks were repaired more efficiently than larger DNA-protein crosslinks in wild-type cells and that their repair was also dependent on the NER pathway[91]. To assess repair of DNA-peptide crosslinks attached to a nucleotide base, an 11mer peptide synthesized

from the substance P protein was crosslinked to the N7 position of guanine on an oligonucleotide and extended onto single-stranded DNA as described above. These DNA-peptide crosslinks were 57% repaired by 8 hours in V79 cells and 26% repaired in V-H1 cells after 8 hours **(Figure 4.1).** These results confirm the hypothesis that plasmids containing smaller DNA-peptide crosslinks attached to the nucleotide base are also more efficiently repaired in wild-type cells and are substrates for repair via the NER pathway. Interestingly, background levels of DPC repair in NER-deficient cells were much higher compared to DPCs attached to the deoxyribose backbone. Therefore, we hypothesize that another DNA repair pathway may be able to repair lesions attached to the DNA base that is not able to remove DPCs attached to the backbone.

The protease Spartan (and not the proteasome) is involved in repair of DPC-containing plasmids.

Previous investigators have provided evidence for the role of the protease Spartan in DPC repair[6,96,176]. However, there is conflicting data regarding the involvement of the proteasome in the degradation of larger DPCs prior to repair[87,92]. To investigate the role of the proteasome in the repair of DPC-containing plasmids using the SSPE-qPCR assay, wild-type Chinese hamster (V79) cells were pretreated with the proteasome inhibitor lactacystin (10μM) for 3 hours prior to transfection with damaged substrates. After 8 hours, plasmids containing an 8-oxo-guanine lesion showed negligible repair (1% higher) in drug

treated cells compared to untreated. Repair of a cholesterol lesion was significantly reduced in drug-treated cells (35% decrease) while DPC repair was slightly higher in cells treated with the inhibitor compared to untreated (19% increase, **Figure 4.2**). Previous investigators have shown that cholesterol lesions are repaired by the NER pathway in mammalian cells[91,182]. Therefore, we were not surprised to see that proteasome inhibition interfered with the NER repair of the cholesterol lesion[46,218,219]. Additionally, our results showed no decrease in repair of DPC-containing plasmids in the presence of a proteasome inhibitor. Suggesting that another protease (besides the proteasome) is involved in the repair of this particular lesion.

Xenopus egg extracts have commonly been used to study the role of the protease Spartan in DPC repair[94]. However, Spartan knockouts are embryonically lethal[208]. Therefore, we used mouse embryonic fibroblasts hemizygous for the Spartan gene to assess its role in the repair of DPC-containing plasmids using SSPE-qPCR[220]. Results from these experiments showed 50% repair of DPC-containing plasmids in both wild-type (MEF) and mutated (MEF7) cells after 3 hours. However, DPC repair in mutants were decreased (59%) compared to wild-type (93%) 8 hours post-transfection **(Figure 4.2).** These results support the hypothesis that hemizygous clones are not able to repair DPC-containing plasmids as efficiently as wild-type cells due to decreased levels of Spartan production, illustrating Spartan's role in DPC repair.

DPCs are repaired *via* homologous recombination in the nucleus of NER-deficient mammalian cells.

Previous experiments performed in bacteria have shown that clones deficient in the NER and HR pathways are hypersensitive to DPC-inducing agents[61]. However, hypersensitivity assays performed in yeast, only indicated a role for the NER pathway while the involvement of the HR pathway in mammalian cells remains unclear[60]. To assess the role of HR in DPC repair using SSPE-qPCR, OGG1-containing plasmids attached to an abasic site were transfected into mammalian cells in the presence of a homologous donor (undamaged M13mp18 plasmid) or a non-homologous donor (pQe30 plasmid). In NER-deficient hamster (V-H1) and human (XPD) cells, DPCs cotransfected with a homologous donor showed significantly increased repair (22% and 73%, respectively) compared to lesions cotransfected with a nonhomologous donor (11% and 14%, respectively). Interestingly, wild-type (V79) cells showed no difference in DPC repair with or without a homologous donor **(Figure 4.3)**. These results support the hypothesis that homologous recombination of DPC-containing plasmids only occurs in the absence of the NER pathway.

Nuclear homologous recombination of DPC-containing plasmids is dependent on the RAD51 protein.

During homologous recombination, 5' ends of DNA are chewed back by nucleases to create 3' overhangs of single-stranded DNA. This single-stranded

DNA is initially coated by the RPA (DNA replication protein A) protein and activates the ATR response (Ataxia Telangiectasia and Rad3-related protein). A RAD51 nucleofilament is then assembled and replaces the RPA coat to begin its search for homology[211]. To confirm the involvement of the HR pathway in the repair of DPC-containing plasmids, NER-deficient human cells (XPD) were pretreated with a RAD51 inhibitor (B02) prior to transfection[213]. We hypothesized that inhibition of the RAD51 protein would block HR repair and show no increase in repair in the presence of a homologous donor. OGG1-linked plasmids showed significantly decreased repair in B02-treated cells (15%) compared to non-drug treated cells (59%) after 3 hours **(Figure 4.4).** However, DNA-peptide crosslinks formed by degrading OGG1-crosslinks with trypsin (see Chesner and Campbell, *DNA Repair*, 2018 for details) showed no difference in repair between drug-treated and non-treated cells. This result is consistent with previous observations from Ide et al. that HR is only involved in the repair of larger DNA-protein crosslinks[92]. However, it is still unclear which repair pathway is responsible for the background levels of repair that occur in the absence of both the NER and HR pathways. Lead candidates include other double-strand break repair pathways such as non-homologous end-joining (NHEJ) and micro-mediated end-joining repair (MMEJ)[49].

Homologous recombination of DPC-containing plasmids is not dependent on the RAD51D protein in the nucleus.

There are multiple paralogs of the RAD51 protein expressed in invertebrates including RAD51B, RAD51C, RAD51D, XRCC2, and XRCC3[221]. To further characterize the involvement of these paralogs in homologous recombination of DPC-containing plasmids, we performed experiments in Chinese hamster ovarian cells deficient in the RAD51D gene[210]. We hypothesized, that cells deficient in the RAD51D gene would not show increased repair of DPC-containing plasmids in the presence of a homologous donor. However, both wild-type (19% vs 33%) and mutated cells (27% vs 47%) showed increased DPC repair in the presence of a homologous donor **(Figure 4.5).** Together with the data presented above, these results support the interpretation that the RAD51 gene but not the RAD51D paralog is essential for homologous recombination of DPC-containing plasmids in the nucleus of mammalian cells.

Repair of DPC-containing plasmids in purified nuclei.

The reagent lipofectamine used in the experiments above is a cationic agent which relies on endocytosis to take up plasmid DNA and deliver it to the nucleus[222]. Since proteolysis is hypothesized to be involved in repair of larger protein crosslinks, we wanted to rule out the possibility that proteolytic or nucleolytic processing during endocytosis could influence DPC repair results. Purified nuclei from wild-type hamster cells (V79) were electroporated with

plasmids containing an 8-oxo-guanine or DPC lesion and repair quantified using SSPE-qPCR. Results from these experiments showed 29% repair of 8-oxo-guanine lesions and 31% repair of DPCs **(Figure 4.6).** As shown, in **Figure 4.3**, DPC-containing lesions were ~30% repaired in V79 cells 8 hours post-transfection. These results confirm that repair of DPC-containing plasmids occurs to a similar extent when electroporated directly into purified nuclei or transfected into intact mammalian cells. Thus, any alterations to the damaged substrate during endocytosis are most likely not a factor in repair.

Above we have presented evidence for the NER and HR pathway in the repair of DPC-containing plasmids in mammalian cells using the SSPE-qPCR assay. However, the mitochondrial genome is also exposed to DPC-inducing agents such as chemotherapeutics and ionizing radiation[223,224]. Surprisingly, little work as has been done to study repair of these lesions in the mitochondria[225]. Since it has been shown that the NER pathway is not present in the mitochondria, we hypothesized that DPCs would be repaired via homologous recombination and that we could quantify the repair using the SSPE-qPCR assay[127]. First, we confirmed that DPCs form on mitochondrial DNA following exposure to the chemotherapeutic cisplatin in human cells.

Treatment of human cells with cisplatin results in higher formation of DPCs.

Human HT1080 cells were treated with or without 100μM cisplatin for 3 hours and mitochondrial DNA purified as described above. KCl/SDS precipitation is a common assay that has been used to quantify DPCs following exposure to a DPC-forming agent[66]. The SDS binds to the protein and, following the addition of KCl, is precipitated out of solution, pulling down any DNA crosslinked to protein. The DNA is then run on a gel and quantified using scanning densitometry to calculate differences between DNA treated or not treated with KCl/SDS. DNA containing a higher number of protein crosslinks will show a larger difference between KCl/SDS treated and nontreated samples. Results from these experiments showed that cells treated with cisplatin showed a significantly larger difference between samples treated or not treated with KCl/SDS than cells not treated with drug. These results support the conclusion that cisplatin-induced DPCs significantly accumulate in mitochondrial DNA **(Figure 4.7).**

DPC-containing plasmids are repaired *via* homologous recombination in mitochondria.

To test the hypothesis that DPCs are repaired *via* homologous recombination in mitochondria, we electroporated DPC-containing plasmids with a non-homologous (qQe30) or homologous donor (M13) into mitochondria purified from wild-type hamster (V79) and human (HEK293T) cells. The mitochondria were

then incubated for 2 hours in a 37°C water bath in the presence of pyruvate, ATP, BSA, and dNTPs for 2 hours, lysed, and repair quantified using SSPE-qPCR. Since it has been shown that mitochondria lack the NER machinery, we predicted that damaged substrates electroporated with pQe30 would not be repaired, while those electroporated with M13 would be repaired *via* homologous recombination. As predicted, neither hamster nor human cells repaired DPC-containing plasmids electroporated with pQe30. However, substrates electroporated with M13 were 11% repaired in hamster cells and 9% repaired in human mitochondria after 2 hours **(Figure 4.8).** To assess the repair kinetics of these plasmids, we performed a time course in which mitochondria recovered for 1, 2, or 4 hours prior to quantification *via* SSPE-qPCR. These results indicated that repair occurred at a near-linear rate over time. Finally, as another confirmation of DPC repair, plasmid DNA recovered from mitochondria was treated with or without KCl/SDS and run on a gel to quantify DNA using scanning densitometry. Plasmid DNA co-electroporated with pQe30 showed a significant difference in DNA intensity between samples treated with or without KCl/SDS whereas samples co-electroporated with M13 showed no significant difference in DNA intensity **(Figure 4.8).** These results support the conclusion that DPC-containing plasmids co-electroporated with M13 were not precipitated out of solution because they were repaired *via* homologous recombination. Overall, these results provide strong evidence for the repair of DPC-containing plasmids *via* homologous recombination in mammalian mitochondria.

Double-strand break-mediated homologous recombination of DPCs in the mitochondria is dependent on the RAD51 (but not the RAD51D) gene.

It is known that meiotic homologous recombination is proceeded by the formation of a double-strand break[58]. Assays examining interchromosomal and intrachromosomal homologous recombination as well as HR on plasmids has been shown to be stimulated by a double-strand break[226-228]. Initiation of homologous recombination has also been shown by targeting double-strand breaks to specific loci using the restriction endonuclease I-*Sce1*[229,230]. Therefore, we hypothesized that creation of a double-strand break at the crosslinking site of the DPC would increase repair. To test this hypothesis, DPCs crosslinked to the *Eco*RI recognition site of the plasmid **(Table 4.1)** were digested with the restriction enzyme *Eco*RI prior to co-electroporation into mitochondria with a homologous donor. As predicted, the presence of a double-strand break facilitated DPC repair, showing a twofold increase in repair after 2 hours (22% in hamster cells and 16% in human cells, **Figure 4.9**).

One of the key steps in homologous recombination is the synthesis of a new DNA strand, requiring the use of deoxynucleotide triphosphates (dNTPs)[231]. To test whether the absence of dNTPs would inhibit mitochondrial DPC repair, we incubated electroporated mitochondria without dNTPs. Even when co-electroporated with a homologous donor, DPC-containing plasmids were not able to be repaired in the absence of dNTPs. Thus confirming that DNA synthesis is an essential process in repairing these damaged substrates.

To test another step in the homologous recombination pathway, we pre-treated human cells with the RAD51 inhibitor B02 prior to mitochondria purification. RAD51 is a key gene that facilitates the search and invasion of a homologous donor during repair[210]. We predicted that without this gene, HR repair of the DPC-containing plasmids would not occur. Interestingly, cells treated with the RAD51 inhibitor showed no DPC repair while Chinese hamster cells deficient in the RAD51D gene were able to repair the damage **(Figure 4.9).** These results demonstrate that the RAD51 (but not the RAD51D paralog) gene is essential in HR repair of DPC-containing plasmids in the mitochondria.

The mitochondrial genome can be used as a donor to repair DPC-containing plasmids.

As shown above, DPC-containing plasmids are only repaired in mitochondria when co-electroporated with a homologous donor plasmid. Therefore, we wanted to test the hypothesis that the mitochondrial genome could be used as a homologous donor for DPC repair. To do this, a 475bp sequence from the human mitochondrial genome was cloned into a plasmid and crosslinked with the OGG1 protein. This plasmid was then electroporated into human mitochondria and repair quantified after 2 hours using SSPE-qPCR. To ensure that the primers used for the SSPE-qPCR do not amplify the mitochondrial genome, one primer was complementary to the mitochondria insert (forward, **Table 4.1**) while the other (reverse, **Table 4.1**) was complementary to the M13 portion of the plasmid.

Results from these experiments showed 17% repair of DPC-containing plasmids after 2 hours **(Figure 4.10).** Thus, confirming the hypothesis that the mitochondrial genome could be used as a donor for repair of DPC-containing plasmids.

V. DISCUSSION

Data presented above confirms and extends observations that both nucleotide excision repair and homologous recombination play a role in DPC repair. **First,** we have extended our previous work and shown that NER is capable of repairing proteins and peptides crosslinked to plasmid DNA *via* a variety of chemical crosslinks. Our past work showed a significant decrease in the repair of the OGG1 protein crosslinked to an abasic site in NER-deficient cells. However, proteins can be attached to DNA via multiple linkages[89]. Therefore, we synthesized three oligonucleotides containing OGG1 crosslinked to the N7 position of guanine or the 5formyl position of cytosine as well as an 11mer peptide crosslinked to the N7 position of guanine to directly compare differences in repair. Results from these experiments confirmed that both types of crosslinks were substrates for the NER pathway and that DNA-peptide crosslinks were repaired more efficiently than larger DNA-protein crosslinks in wild-type cells. Interestingly, repair of these adducts in NER-deficient hamster cells was higher than previously seen using crosslinks attached to an abasic site on DNA. These results could indicate that proteins attached to the nucleotide base may be

substrates for other repair pathways such as non-homologous end-joining and micro-mediated end-joining. Additionally, repair of OGG1 crosslinked to 5formyl cytosine was significantly decreased in wild-type hamster cells compared to lesions attached to the N7 guanine position. Thus suggesting that some lesions are repaired more efficiently than others and that the nature of the chemical crosslink influences DPC repair.

Second, we utilized SSPE-qPCR to examine the role of HR in nuclear DPC repair. Other investigators have used hypersensitivity assays with mutants from bacteria, yeast, and mammalian cells to show a role for homologous recombination in the repair of DNA-protein crosslinks[61,62,232]. However, DPC-forming agents such as formaldehyde induce other types of damage besides DPCs[233]. Studies performed in *E. coli* have proposed a size limit for repair of DPCs by the NER pathway and suggested that DPCs larger than 10 kDa are repaired via HR[2,92]. Other models using *Xenopus* egg extracts have proposed that larger DNA-protein crosslinks are proteolyzed into smaller adducts and then bypassed by the replication machinery during translesion synthesis[101]. To gain a better understanding of the role of homologous recombination in mammalian cells, we co-transfected OGG1-linked plasmids with a homologous donor into NER-deficient hamster and human cells and studied their repair using SSPE-qPCR. One advantage of using this assay to study HR, is that intermediates such as proteolyzed DNA-peptide crosslinks or double-strand breaks will block the Taq polymerase during strand extension, ensuring that proteolysis or translesion

synthesis are not quantified as repair events. Results from these experiments showed significantly increased repair of DPCs *via* HR in NER-deficient cells. We also predicted that providing a homologous donor for repair of these DPC-containing plasmids in wild-type cells would increase repair. Interestingly, wild-type cells co-transfected with a damaged substrate and donor plasmid did not show an increase in DPC repair. These results suggest that normal cells rely on the NER pathway as a primary mechanism to repair these lesions and that HR only occurs in the absence of the NER pathway. It would be interesting to investigate, in future experiments, how DPCs are repaired in cells deficient in both the NER and HR pathways.

Third, we confirmed the role of nuclear HR in repair of DPC-containing plasmids by pre-treating NER-deficient cells with a RAD51 inhibitor prior to transfection. We predicted that inhibition an essential HR protein would prevent DPC repair. Results from these experiments showed that repair of DPC-containing plasmids was significantly decreased in cells treated with the RAD51 inhibitor. Next, we examined nuclear DPC-repair in the absence of a RAD51 paralog. RAD51 paralogs form 2 distinct complexes: RAD51B-RAD51C-RAD51D-XRCC2 (BCDX2) and RAD51C-XRCC3 (CX3)[234]. SiRNA studies of the RAD51 paralogs have indicated a role for the BCDX2 complex in the recruitment of RAD51 to Isce1-induced double-strand breaks[235]. Therefore, we predicted hamster cells deficient in the RAD51D paralog would inhibit the recruitment of RAD51 and prevent DPC repair via HR. However, RAD51D KO cells showed no

difference in the repair of DPC-containing plasmids compared to wild-type in the presence of a homologous donor. It is known that HR can also occur *via* a RAD52-mediated pathway[236]. Therefore, future studies will examine the role of other RAD51 paralogs as well as inhibition of the RAD52 protein in the repair of DPC-containing plasmids. Another interesting observation from these studies was that pretreatment of cells with a RAD51 inhibitor showed no difference in repair of DNA-peptide crosslinks compared to untreated. Although these results are consistent with previous observations that HR is involved in the repair of DPCs larger than 10 kDa, it is unclear how these DNA-peptide crosslinks are repaired in the absence of NER[92]. Future studies will examine other double-strand break repair pathways such as non-homologous end-joining (NHEJ) by pre-treating cells with a protein kinase inhibitor prior to transfection.

The data presented above convincingly demonstrates nuclear repair of DPC-containing plasmids *via* HR in the absence of the NER pathway. Since mitochondria have been shown to lack the NER pathway, it seemed obvious to hypothesize that repair of these lesions in mitochondria would also involve the HR pathway. **Finally,** we used SSPE-qPCR to investigate the role of HR in repair of DPC-containing plasmids electroporated into purified mitochondria.

DPC formation is known to occur in mitochondria following exposure to crosslinking agents such as formaldehyde and oxidative processes[237]. However, until now, no mechanism has been proposed for their repair. In fact, Borisov et al. saw no decrease in mitochondrial DPC accumulation over time in the brain and

spleen of rats following exposure to radiation and suggested that mitochondria are not capable of repairing DPCs[238]. However, results from the experiments above indicate that DPC-containing plasmids electroporated into mitochondria are repaired in the presence of a homologous donor plasmid or a homologous portion of the mitochondrial genome. Further characterization of HR repair in the mitochondria was reflective of results obtained in the nucleus. Homologous recombination of DPC-containing plasmids was prevented in the presence of a RAD51 inhibitor but was still able to occur in the mitochondria of RAD51D-deficient cells.

As discussed above, homologous recombination is stimulated by the formation of double-strand breaks[239]. Therefore, we hypothesized that DPCs created at the site of a double-strand break, would show higher amounts of repair. As predicted, plasmids cut with a restriction enzyme at the crosslinking site showed increased HR repair. Finally, we confirmed that HR repair of DPC-containing plasmids involved strand synthesis by incubating electroporated mitochondria in the absence of dNTPs. Results from these experiments showed that DPC repair was not able to occur without dNTPs, indicating that DNA synthesis is required for HR repair of these plasmids.

Other models of DPC repair such as proteolysis have yet to be investigated in the mitochondria. It would also be interesting to assess the repair efficiency of other types of crosslinks (i.e. proteins crosslinked to the nucleotide base) to gain a greater understanding of DPC repair mechanisms in the

mitochondria. Insight into these pathways can ultimately provide new avenues for cancer treatments. For example, work done by Shauna Kelly's group has shown that targeting the topoisomerase II inhibitor doxorubicin to mitochondria is toxic to drug-resistant cancer cells,[240] indicating a role for mitochondria-targeting DPC-forming drugs in the treatment of cancer[158,241,242].

Overall, the work above details initial observations of DPC repair *via* HR. However, this system can be further exploited to gain a greater understanding of HR repair mechanisms in the mitochondria and the repair of other lesions such as double-strand breaks. Thus far, indirect evidence has been given for the NHEJ and HR double-strand break repair pathways in mitochondria [138,243]. Further work using the method described above could provide a more detailed mechanism of these processes in mitochondria. For example, capture experiments of biotin-labeled oligonucleotides could be used to pull-down repair intermediates and identify repair proteins recruited to the lesion. Taken together, this work is the first to provide convincing evidence for homologous recombinational repair of DPC-containing plasmids in the nucleus and mitochondria using a new SSPE-qPCR assay.

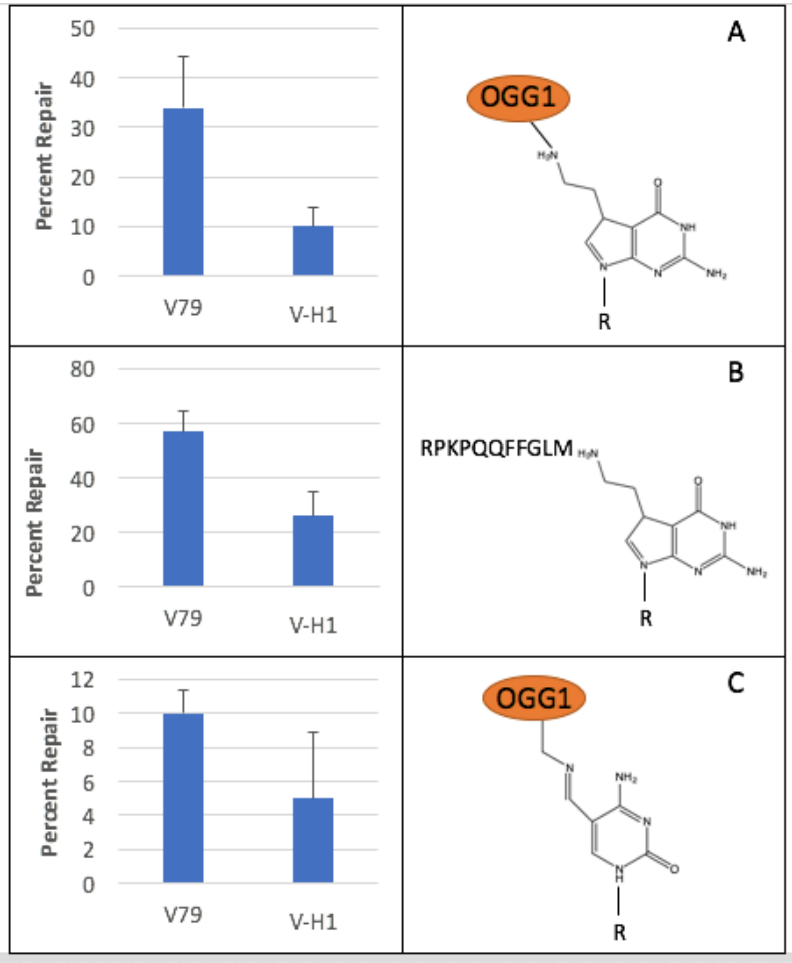

Figure 4.1: Decreased repair of DPC-containing plasmids in NER-deficient hamster cells. Plasmids containing the OGG1 protein crosslinked to a 7-deaza-guanine residue (A), 11-mer peptide crosslinked to a 7-deaza-guanine residue (B) or OGG1 protein crosslinked to a 5-formyl-cytosine residue were transfected into wild-type Chinese hamster lung fibroblasts (V79) or isogenic NER-deficient cells (V-H1). Cells recovered for 8 hours, were lysed, and repair quantified using SSPE-qPCR (see methods for details). Values depict mean percent repair ± SEM, N=3.

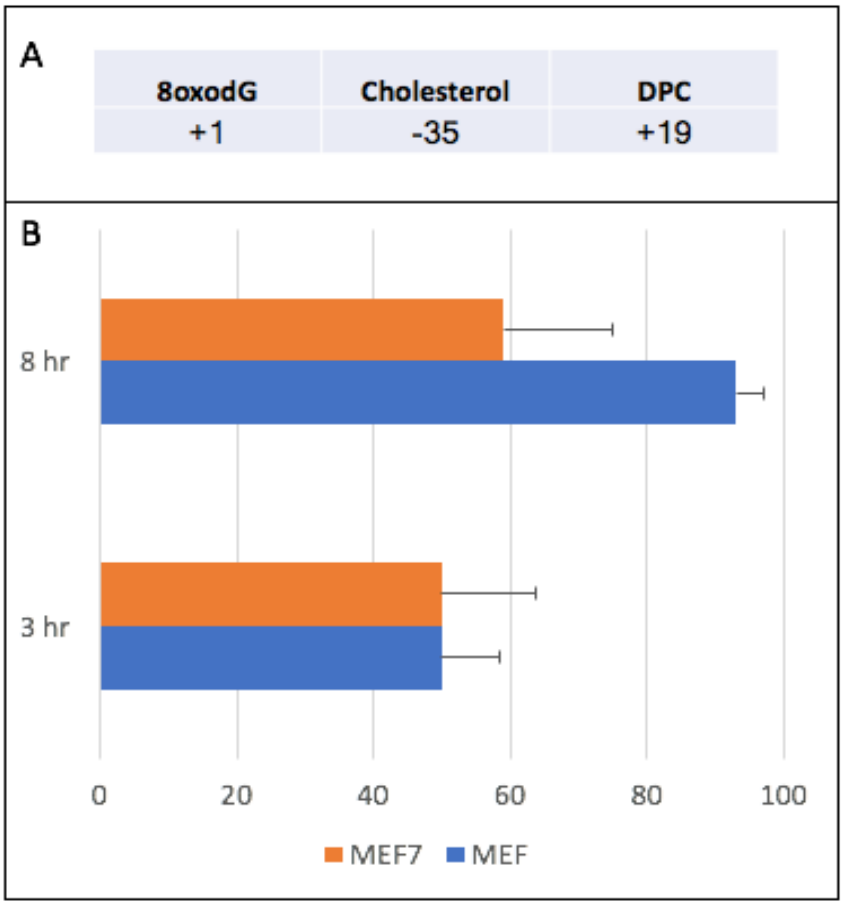

Figure 4.2: DPC repair is dependent on the protease Spartan and not the proteasome. A: Wild-type Chinese hamster (V79) cells were or were not incubated in the presence of the proteasome inhibitor lactacystin (10μM) for 3 hours prior to the transfection of damaged substrates. Values given indicate the difference in percent repair (calculated using SSPE-qPCR) between cells treated or not treated with drug. **B:** Wild-type mouse embryonic fibroblasts (MEF) and hemizygous clones (MEF7) deficient in the protease Spartan were transfected with DPC-containing plasmids and repair calculated using SSPE-qPCR at 3 and 8 hours. Values depict mean percent repair ± SEM, N=3.

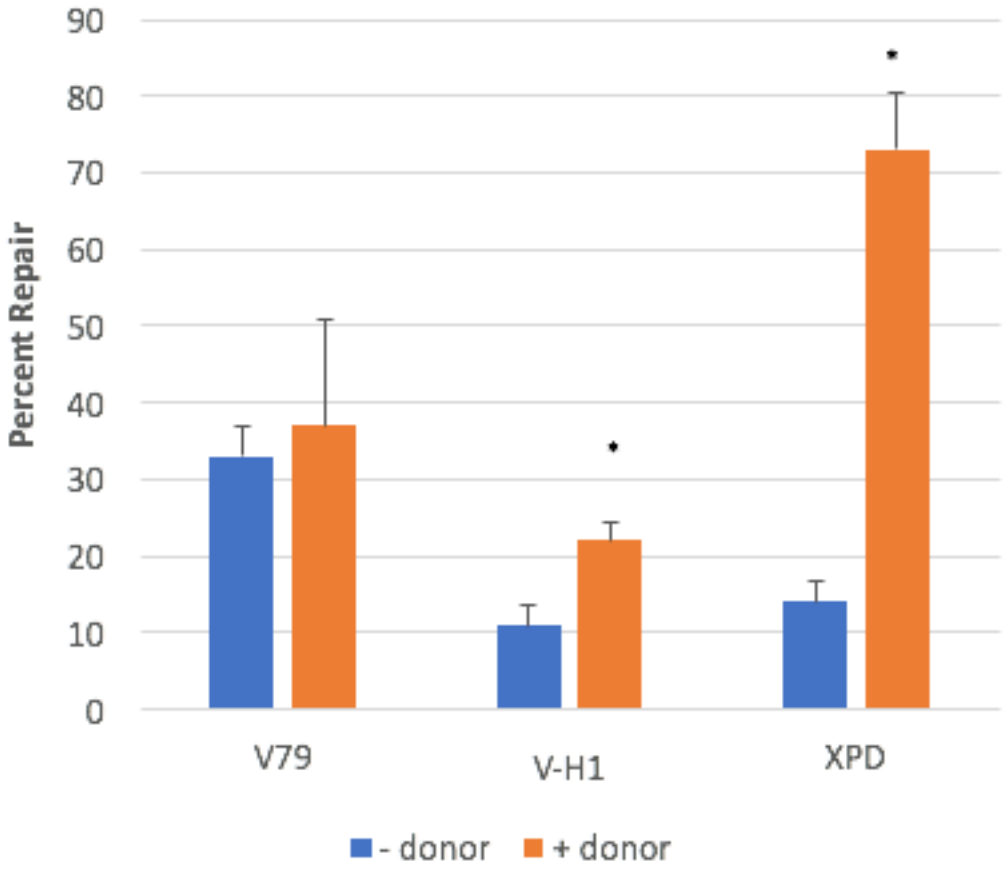

Figure 4.3: Increased repair of DPC-containing plasmids crosslinked to the deoxyribose in NER-deficient cells with a homologous donor. OGG1-containing plasmids were co-transfected with either a homologous (+ donor) or non-homologous donor (- donor) into hamster (V79 and V-H1) or human (XPD) cells. Cells recovered for 8 hours, were lysed, and repair quantified using SSPE-qPCR (see methods for details). Values depict mean percent repair ± SEM, N=3, $p<0.05$.

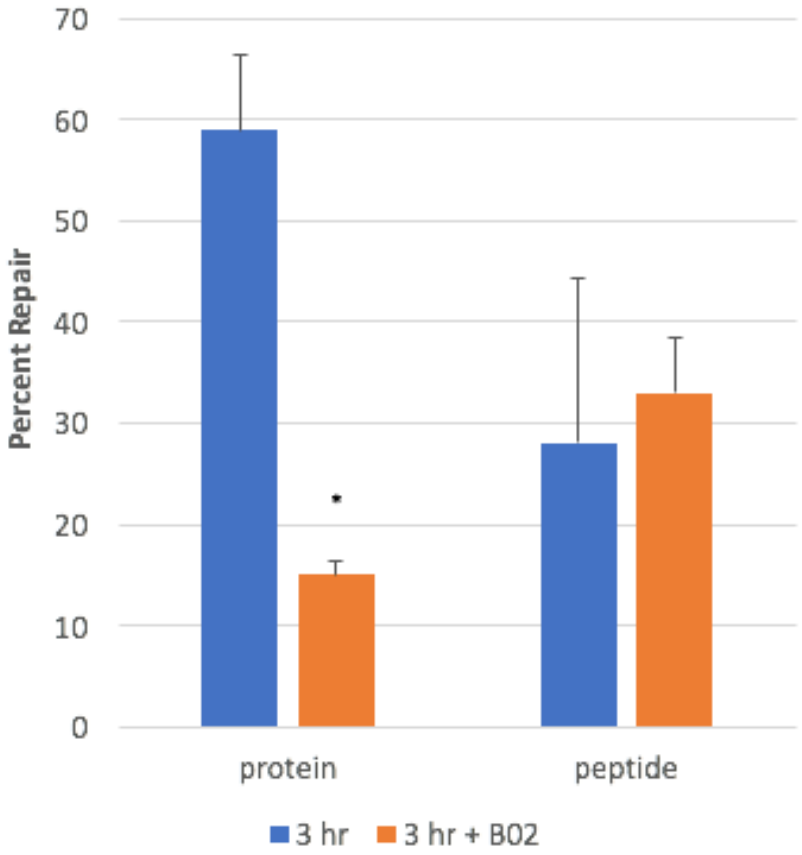

Figure 4.4: Decreased homologous recombination of DNA-protein crosslinks but not DNA-peptide crosslinks in the presence of a RAD51 inhibitor. NER-deficient human fibroblasts (XPD) were incubated with or without the RAD51 inhibitor B02 (5μM) for 1 hour prior to transfection with plasmids crosslinked to hOGG1 or trypsin-digested hOGG1 with or without a homologous donor. Cells recovered for 3 hours, were lysed, and repair quantified using SSPE-qPCR (see methods for details). Percent HR repair was calculated by subtracting repair in the presence of a homologous donor from repair in the absence of a donor. Values depict mean percent repair ± SEM, N=5, $p<0.05$.

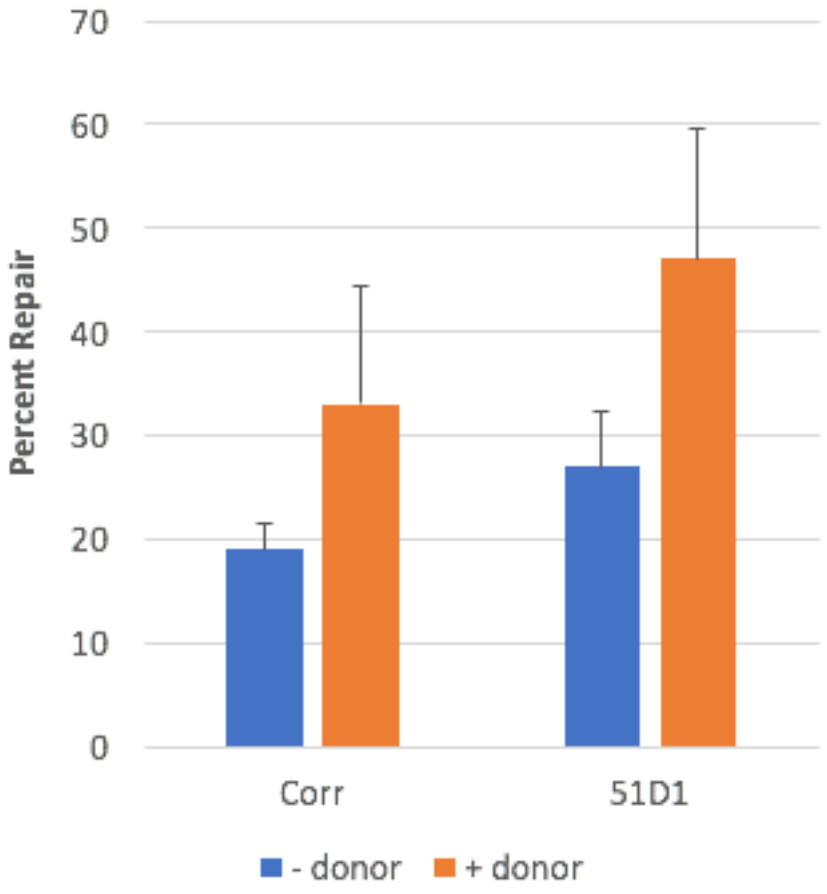

Figure 4.5: Homologous recombination of DPC-containing plasmids is not dependent on RAD51D. Plasmids crosslinked to hOGG1 to the deoxyribose were co-transfected with either a homologous (W/ donor) or non-homologous donor (W/o donor) into Chinese hamster ovarian AA8 cells deficient in the RAD51D gene (51D1) and isogenic corrected cells (Corr). Cells recovered for 8 hours, were lysed, and repair quantified using SSPE-qPCR (see methods for details). Values depict mean percent repair ± SEM, N=3, $p<0.05$.

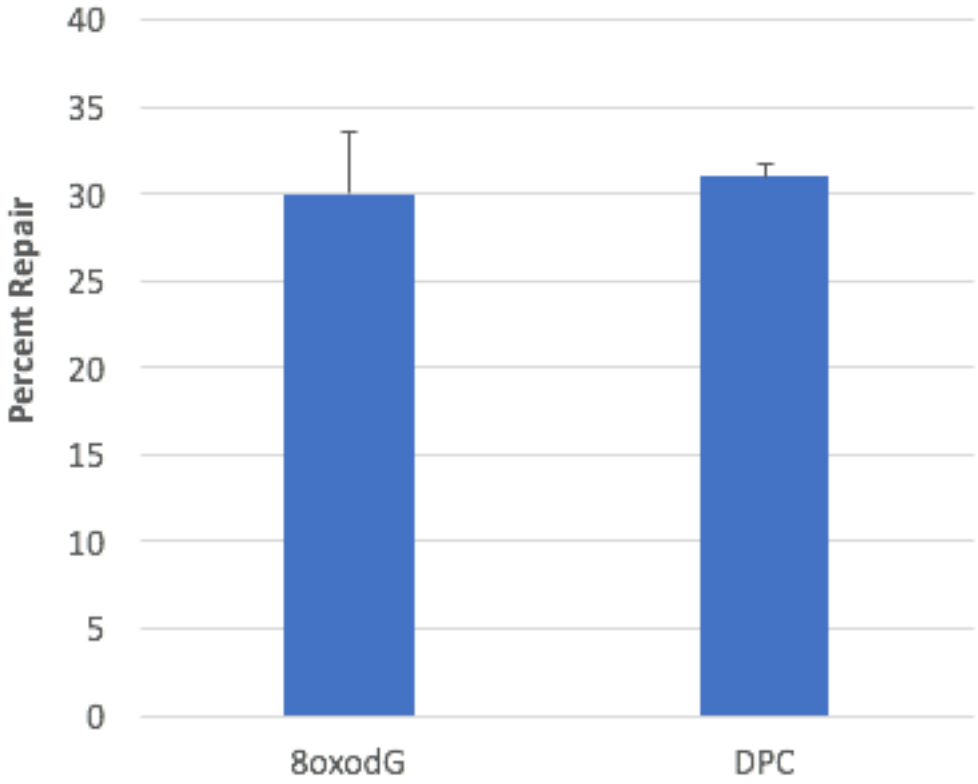

Figure 4.6: Repair of damaged plasmids in purified nuclei. Plasmids containing either an 8-oxo-guanine modification or OGG1 crosslink were electroporated into purified nuclei from wild-type hamster cells, incubated at 37°C for 2 hours, and repair quantified using SSPE-qPCR. Values depict mean percent repair ± SEM, N=3.

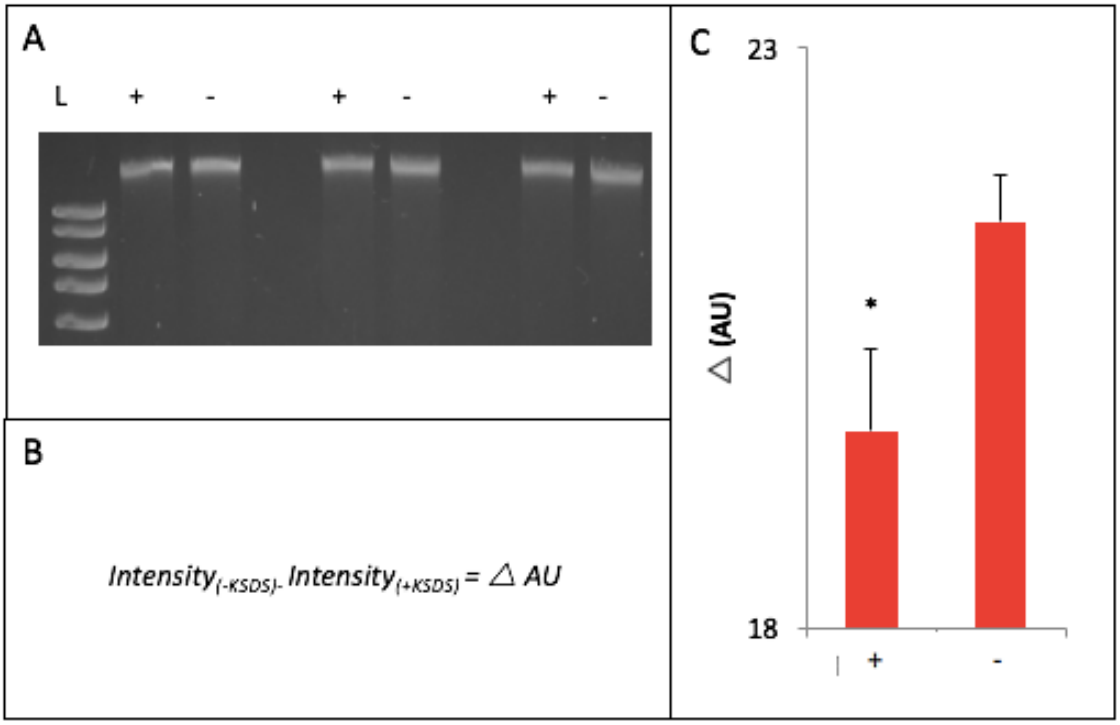

Figure 4.7: Formation of cisplatin-induced DNA-protein crosslinks in human cells. Human HT1080 cells were treated with 100μM cisplatin and mitochondrial DNA purified as described in methods. **A:** Purified DNA was then treated (+) or not treated (-) with KCl/SDS and run on a gel. **B:** Density of gel bands were quantified using ImageJ and difference in arbitrary units (AU) calculated. **C:** Average difference in density calculated from three experiments. Values depict mean percent repair ± SEM, N=3, $p<0.05$.

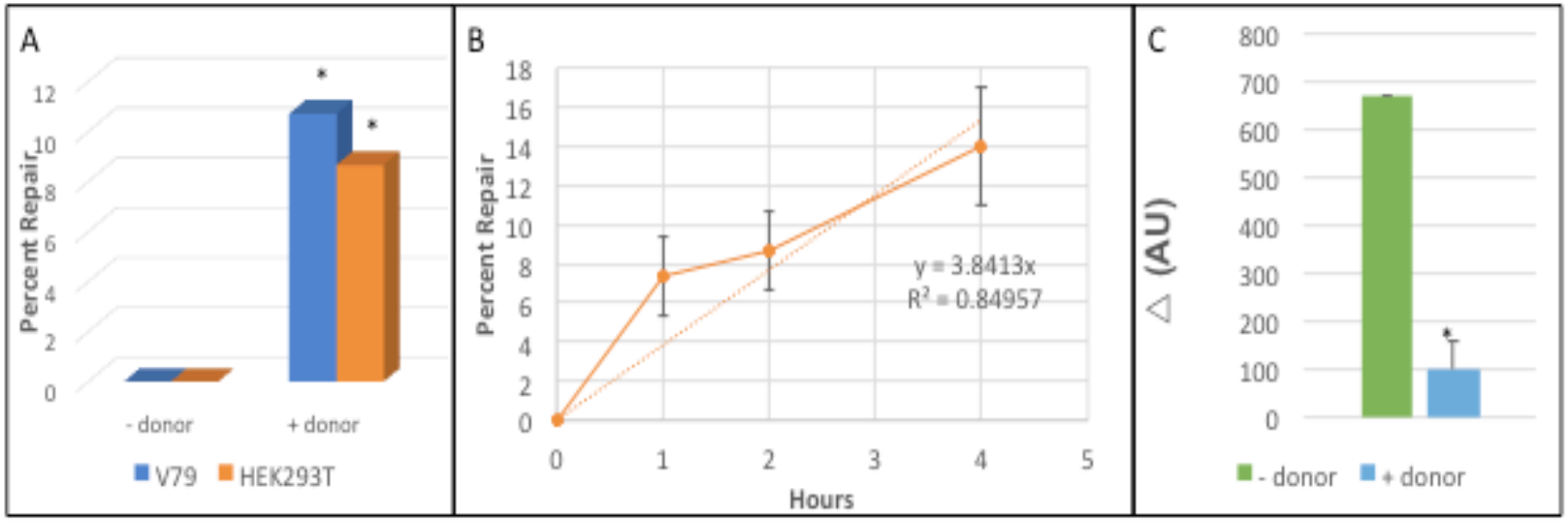

Figure 4.8: DPC-containing plasmids are repaired via homologous recombination in purified mitochondria.

A: DPC-containing plasmids were electroporated in hamster (V79) and human (HEK293T) mitochondria with (+donor) or without (-donor), allowed to recover for 2 hours, and repair quantified using SSPE-qPCR. **B:** Repair in HEK293T mitochondria at 1, 2, and 4 hours. **C:** DNA recovered from (A) were divided in half, treated with or without KCl/SDS, run on a gel, and density quantified using Image J. The difference in density was then calculated and plotted on the graph. Values depict mean percent repair ± SEM, N=3, $p<0.05$.

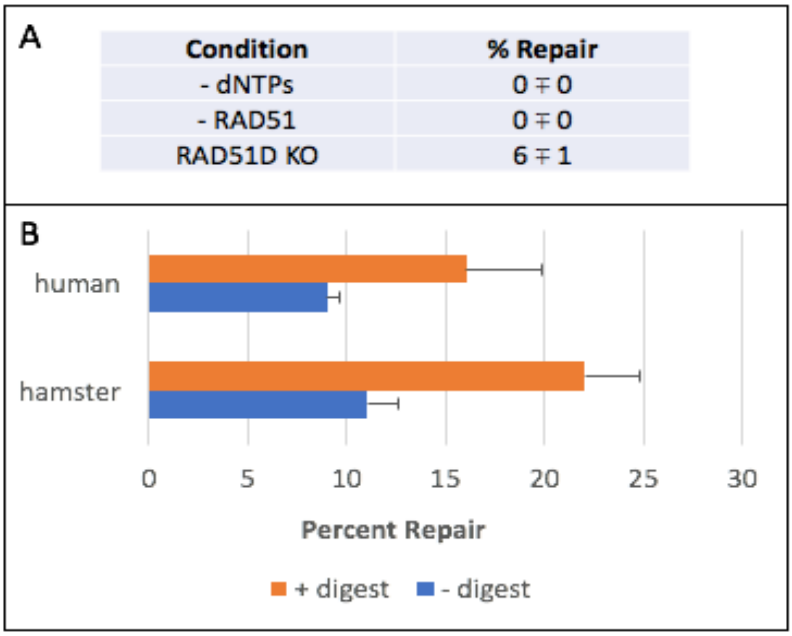

Figure 4.9: Mitochondrial repair of DPCs in dependent on dNTPs and the RAD51 protein. A: (-dNTPs) refers to DPC-containing plasmids were electroporated into human HEK293T mitochondria with an undamaged, homologous donor and allowed to recover for two hours in the absence of deoxynucleotide triphosphates. (-RAD51) refers to HEK293T cells were pretreated with the RAD51 inhibitor B02 (5μM) for one hour prior to mitochondrial purification. RAD51D KO refers to Chinese hamster ovarian cells that are deficient in the RAD51D gene. **B:** DPC-containing plasmids were digested with (+digest) or without (-digest) the restriction enzyme EcoRI adjacent to the crosslinking site and electroporated in wild-type (V79) cells. All DPC-containing plasmids were electroporated with a homologous donor, incubated for 2 hours, and repair calculated using SSPE-qPCR. Values depict mean percent repair ± SEM, N=3.

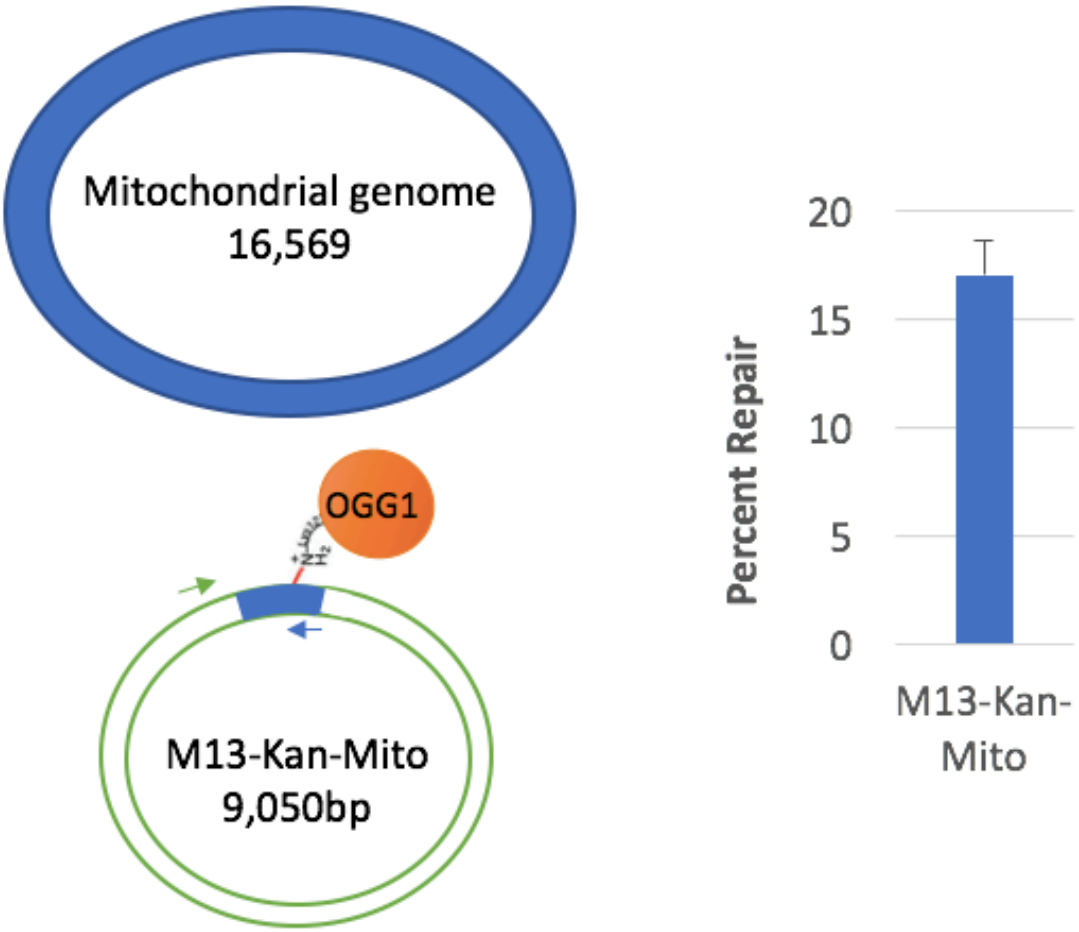

Figure 4.10: Repair of DPC-containing plasmids using the mitochondrial genome as a homologous donor. A plasmid containing 475bp of homology (blue) with the mitochondrial genome was crosslinked with OGG1, electroporated in HEK293T cells, allowed to recover for 2 hours, and repair quantified with SSPE-qPCR using primers complementary to the mitochondrial insert (blue arrow) and to the M13 plasmid (green arrow). Values depict mean percent repair ± SEM, N=3.

Chapter 5

Discussion

DNA-damaging chemotherapeutics are used to treat a wide variety of cancers[1]. Unfortunately, cancers can develop resistance to these drugs[244]. It has been shown that increased expression of DNA repair proteins is correlated with drug resistance[245]. DNA-protein crosslinks (DPCs) are one of the toxic lesions formed by these chemotherapeutics. However, because DPCs are induced with other types of DNA damage, it is unclear what role DPC repair mechanisms play in chemotherapeutic resistance. The goal of this research was to gain insight into the pathways involved into DPC repair by studying the repair of synthetic DPCs crosslinked to plasmid DNA and transfected into mammalian cells.

From this work, a new assay termed strand-specific primer extension-quantitative polymerase chain reaction (SSPE-qPCR) was developed and used to quantify DPC-containing plasmids (as well as other lesions) transfected into mammalian cells of different genetic backgrounds and recovered over time. The important feature of this assay lies in the multiple rounds of primer extension that recovered plasmids are subjected to using Taq polymerase and a primer complementary to the originally damaged strand. Unrepaired adducts blocked extension of these primers and did not generate any additional DNA strands. However, repaired DNA was extended during this step and produced additional DNA strands. QPCR was then used to quantify how many additional strands of DNA were produced during primer extension and calculate what percent of recovered plasmids had been repaired. Another unique feature of the assay was that conditions such as protein size, sequence context, and nature of the

chemical crosslink could be altered to assess how these factors influenced repair. This assay was then exploited to investigate the role of nucleotide excision repair (NER), homologous recombination (HR), and proteolysis in the repair of DPCs in the nucleus.

As mentioned above, DPCs are formed by endogenous and exogenous agents randomly throughout the genome. However, mitochondrial DNA is also susceptible to these DNA-damaging agents and the formation of DNA-protein crosslinks[225]. Because mitochondria are frequently exposed to oxidative damage, repair pathways such as base excision repair have been a main focus in mitochondrial DNA repair research[246]. To examine DPC repair in the mitochondria, the SSPE-qPCR assay was used to quantify the repair of DPC-containing plasmids electroporated into purified mitochondria. Incubation of the damaged substrate in the presence of pyruvate, BSA, dNTPs, and ATP was sufficient to examine repair events over a time course of 4 hours. Results from these experiments showed a role for the homologous recombination pathway in DPC repair, providing the first evidence for DPC repair in this organelle. These experiments validate future use of this assay to gain a greater understanding of DPC and HR repair in mitochondria.

Overall, this work has contributed to current literature aimed to better understand DNA repair mechanisms in order to advance chemotherapeutic treatment of cancer patients. Once understood, these pathways can then be exploited to increase the efficacy of DNA-damaging drugs. An example of this

therapeutic strategy is the combinational use of temazolamide and O6-benzylguanine in treating drug-resistant glioma[247]. Temzazolamide is a chemotherapeutic which alkylates DNA and is used to treat malignant glioma. However, patients who are resistant to this drug have a poor prognosis for survival. O6-benzylguanine is a repair substrate for the enzyme O6-alkylguanine-DNA alkyltransferase (AGT) and can irreversibly inactive AGT in order to increase the effectiveness of temozolomide[248]. In this case, understanding how alkylated DNA is repaired in cells, improved the therapeutic efficacy of temozolomide by using a combination therapy involving a DNA repair substrate. Considering the large number of chemotherapeutics which induce DNA-protein crosslinks, it is logical to predict that a similar strategy could be used in cancers resistant to DPC-inducing agents. Thus, understanding the repair mechanisms involved in DPC repair can be used to improve therapeutic strategies and ultimately save lives.

Chapter 6

Future Directions

The work presented above has contributed to the field by providing a new assay to gain insight into the repair mechanisms of polymerase-blocking lesions on exogenous DNA in mammalian cells. Future work can utilize this assay to gain further insight into repair mechanisms of specific lesions in the nucleus and mitochondria. For example, it would be interesting to investigate the role of proteolysis in the repair of larger DNA-protein crosslinks (DPCs).

Current studies suggest that proteins larger than 10 kDa are digested into smaller peptides prior to removal[92]. However, it is still unclear what protease is responsible for the degradation and how the enzyme is recruited to the damage. To address this question, a biotinylated, DPC-containing oligonucleotide could be electroporated into purified nuclei, recovered, and analyzed using mass spectrometry. Using this method, one could identify the sequence of the remaining DNA-peptide on the oligonucleotide and gain insight into the protease responsible by examining its recognition sequence. Polyubiquitination is a modification used to signal protein degradation by the proteasome[249]. To assess the role of ubiquitin in proteolysis signaling during DPC repair, substrates recovered from cells at early time points could be analyzed for ubiquitin *via* western blot[250]. Another strategy would be to treat plasmids containing larger DPCs with acetyl succinimide to modify lysine residues and prevent ubiquitination[251]. Decreased repair of these substrates would confirm a role for ubiquitin modification in their repair. Researchers have also shown the protease Spartan to be involved in the proteolysis of DPCs[176]. However, most studies have

been performed in extracts since knock-out cells are embryonically lethal[100]. To assess the role of Spartan in DPC repair in intact cells, a cell line could be created in which the expression of Spartan is controlled under an inducible promoter. Using this strategy, it could be determined how much Spartan is needed to see repair of DPC-containing plasmids. Alternatively, cells transfected with a plasmid that expressed flag-tagged Spartan and could be used to pull-down DPC-containing plasmids *via* immunoprecipitation.

Another future direction of this work would be to further investigate mitochondrial repair mechanisms. For example, although proteolysis is believed to play a role in nuclear DPC repair, it is unclear if the same proteases (or any) are involved in mitochondrial DPC repair. This could be examined by electroporating DPC-containing plasmids of multiple sizes in purified mitochondria to assess their repair rate. Faster repair of DNA-peptide crosslinks would support the existence of a rate-limiting proteolysis step during repair. SiRNA knockdown of different mitochondrial proteases could then be used to identify which protease influences repair of larger DPC-containing plasmids. Although we have provided evidence for the repair of DPCs *via* mitochondrial homologous recombination, future experiments could investigate the recruitment of this repair machinery to the damaged site. For example, following electroporation, DPC-containing oligonucleotides could be treated with formaldehyde to crosslink protein recruited to the site of damage[252]. These proteins can then be released upon heating, resolved on a protein gel, and cut

out of the gel for identification *via* mass spectrometry. This strategy could be used to gain insight into the homologous recombination of double-strand breaks as well as DNA-protein crosslinks in the mitochondria. Sequence analysis of the recovered substrates could also assess repair-induced mutagenesis.

Although nucleotide excision repair (NER) and homologous recombination (HR) are thought to be the primary pathways involved in DPC repair, cancerous cells can have defects in repair proteins, resulting in dysfunctional pathways[107]. Therefore, it is important to understand what other mechanisms are able to repair DPCs in the absence of the NER and HR pathway. One candidate for this repair is the non-homologous end-joining pathway (NHEJ) which is known to repair double-strand breaks[253]. This could be investigated by pretreating NER-deficient cells with a NHEJ inhibitor (such as a protein kinase inhibitor) prior to transfection with a damaged plasmid in the absence of a homologous donor.

Insight into the role of the mechanisms described above in DPC repair could one day be used clinically in the development of inhibitors to prevent DPC repair and increase the effectiveness of DPC-forming chemotherapeutics.

Bibliography

1 Barker, S., Weinfeld, M. & Murray, D. DNA-protein crosslinks: their induction, repair, and biological consequences. *Mutat Res.* **589** (2), 111-135, doi:10.1016/j.mrrev.2004.11.003, (2005).
2 Ide, H., Shoulkamy, M. I., Nakano, T., Miyamoto-Matsubara, M. & Salem, A. M. H. Repair and biochemical effects of DNA–protein crosslinks. *Mutation Research/Fundamental and Molecular Mechanisms of Mutagenesis.* **711** (1), 113-122, doi:https://doi.org/10.1016/j.mrfmmm.2010.12.007, (2011).
3 Groehler, A. t., Degner, A. & Tretyakova, N. Y. Mass Spectrometry-Based Tools to Characterize DNA-Protein Cross-Linking by Bis-Electrophiles. *Basic Clin Pharmacol Toxicol.* **121** 63–77, doi:10.1111/bcpt.12751, (2016).
4 Loeber, R. L. *et al.* Proteomic analysis of DNA-protein cross-linking by antitumor nitrogen mustards. *Chem Res Toxicol.* **22** (6), 1151-1162, doi:10.1021/tx900078y, (2009).
5 Qiu, H. & Wang, Y. Exploring DNA-binding Proteins with In Vivo Chemical Cross-linking and Mass Spectrometry. *Journal of proteome research.* **8** (4), 1983-1991 (2009).
6 Stingele, J., Habermann, B. & Jentsch, S. DNA–protein crosslink repair: proteases as DNA repair enzymes. *Trends in Biochemical Sciences.* **40** (2), 67-71, doi:http://dx.doi.org/10.1016/j.tibs.2014.10.012, (2015).
7 Loeber, R. *et al.* Cross-linking of the DNA repair protein O(6)-alkylguanine DNA alkyltransferase to DNA in the presence of antitumor nitrogen mustards. *Chemical research in toxicology.* **21** (4), 787-795, doi:10.1021/tx7004508, (2008).
8 Barker, S., Weinfeld, M., Zheng, J., Li, L. & Murray, D. Identification of mammalian proteins cross-linked to DNA by ionizing radiation. *J Biol Chem.* **280** (40), 33826-33838, doi:10.1074/jbc.M502477200, (2005).
9 Chvalova, K., Brabec, V. & Kasparkova, J. Mechanism of the formation of DNA-protein cross-links by antitumor cisplatin. *Nucleic Acids Res.* **35** (6), 1812-1821, doi:10.1093/nar/gkm032, (2007).
10 Pommier, Y. Topoisomerase I inhibitors: camptothecins and beyond. *Nat Rev Cancer.* **10** (1474-175X (Print)), 789-802 (2006).
11 Smith, P. J., Bell, S. M., Dee, A. & Sykes, H. Involvement of DNA topoisomerase II in the selective resistance of a mammalian cell mutant to DNA minor groove ligands: ligand-induced DNA—protein crosslinking and responses to topoisomerase poisons. *Carcinogenesis.* **11** (4), 659-665, doi:10.1093/carcin/11.4.659, (1990).
12 Sczepanski, J. T., Wong, R. S., McKnight, J. N., Bowman, G. D. & Greenberg, M. M. Rapid DNA–protein cross-linking and strand scission by an abasic site in a nucleosome core particle. *Proceedings of the National Academy of Sciences.* **107** (52), 22475-22480, doi:10.1073/pnas.1012860108, (2010).

13 Hill, J. W. & Evans, M. K. Dimerization and opposite base-dependent catalytic impairment of polymorphic S326C OGG1 glycosylase. *Nucleic Acids Research.* **34** (5), 1620-1632, doi:10.1093/nar/gkl060, (2006).
14 Lindahl, T. Instability and decay of the primary structure of DNA. *Nature.* **362** 709, doi:10.1038/362709a0, (1993).
15 Quinones, J. L. *et al.* Enzyme mechanism-based, oxidative DNA-protein cross-links formed with DNA polymerase beta in vivo. *Proc Natl Acad Sci U S A.* **112** (28), 8602-8607, doi:10.1073/pnas.1501101112, (2015).
16 Michaelson-Richie, E. D. *et al.* DNA-protein cross-linking by 1,2,3,4-diepoxybutane. *J Proteome Res.* **9** (9), 4356-4367, doi:10.1021/pr1000835, (2010).
17 Gherezghiher, T. B., Ming, X., Villalta, P. W., Campbell, C. & Tretyakova, N. Y. 1,2,3,4-Diepoxybutane-induced DNA-protein cross-linking in human fibrosarcoma (HT1080) cells. *J Proteome Res.* **12** (5), 2151-2164, doi:10.1021/pr3011974, (2013).
18 Loeber, R., Rajesh, M., Fang, Q., Pegg, A. E. & Tretyakova, N. Cross-Linking of the Human DNA Repair Protein O6-Alkylguanine DNA Alkyltransferase to DNA in the Presence of 1,2,3,4-Diepoxybutane. *Chemical Research in Toxicology.* **19** (5), 645-654, doi:10.1021/tx0600088, (2006).
19 Kotapati, S. *et al.* Polymerase Bypass of N(6)-Deoxyadenosine Adducts Derived from Epoxide Metabolites of 1,3-Butadiene. *Chemical research in toxicology.* **28** (7), 1496-1507, doi:10.1021/acs.chemrestox.5b00166, (2015).
20 Kotapati, S. *et al.* Translesion Synthesis across 1,N(6)-(2-Hydroxy-3-hydroxymethylpropan-1,3-diyl)-2′ -deoxyadenosine (1,N(6)-γ-HMHP-dA) Adducts by Human and Archebacterial DNA Polymerases. *The Journal of Biological Chemistry.* **287** (46), 38800-38811, doi:10.1074/jbc.M112.396788, (2012).
21 Wickramaratne, S. & Tretyakova, N. Y. Structural Elucidation of DNA-Protein Crosslinks Using Reductive Desulfurization and Liquid Chromatography-Tandem Mass Spectrometry. *Chembiochem : a European journal of chemical biology.* **15** (3), 353-355, doi:10.1002/cbic.201300757, (2014).
22 Johnson, L. A. A. *et al.* Formation of Cyclophosphamide Specific DNA Adducts in Hematological Diseases. *Pediatric blood & cancer.* **58** (5), 708-714, doi:10.1002/pbc.23254, (2012).
23 Michaelson-Richie, E. D. *et al.* Mechlorethamine-Induced DNA-Protein Cross-Linking in Human Fibrosarcoma (HT1080) Cells. *Journal of proteome research.* **10** (6), 2785-2796, doi:10.1021/pr200042u, (2011).
24 Tretyakova, N. Y., Groehler, A. & Ji, S. DNA-Protein Cross-links: Formation, Structural Identities, and Biological Outcomes. *Accounts of chemical research.* **48** (6), 1631-1644, doi:10.1021/acs.accounts.5b00056, (2015).
25 Swenberg, J. A. *et al.* Endogenous versus exogenous DNA adducts: their role in carcinogenesis, epidemiology, and risk assessment. *Toxicol Sci.* **120** (1096-0929 (Electronic)), 130-145 (2011).

26 Jena, N. R. DNA damage by reactive species: Mechanisms, mutation and repair. *J Biosci.* **37** (0973-7138 (Electronic)), 503-517 (2012).
27 Nakano, T. *et al.* T7 RNA Polymerases Backed up by Covalently Trapped Proteins Catalyze Highly Error Prone Transcription. *The Journal of Biological Chemistry.* **287** (9), 6562-6572, doi:10.1074/jbc.M111.318410, (2012).
28 Kuo, H. K., Griffith, J. D. & Kreuzer, K. N. 5-Azacytidine–Induced Methyltransferase-DNA Adducts Block DNA Replication <em>In vivo</em&gt. *Cancer Research.* **67** (17), 8248 (2007).
29 Palii, S. S., Van Emburgh Bo Fau - Sankpal, U. T., Sankpal Ut Fau - Brown, K. D., Brown Kd Fau - Robertson, K. D. & Robertson, K. D. DNA methylation inhibitor 5-Aza-2'-deoxycytidine induces reversible genome-wide DNA damage that is distinctly influenced by DNA methyltransferases 1 and 3B. *Mol Cell Biol.* **28** (1098-5549 (Electronic)), 752-771 (2008).
30 Orta, M. L. *et al.* 5-Aza-2′ -deoxycytidine causes replication lesions that require Fanconi anemia-dependent homologous recombination for repair. *Nucleic Acids Research.* **41** (11), 5827-5836, doi:10.1093/nar/gkt270, (2013).
31 Klages-Mundt, N. L. & Li, L. Formation and Repair of DNA-Protein Crosslink Damage. *Science China. Life sciences.* **60** (10), 1065-1076, doi:10.1007/s11427-017-9183-4, (2017).
32 Smith, K. C. Dose dependent decrease in extractability of DNA from bacteria following irradiation with ultraviolet light or with visible light plus dye. *Biochem Biophys Res Commun.* **8** (0006-291X (Print)), 157-163 (1962).
33 Nishioka, H. Lethal and mutagenic action of formaldehyde in Hcr + and Hcr - strains of Escherichia coli. *Mutat Res.* **17** (2), 261-265 (1973).
34 Takahashi, K., Morita, T. & Kawazoe, Y. Mutagenic characteristics of formaldehyde on bacterial systems. *Mutat Res.* **156** (3), 153-161 (1985).
35 Spivak, G. Nucleotide excision repair in humans. *DNA Repair (Amst).* **36** 13-18, doi:10.1016/j.dnarep.2015.09.003, (2015).
36 Reardon, J. T. & Sancar, A. in *Progress in Nucleic Acid Research and Molecular Biology* Vol. 79 183-235 (Academic Press, 2005).
37 Mellon, I., Spivak, G. & Hanawalt, P. C. Selective removal of transcription-blocking DNA damage from the transcribed strand of the mammalian DHFR gene. *Cell.* **51** (2), 241-249, doi:https://doi.org/10.1016/0092-8674(87)90151-6, (1987).
38 Gillet, L. C. J. & Schärer, O. D. Molecular Mechanisms of Mammalian Global Genome Nucleotide Excision Repair. *Chemical Reviews.* **106** (2), 253-276, doi:10.1021/cr040483f, (2006).
39 Vermeulen, W. & Fousteri, M. Mammalian Transcription-Coupled Excision Repair. *Cold Spring Harbor Perspectives in Biology.* **5** (8), a012625, doi:10.1101/cshperspect.a012625, (2013).
40 Saijo, M. The role of Cockayne syndrome group A (CSA) protein in transcription-coupled nucleotide excision repair. *Mechanisms of Ageing and*

Development. **134** (5), 196-201, doi:https://doi.org/10.1016/j.mad.2013.03.008, (2013).
41 Cockayne, E. A. Dwarfism with retinal atrophy and deafness. *Archives of Disease in Childhood.* **11** (61), 1-8 (1936).
42 Black, J. O. Xeroderma Pigmentosum. *Head and Neck Pathology.* **10** (2), 139-144, doi:10.1007/s12105-016-0707-8, (2016).
43 Huang, J. C., Svoboda, D. L., Reardon, J. T. & Sancar, A. Human nucleotide excision nuclease removes thymine dimers from DNA by incising the 22nd phosphodiester bond 5' and the 6th phosphodiester bond 3' to the photodimer. *Proceedings of the National Academy of Sciences of the United States of America.* **89** (8), 3664-3668 (1992).
44 Fuss, J. O. & Tainer, J. A. XPB and XPD helicases in TFIIH orchestrate DNA duplex opening and damage verification to coordinate repair with transcription and cell cycle via CAK kinase. *DNA repair.* **10** (7), 697-713, doi:10.1016/j.dnarep.2011.04.028, (2011).
45 Schärer, O. D. Nucleotide Excision Repair in Eukaryotes. *Cold Spring Harbor Perspectives in Biology.* **5** (10), a012609, doi:10.1101/cshperspect.a012609, (2013).
46 Hu, J. *et al.* Nucleotide Excision Repair in Human Cells: FATE OF THE EXCISED OLIGONUCLEOTIDE CARRYING DNA DAMAGE IN VIVO. *The Journal of Biological Chemistry.* **288** (29), 20918-20926, doi:10.1074/jbc.M113.482257, (2013).
47 Jasin, M. & Rothstein, R. Repair of Strand Breaks by Homologous Recombination. *Cold Spring Harbor Perspectives in Biology.* **5** (11), a012740, doi:10.1101/cshperspect.a012740, (2013).
48 Krejci, L., Altmannova, V., Spirek, M. & Zhao, X. Homologous recombination and its regulation. *Nucleic Acids Research.* **40** (13), 5795-5818, doi:10.1093/nar/gks270, (2012).
49 Mehta, A. & Haber, J. E. Sources of DNA Double-Strand Breaks and Models of Recombinational DNA Repair. *Cold Spring Harbor Perspectives in Biology.* **6** (9), a016428, doi:10.1101/cshperspect.a016428, (2014).
50 Symington, L. S. End Resection at Double-Strand Breaks: Mechanism and Regulation. *Cold Spring Harbor Perspectives in Biology.* **6** (8), a016436, doi:10.1101/cshperspect.a016436, (2014).
51 Liu, J., Doty, T., Gibson, B. & Heyer, W.-D. Human BRCA2 protein promotes RAD51 filament formation on RPA-covered ssDNA. *Nature structural & molecular biology.* **17** (10), 1260-1262, doi:10.1038/nsmb.1904, (2010).
52 Barzel, A. & Kupiec, M. Finding a match: how do homologous sequences get together for recombination? *Nature Reviews Genetics.* **9** 27, doi:10.1038/nrg2224, (2008).
53 San Filippo, J., Sung, P. & Klein, H. Mechanism of Eukaryotic Homologous Recombination. *Annual Review of Biochemistry.* **77** (1), 229-257, doi:10.1146/annurev.biochem.77.061306.125255, (2008).

54 Wyatt, H. D. M. & West, S. C. Holliday Junction Resolvases. *Cold Spring Harbor Perspectives in Biology.* **6** (9), a023192, doi:10.1101/cshperspect.a023192, (2014).
55 Bizard, A. H. & Hickson, I. D. The Dissolution of Double Holliday Junctions. *Cold Spring Harbor Perspectives in Biology.* **6** (7), a016477, doi:10.1101/cshperspect.a016477, (2014).
56 Schwartz, E. K. & Heyer, W.-D. Processing of joint molecule intermediates by structure-selective endonucleases during homologous recombination in eukaryotes. *Chromosoma.* **120** (2), 109-127, doi:10.1007/s00412-010-0304-7, (2011).
57 Morrical, S. W. DNA-Pairing and Annealing Processes in Homologous Recombination and Homology-Directed Repair. *Cold Spring Harbor Perspectives in Biology.* **7** (2), a016444, doi:10.1101/cshperspect.a016444, (2015).
58 Bee, L., Fabris, S., Cherubini, R., Mognato, M. & Celotti, L. The efficiency of homologous recombination and non-homologous end joining systems in repairing double-strand breaks during cell cycle progression. *PLoS One.* **8** (7), e69061, doi:10.1371/journal.pone.0069061, (2013).
59 Daley, J. M., Gaines, W. A., Kwon, Y. & Sung, P. Regulation of DNA Pairing in Homologous Recombination. *Cold Spring Harbor Perspectives in Biology.* **6** (11), a017954, doi:10.1101/cshperspect.a017954, (2014).
60 Chanet, R., Izard, C. & Moustacchi, E. Genetic effects of formaldehyde in yeast. II. Influence of ploidly and of mutations affecting radiosensitivity on its lethal effect. *Mutat Res.* **35** (1), 29-38 (1976).
61 Nakano, T. *et al.* Nucleotide excision repair and homologous recombination systems commit differentially to the repair of DNA-protein crosslinks. *Mol Cell.* **28** (1), 147-158, doi:10.1016/j.molcel.2007.07.029, (2007).
62 de Graaf, B., Clore, A. & McCullough, A. K. Cellular pathways for DNA repair and damage tolerance of formaldehyde-induced DNA-protein crosslinks. *DNA Repair (Amst).* **8** (10), 1207-1214, doi:10.1016/j.dnarep.2009.06.007, (2009).
63 Kumari, A., Lim, Y. X., Newell, A. H., Olson, S. B. & McCullough, A. K. Formaldehyde-induced genome instability is suppressed by an XPF-dependent pathway. *DNA Repair (Amst).* **11** (3), 236-246, doi:10.1016/j.dnarep.2011.11.001, (2012).
64 Speit, G., Schutz, P. & Merk, O. Induction and repair of formaldehyde-induced DNA-protein crosslinks in repair-deficient human cell lines. *Mutagenesis.* **15** (1), 85-90 (2000).
65 Yu, R. *et al.* Formation, Accumulation, and Hydrolysis of Endogenous and Exogenous Formaldehyde-Induced DNA Damage. *Toxicological Sciences.* **146** (1), 170-182, doi:10.1093/toxsci/kfv079, (2015).
66 Zhitkovich, A. & Costa, M. A simple, sensitive assay to detect DNA-protein crosslinks in intact cells and in vivo. *Carcinogenesis.* **13** (8), 1485-1489 (1992).

67 Liu Lf Fau - Rowe, T. C., Rowe Tc Fau - Yang, L., Yang L Fau - Tewey, K. M., Tewey Km Fau - Chen, G. L. & Chen, G. L. Cleavage of DNA by mammalian DNA topoisomerase II. *J Biol Chem.* **258** (0021-9258 (Print)), 15365-15370 (1983).
68 Chiu, S. M., Sokany, N. M., Friedman, L. R. & Oleinick, N. L. Differential processing of ultraviolet or ionizing radiation-induced DNA-protein cross-links in Chinese hamster cells. *Int J Radiat Biol Relat Stud Phys Chem Med.* **46** (6), 681-690 (1984).
69 Merk, O., Reiser, K. & Speit, G. Analysis of chromate-induced DNA-protein crosslinks with the comet assay. *Mutat Res.* **471** (1-2), 71-80 (2000).
70 Merk, O. & Speit, G. Detection of crosslinks with the comet assay in relationship to genotoxicity and cytotoxicity. *Environ Mol Mutagen.* **33** (0893-6692 (Print)), 167-172 (1999).
71 Shoulkamy, M. I. *et al.* Detection of DNA–protein crosslinks (DPCs) by novel direct fluorescence labeling methods: distinct stabilities of aldehyde and radiation-induced DPCs. *Nucleic Acids Research.* **40** (18), e143-e143, doi:10.1093/nar/gks601, (2012).
72 Kiianitsa, K. & Maizels, N. A rapid and sensitive assay for DNA–protein covalent complexes in living cells. *Nucleic Acids Research.* **41** (9), e104-e104, doi:10.1093/nar/gkt171, (2013).
73 Kiianitsa, K. & Maizels, N. Ultrasensitive isolation, identification and quantification of DNA–protein adducts by ELISA-based RADAR assay. *Nucleic Acids Research.* **42** (13), e108-e108, doi:10.1093/nar/gku490, (2014).
74 Cress, A. E., Kurath, K. M., Stea, B. & Bowden, G. T. The crosslinking of nuclear protein to DNA using ionizing radiation. *Journal of Cancer Research and Clinical Oncology.* **116** (4), 324-330, doi:10.1007/BF01612913, (1990).
75 Loeber, R. L. *et al.* Proteomic Analysis of DNA-Protein Cross-Linking by Antitumor Nitrogen Mustards. *Chemical research in toxicology.* **22** (6), 1151-1162, doi:10.1021/tx900078y, (2009).
76 Ong, S. E. *et al.* Stable isotope labeling by amino acids in cell culture, SILAC, as a simple and accurate approach to expression proteomics. *Mol Cell Proteomics.* **5** (1535-9476 (Print)), 376-386 (2002).
77 Rajesh, M., Wang, G., Jones, R. & Tretyakova, N. Stable Isotope Labeling−Mass Spectrometry Analysis of Methyl- and Pyridyloxobutyl-Guanine Adducts of 4-(Methylnitrosamino)-1-(3-pyridyl)-1-butanone in p53-Derived DNA Sequences. *Biochemistry.* **44** (6), 2197-2207, doi:10.1021/bi0480032, (2005).
78 Tretyakova, N., Goggin, M. & Janis, G. Quantitation of DNA adducts by stable isotope dilution mass spectrometry. *Chemical research in toxicology.* **25** (10), 2007-2035, doi:10.1021/tx3002548, (2012).
79 Groehler, A. *et al.* Oxidative cross-linking of proteins to DNA following ischemia-reperfusion injury. *Free Radical Biology and Medicine.* **120** 89-101, doi:https://doi.org/10.1016/j.freeradbiomed.2018.03.010, (2018).

80 Sangaraju, D., Villalta, P. W., Wickramaratne, S., Swenberg, J. & Tretyakova, N. NanoLC/ESI(+) HRMS(3) Quantitation of DNA Adducts Induced by 1,3-Butadiene. *Journal of the American Society for Mass Spectrometry.* **25** (7), 1124-1135, doi:10.1007/s13361-014-0916-x, (2014).
81 Malayappan, B. *et al.* Quantitative High-Performance Liquid Chromatography–Electrospray Ionization Tandem Mass Spectrometry Analysis of Bis-N7-Guanine DNA–DNA Cross-Links in White Blood Cells of Cancer Patients Receiving Cyclophosphamide Therapy. *Analytical Chemistry.* **82** (9), 3650-3658, doi:10.1021/ac902923s, (2010).
82 Groehler, A. t., Villalta, P. W., Campbell, C. & Tretyakova, N. Covalent DNA-Protein Cross-Linking by Phosphoramide Mustard and Nornitrogen Mustard in Human Cells. *Chem Res Toxicol.* **29** (2), 190-202, doi:10.1021/acs.chemrestox.5b00430, (2016).
83 Sangaraju, D. *et al.* Capillary HPLC-Accurate Mass MS/MS Quantitation of N7-(2, 3, 4-trihydroxybut-1-yl)-guanine Adducts of 1,3-Butadiene in Human Leukocyte DNA. *Chemical research in toxicology.* **26** (10), 1486-1497, doi:10.1021/tx400213m, (2013).
84 Yeo, J. E. *et al.* Synthesis of Site-Specific DNA–Protein Conjugates and Their Effects on DNA Replication. *ACS Chemical Biology.* **9** (8), 1860-1868, doi:10.1021/cb5001795, (2014).
85 Ahn, B., Kang, D., Kim, H. & Wei, Q. Repair of mitomycin C cross-linked DNA in mammalian cells measured by a host cell reactivation assay. *Mol Cells.* **18** (2), 249-255 (2004).
86 Pande, P. *et al.* Mutagenicity of a Model DNA-Peptide Cross-Link in Human Cells: Roles of Translesion Synthesis DNA Polymerases. *Chemical research in toxicology.* **30** (2), 669-677, doi:10.1021/acs.chemrestox.6b00397, (2017).
87 Baker, D. J. *et al.* Nucleotide excision repair eliminates unique DNA-protein cross-links from mammalian cells. *J Biol Chem.* **282** (31), 22592-22604, doi:10.1074/jbc.M702856200, (2007).
88 Kotandeniya, D. *et al.* Mass Spectrometry Based Approach to Study the Kinetics of O(6)-Alkylguanine DNA Alkyltransferase Mediated Repair of O(6)-pyridyloxobutyl-2′ -deoxyguanosine Adducts in DNA. *Chemical research in toxicology.* **24** (11), 1966-1975, doi:10.1021/tx2002993, (2011).
89 Wickramaratne, S. *et al.* Error-prone Translesion Synthesis Past DNA-Peptide Cross-links Conjugated to the Major Groove of DNA via C5 of Thymidine. *The Journal of Biological Chemistry.* **290** (2), 775-787, doi:10.1074/jbc.M114.613638, (2015).
90 Chesner, L. N. & Campbell, C. A Simple, Rapid, and Quantitative Assay to Measure Repair of DNA-protein Crosslinks on Plasmids Transfected into Mammalian Cells. LID - 10.3791/57413 [doi]. *J Vis Exp.* **5** (1940-087X (Electronic)), (2018).
91 Chesner, L. N. & Campbell, C. A quantitative PCR-based assay reveals that nucleotide excision repair plays a predominant role in the removal of DNA-

protein crosslinks from plasmids transfected into mammalian cells. *DNA Repair (Amst).* **62** (1568-7856 (Electronic)), 18-27 (2018).
92 Nakano, T. *et al.* Homologous recombination but not nucleotide excision repair plays a pivotal role in tolerance of DNA-protein cross-links in mammalian cells. *J Biol Chem.* **284** (40), 27065-27076, doi:10.1074/jbc.M109.019174, (2009).
93 Stingele, J., Schwarz, M. S., Bloemeke, N., Wolf, P. G. & Jentsch, S. A DNA-dependent protease involved in DNA-protein crosslink repair. *Cell.* **158** (2), 327-338, doi:10.1016/j.cell.2014.04.053, (2014).
94 Stingele, J. *et al.* Mechanism and Regulation of DNA-Protein Crosslink Repair by the DNA-Dependent Metalloprotease SPRTN. *Molecular Cell.* **64** (4), 688-703, doi:10.1016/j.molcel.2016.09.031, (2016).
95 Vaz, B. *et al.* Metalloprotease SPRTN/DVC1 Orchestrates Replication-Coupled DNA-Protein Crosslink Repair. (1097-4164 (Electronic)).
96 Morocz, M. *et al.* DNA-dependent protease activity of human Spartan facilitates replication of DNA-protein crosslink-containing DNA. *Nucleic Acids Res.* **45** (6), 3172–3188, doi:10.1093/nar/gkw1315, (2017).
97 Lopez-Mosqueda, J. *et al.* SPRTN is a mammalian DNA-binding metalloprotease that resolves DNA-protein crosslinks. *eLife.* **5** e21491, doi:10.7554/eLife.21491, (2016).
98 Maskey, R. S. *et al.* Spartan deficiency causes accumulation of Topoisomerase 1 cleavage complexes and tumorigenesis. *Nucleic Acids Res.* **45** (8), 4564-4576, doi:10.1093/nar/gkx107, (2017).
99 Machida, Y., Kim, M. S. & Machida, Y. J. Spartan/C1orf124 is important to prevent UV-induced mutagenesis. *Cell Cycle.* **11** (18), 3395-3402, doi:10.4161/cc.21694, (2012).
100 Lessel, D. *et al.* Mutations in SPRTN cause early onset hepatocellular carcinoma, genomic instability and progeroid features. *Nature Genetics.* **46** (11), 1239-1244 (2014).
101 Duxin, J. P., Dewar, J. M., Yardimci, H. & Walter, J. C. Repair of a DNA-Protein Crosslink by Replication-Coupled Proteolysis. *Cell.* **159** (2), 346-357, doi:10.1016/j.cell.2014.09.024, (2014).
102 Duxin, J. P. & Walter, J. C. What is the DNA repair defect underlying Fanconi anemia? *Current Opinion in Cell Biology.* **37** 49-60, doi:https://doi.org/10.1016/j.ceb.2015.09.002, (2015).
103 Gómez-Herreros, F. *et al.* TDP2–Dependent Non-Homologous End-Joining Protects against Topoisomerase II–Induced DNA Breaks and Genome Instability in Cells and In Vivo. *PLoS Genetics.* **9** (3), e1003226, doi:10.1371/journal.pgen.1003226, (2013).
104 Hoa, Nguyen N. *et al.* Mre11 Is Essential for the Removal of Lethal Topoisomerase 2 Covalent Cleavage Complexes. *Molecular Cell.* **64** (3), 580-592, doi:https://doi.org/10.1016/j.molcel.2016.10.011, (2016).

105 Andreassen, P. R. & Ren, K. Fanconi anemia proteins, DNA interstrand crosslink repair pathways, and cancer therapy. *Curr Cancer Drug Targets.* **9** (1), 101-117 (2009).
106 Mathew, C. G. Fanconi anaemia genes and susceptibility to cancer. *Oncogene.* **25**, doi:10.1038/sj.onc.1209878, (2006).
107 Walden, H. & Deans, A. J. The Fanconi anemia DNA repair pathway: structural and functional insights into a complex disorder. *Annu Rev Biophys.* **43** 257-278, doi:10.1146/annurev-biophys-051013-022737, (2014).
108 Alexeyev, M., Shokolenko, I., Wilson, G. & LeDoux, S. The Maintenance of Mitochondrial DNA Integrity—Critical Analysis and Update. *Cold Spring Harbor Perspectives in Biology.* **5** (5), a012641, doi:10.1101/cshperspect.a012641, (2013).
109 Tatarenkov, A. & Avise, J. C. Rapid concerted evolution in animal mitochondrial DNA. *Proceedings of the Royal Society B: Biological Sciences.* **274** (1619), 1795-1798, doi:10.1098/rspb.2007.0169, (2007).
110 Brown, W. M., George, M. & Wilson, A. C. Rapid evolution of animal mitochondrial DNA. *Proceedings of the National Academy of Sciences of the United States of America.* **76** (4), 1967-1971 (1979).
111 Ballard, J. W. & Whitlock, M. C. The incomplete natural history of mitochondria. *Mol Ecol.* **13** (0962-1083 (Print)), 729-744 (2004).
112 Iborra, F. J., Kimura, H. & Cook, P. R. The functional organization of mitochondrial genomes in human cells. *BMC Biology.* **2** 9-9, doi:10.1186/1741-7007-2-9, (2004).
113 Hoogenraad, N. J., Ward, L. A. & Ryan, M. T. Import and assembly of proteins into mitochondria of mammalian cells. *Biochimica et Biophysica Acta (BBA) - Molecular Cell Research.* **1592** (1), 97-105, doi:https://doi.org/10.1016/S0167-4889(02)00268-9, (2002).
114 Podratz, J. L. *et al.* Cisplatin induced Mitochondrial DNA Damage In Dorsal Root Ganglion Neurons. *Neurobiology of disease.* **41** (3), 661-668, doi:10.1016/j.nbd.2010.11.017, (2011).
115 Gustafsson, C. M., Falkenberg, M. & Larsson, N.-G. Maintenance and Expression of Mammalian Mitochondrial DNA. *Annual Review of Biochemistry.* **85** (1), 133-160, doi:10.1146/annurev-biochem-060815-014402, (2016).
116 Larsen, N. B., Rasmussen M Fau - Rasmussen, L. J. & Rasmussen, L. J. Nuclear and mitochondrial DNA repair: similar pathways? *Mitochondrion.* **2** (1567-7249 (Print)), 89-108 (2005).
117 Rydberg, B. & Lindahl, T. Nonenzymatic methylation of DNA by the intracellular methyl group donor S-adenosyl-L-methionine is a potentially mutagenic reaction. *The EMBO Journal.* **1** (2), 211-216 (1982).
118 De Bont, R. & van Larebeke, N. Endogenous DNA damage in humans: a review of quantitative data. *Mutagenesis.* **19** (0267-8357 (Print)), 169-185 (2004).

119 Wunderlich, V., Schütt, M., Böttger, M. & Graffi, A. Preferential alkylation of mitochondrial deoxyribonucleic acid by N-methyl-N-nitrosourea. *Biochemical Journal.* **118** (1), 99-109 (1970).
120 Tomasi, A. *et al.* Free-radical metabolism of carbon tetrachloride in rat liver mitochondria. A study of the mechanism of activation. *Biochemical Journal.* **246** (2), 313-317 (1987).
121 Jung, D., Cho, Y., Collins, L. B., Swenberg, J. A. & Di Giulio, R. T. Effects of benzo[a]pyrene on mitochondrial and nuclear DNA damage in Atlantic killifish (Fundulus heteroclitus) from a creosote-contaminated and reference site. *Aquatic toxicology (Amsterdam, Netherlands).* **95** (1), 44-51, doi:10.1016/j.aquatox.2009.08.003, (2009).
122 Kamiya, H. SURVEY AND SUMMARY: Mutagenic potentials of damaged nucleic acids produced by reactive oxygen/nitrogen species: approaches using synthetic oligonucleotides and nucleotides. *Nucleic Acids Research.* **31** (2), 517-531 (2003).
123 El-Khamisy, S. F. & Caldecott, K. W. DNA single-strand break repair and spinocerebellar ataxia with axonal neuropathy-1. *Neuroscience.* **145** (4), 1260-1266, doi:https://doi.org/10.1016/j.neuroscience.2006.08.048, (2007).
124 Croteau, D. L., Stierum, R. H. & Bohr, V. A. Mitochondrial DNA repair pathways. *Mutation Research/DNA Repair.* **434** (3), 137-148, doi:https://doi.org/10.1016/S0921-8777(99)00025-7, (1999).
125 Murphy, Michael P. How mitochondria produce reactive oxygen species. *Biochemical Journal.* **417** (Pt 1), 1-13, doi:10.1042/BJ20081386, (2009).
126 Thorslund, T., Sunesen, M., Bohr, V. A. & Stevnsner, T. Repair of 8-oxoG is slower in endogenous nuclear genes than in mitochondrial DNA and is without strand bias. *DNA Repair.* **1** (4), 261-273, doi:https://doi.org/10.1016/S1568-7864(02)00003-4, (2002).
127 Clayton, D. A., Doda, J. N. & Friedberg, E. C. The Absence of a Pyrimidine Dimer Repair Mechanism in Mammalian Mitochondria. *Proceedings of the National Academy of Sciences.* **71** (7), 2777 (1974).
128 Miyaki, M., Yatagai, K. & Ono, T. Strand breaks of mammalian mitochondrial DNA induced by carcinogens. *Chemico-Biological Interactions.* **17** (3), 321-329, doi:https://doi.org/10.1016/0009-2797(77)90095-3, (1977).
129 Lakshmipathy, U. & Campbell, C. Antisense-mediated decrease in DNA ligase III expression results in reduced mitochondrial DNA integrity. *Nucleic Acids Research.* **29** (3), 668-676 (2001).
130 Donahue, S. L., Corner, B. E., Bordone, L. & Campbell, C. Mitochondrial DNA ligase function in Saccharomyces cerevisiae. *Nucleic Acids Research.* **29** (7), 1582-1589 (2001).
131 Thyagarajan, B., Padua, R. A. & Campbell, C. Mammalian Mitochondria Possess Homologous DNA Recombination Activity. *Journal of Biological Chemistry.* **271** (44), 27536-27543 (1996).

132 Zhou, J., Liu, L. & Chen, J. Mitochondrial DNA Heteroplasmy in Candida glabrata after Mitochondrial Transformation. *Eukaryotic Cell.* **9** (5), 806-814, doi:10.1128/EC.00349-09, (2010).
133 Mileshina, D., Koulintchenko, M., Konstantinov, Y. & Dietrich, A. Transfection of plant mitochondria and in organello gene integration. *Nucleic Acids Research.* **39** (17), e115-e115, doi:10.1093/nar/gkr517, (2011).
134 Bacman, S. R., Williams, S. L. & Moraes, C. T. Intra- and inter-molecular recombination of mitochondrial DNA after in vivo induction of multiple double-strand breaks. *Nucleic Acids Research.* **37** (13), 4218-4226, doi:10.1093/nar/gkp348, (2009).
135 Lakshmipathy, U. & Campbell, C. Double strand break rejoining by mammalian mitochondrial extracts. *Nucleic Acids Research.* **27** (4), 1198-1204 (1999).
136 Coffey, G., Lakshmipathy, U. & Campbell, C. Mammalian mitochondrial extracts possess DNA end-binding activity. *Nucleic Acids Research.* **27** (16), 3348-3354 (1999).
137 Coffey, G. & Campbell, C. An alternate form of Ku80 is required for DNA end-binding activity in mammalian mitochondria. *Nucleic Acids Research.* **28** (19), 3793-3800 (2000).
138 Tadi, S. K. *et al.* Microhomology-mediated end joining is the principal mediator of double-strand break repair during mitochondrial DNA lesions. *Molecular Biology of the Cell.* **27** (2), 223-235, doi:10.1091/mbc.E15-05-0260, (2016).
139 De, A. & Campbell, C. A novel interaction between DNA ligase III and DNA polymerase γ plays an essential role in mitochondrial DNA stability. *Biochemical Journal.* **402** (Pt 1), 175-186, doi:10.1042/BJ20061004, (2007).
140 Gross Nj Fau - Rabinowitz, M. & Rabinowitz, M. Synthesis of new strands of mitochondrial and nuclear deoxyribonucleic acid by semiconservative replication. *J Biol Chem.* **244** (0021-9258 (Print)), 1563-1566 (1969).
141 King, M. P. & Attardi, G. Human cells lacking mtDNA: repopulation with exogenous mitochondria by complementation. *Science.* **246** (4929), 500 (1989).
142 Kukat, A. *et al.* Generation of ρ(0) cells utilizing a mitochondrially targeted restriction endonuclease and comparative analyses. *Nucleic Acids Research.* **36** (7), e44-e44, doi:10.1093/nar/gkn124, (2008).
143 Moretton, A. *et al.* Selective mitochondrial DNA degradation following double-strand breaks. *PLOS ONE.* **12** (4), e0176795, doi:10.1371/journal.pone.0176795, (2017).
144 Shokolenko, I., Venediktova, N., Bochkareva, A., Wilson, G. L. & Alexeyev, M. F. Oxidative stress induces degradation of mitochondrial DNA. *Nucleic Acids Research.* **37** (8), 2539-2548, doi:10.1093/nar/gkp100, (2009).
145 Sordet, O., Khan Qa Fau - Pommier, Y. & Pommier, Y. Apoptotic topoisomerase I-DNA complexes induced by oxygen radicals and

mitochondrial dysfunction. *Cell Cycle.* **9** (1551-4005 (Electronic)), 1095-1097 (2004).
146 Hamon, M.-P., Bulteau, A.-L. & Friguet, B. Mitochondrial proteases and protein quality control in ageing and longevity. *Ageing Research Reviews.* **23** 56-66, doi:https://doi.org/10.1016/j.arr.2014.12.010, (2015).
147 Lee, H. R. & Johnson, K. A. Fidelity of the human mitochondrial DNA polymerase. *J Biol Chem.* **281** (0021-9258 (Print)), 36236-36240 (2006).
148 Pinto, M., Pickrell, A. M., Fukui, H. & Moraes, C. T. Mitochondrial DNA damage in a mouse model of Alzheimer's disease decreases amyloid beta plaque formation. *Neurobiology of aging.* **34** (10), 2399-2407, doi:10.1016/j.neurobiolaging.2013.04.014, (2013).
149 Pickrell, A. M., Pinto, M. & Moraes, C. T. Mouse Models of Parkinson 's Disease Associated with Mitochondrial Dysfunction. *Molecular and cellular neurosciences.* **55** 87-94, doi:10.1016/j.mcn.2012.08.002, (2013).
150 Laloi-Michelin, M. *et al.* Kearns Sayre syndrome: an unusual form of mitochondrial diabetes. *Diabetes & Metabolism.* **32** (2), 182-186, doi:https://doi.org/10.1016/S1262-3636(07)70267-7, (2006).
151 Santos, R. X. *et al.* Mitochondrial DNA Oxidative Damage and Repair in Aging and Alzheimer's Disease. *Antioxidants & Redox Signaling.* **18** (18), 2444-2457, doi:10.1089/ars.2012.5039, (2013).
152 Wang, X., Pickrell, A. M., Zimmers, T. A. & Moraes, C. T. Increase in Muscle Mitochondrial Biogenesis Does Not Prevent Muscle Loss but Increased Tumor Size in a Mouse Model of Acute Cancer-Induced Cachexia. *PLoS ONE.* **7** (3), e33426, doi:10.1371/journal.pone.0033426, (2012).
153 Wang, X. *et al.* Transient systemic mtDNA damage leads to muscle wasting by reducing the satellite cell pool. *Human Molecular Genetics.* **22** (19), 3976-3986, doi:10.1093/hmg/ddt251, (2013).
154 Wang, X. & Moraes, C. T. Increases in mitochondrial biogenesis impair carcinogenesis at multiple levels. *Molecular Oncology.* **5** (5), 399-409, doi:10.1016/j.molonc.2011.07.008, (2011).
155 Jean, S. R. *et al.* Mitochondrial Targeting of Doxorubicin Eliminates Nuclear Effects Associated with Cardiotoxicity. *ACS Chemical Biology.* **10** (9), 2007-2015, doi:10.1021/acschembio.5b00268, (2015).
156 Rin Jean, S. *et al.* Molecular Vehicles for Mitochondrial Chemical Biology and Drug Delivery. *ACS Chemical Biology.* **9** (2), 323-333, doi:10.1021/cb400821p, (2014).
157 Horton Kristin, L., Pereira Mark, P., Stewart Kelly, M., Fonseca Sonali, B. & Kelley Shana, O. Tuning the Activity of Mitochondria‐Penetrating Peptides for Delivery or Disruption. *ChemBioChem.* **13** (3), 476-485, doi:10.1002/cbic.201100415, (2012).
158 Buondonno, I. *et al.* Mitochondria-Targeted Doxorubicin: A New Therapeutic Strategy against Doxorubicin-Resistant Osteosarcoma. *Molecular Cancer Therapeutics.* **15** (11), 2640 (2016).

159 Cheung-Ong, K., Giaever, G. & Nislow, C. DNA-Damaging Agents in Cancer Chemotherapy: Serendipity and Chemical Biology. *Chemistry & Biology.* **20** (5), 648-659, doi:https://doi.org/10.1016/j.chembiol.2013.04.007, (2013).
160 Roos, W. P. & Kaina, B. DNA damage-induced cell death: From specific DNA lesions to the DNA damage response and apoptosis. *Cancer Letters.* **332** (2), 237-248, doi:https://doi.org/10.1016/j.canlet.2012.01.007, (2013).
161 Middleton, M. R. & Margison, G. P. Improvement of chemotherapy efficacy by inactivation of a DNA-repair pathway. *The Lancet Oncology.* **4** (1), 37-44, doi:https://doi.org/10.1016/S1470-2045(03)00959-8, (2003).
162 Zamble, D. B. & Lippard, S. J. Cisplatin and DNA repair in cancer chemotherapy. *Trends in Biochemical Sciences.* **20** (10), 435-439, doi:https://doi.org/10.1016/S0968-0004(00)89095-7, (1995).
163 Annovazzi, L., Mellai, M. & Schiffer, D. Chemotherapeutic Drugs: DNA Damage and Repair in Glioblastoma. *Cancers.* **9** (6), 57, doi:10.3390/cancers9060057, (2017).
164 Sanderson, B. J. S. & Shield, A. J. Mutagenic damage to mammalian cells by therapeutic alkylating agents. *Mutation Research/Fundamental and Molecular Mechanisms of Mutagenesis.* **355** (1), 41-57, doi:https://doi.org/10.1016/0027-5107(96)00021-8, (1996).
165 Helleday, T., Petermann, E., Lundin, C., Hodgson, B. & Sharma, R. A. DNA repair pathways as targets for cancer therapy. *Nature Reviews Cancer.* **8** 193, doi:10.1038/nrc2342
https://http://www.nature.com/articles/nrc2342 - supplementary-information, (2008).
166 Fan, C. H. *et al.* O(6)-methylguanine DNA methyltransferase as a promising target for the treatment of temozolomide-resistant gliomas. *Cell Death & Disease.* **4** (10), e876, doi:10.1038/cddis.2013.388, (2013).
167 Fojo, T. Cancer, DNA repair mechanisms, and resistance to chemotherapy. *J Natl Cancer Inst.* **93** (19), 1434-1436 (2001).
168 Tretyakova, N. Y. *et al.* DNA-reactive protein monoepoxides induce cell death and mutagenesis in mammalian cells. *Biochemistry.* **52** (18), 3171-3181, doi:10.1021/bi400273m, (2013).
169 Cheung-Ong, K., Giaever, G. & Nislow, C. DNA-damaging agents in cancer chemotherapy: serendipity and chemical biology. *Chem Biol.* **20** (5), 648-659, doi:10.1016/j.chembiol.2013.04.007, (2013).
170 Fuss, J. O. & Cooper, P. K. DNA Repair: Dynamic Defenders against Cancer and Aging. *PLOS Biology.* **4** (6), e203, doi:10.1371/journal.pbio.0040203, (2006).
171 Dizdaroglu, M. & Gajewski, E. Structure and mechanism of hydroxyl radical-induced formation of a DNA-protein cross-link involving thymine and lysine in nucleohistone. *Cancer Res.* **49** (13), 3463-3467 (1989).
172 Stingele, J., Bellelli, R. & Boulton, S. J. Mechanisms of DNA-protein crosslink repair. (1471-0080 (Electronic)).

173 Kohn Kw Fau - Erickson, L. C., Erickson Lc Fau - Ewig, R. A., Ewig Ra Fau - Friedman, C. A. & Friedman, C. A. Fractionation of DNA from mammalian cells by alkaline elution. *Biochemistry.* **19** (15), 4629-4637 (1976).
174 Ewig Ra Fau - Kohn, K. W. & Kohn, K. W. DNA damage and repair in mouse leukemia L1210 cells treated with nitrogen mustard, 1,3-bis(2-chloroethyl)-1-nitrosourea, and other nitrosoureas. *Cancer Res.* **37** (0008-5472 (Print)), 2114-2122 (1977).
175 Ewig Ra Fau - Kohn, K. W. & Kohn, K. W. DNA-protein cross-linking and DNA interstrand cross-linking by haloethylnitrosoureas in L1210 cells. *Cancer Res.* **38** (0008-5472 (Print)), 3197-3203 (1978).
176 Vaz, B. *et al.* Metalloprotease SPRTN/DVC1 Orchestrates Replication-Coupled DNA-Protein Crosslink Repair. *Mol Cell.* **64** (1097-4164 (Electronic)), 704-719 (2016).
177 Fromme, J. C., Bruner, S. D., Yang, W., Karplus, M. & Verdine, G. L. Product-assisted catalysis in base-excision DNA repair. *Nat Struct Biol.* **10** (3), 204-211, doi:10.1038/nsb902, (2003).
178 Hirt, B. Selective extraction of polyoma DNA from infected mouse cell cultures. *J Mol Biol.* **26** (2), 365-369 (1967).
179 Lee, H. W. *et al.* Monitoring repair of DNA damage in cell lines and human peripheral blood mononuclear cells. *Anal Biochem.* **365** (2), 246-259, doi:10.1016/j.ab.2007.03.016, (2007).
180 Sikorsky, J. A., Primerano, D. A., Fenger, T. W. & Denvir, J. DNA damage reduces Taq DNA polymerase fidelity and PCR amplification efficiency. *Biochemical and biophysical research communications.* **355** (2), 431-437, doi:10.1016/j.bbrc.2007.01.169, (2007).
181 Wickramaratne, S., Mukherjee, S., Villalta, P. W., Scharer, O. D. & Tretyakova, N. Y. Synthesis of sequence-specific DNA-protein conjugates via a reductive amination strategy. *Bioconjug Chem.* **24** (9), 1496-1506, doi:10.1021/bc400018u, (2013).
182 George, J. W. *et al.* Restoration of nucleotide excision repair in a helicase-deficient XPD mutant from intragenic suppression by a trichothiodystrophy mutation. *Mol Cell Biol.* **21** (21), 7355-7365, doi:10.1128/mcb.21.21.7355-7365.2001, (2001).
183 Minko, I. G. *et al.* Initiation of Repair of DNA−Polypeptide Cross-Links by the UvrABC Nuclease. *Biochemistry.* **44** (8), 3000-3009, doi:10.1021/bi0478805, (2005).
184 Minko, I. G., Zou Y Fau - Lloyd, R. S. & Lloyd, R. S. Incision of DNA-protein crosslinks by UvrABC nuclease suggests a potential repair pathway involving nucleotide excision repair. *Proc Natl Acad Sci U S A.* **99** (0027-8424 (Print)), 1905-1909, doi:D - NLM: PMC122292 EDAT- 2002/02/14 10:00 MHDA- 2002/03/26 10:01 CRDT- 2002/02/14 10:00 AID - 10.1073/pnas.042700399 [doi] AID - 042700399 [pii] PST - ppublish, (2002).

185 Reardon, J. T. & Sancar, A. Repair of DNA-polypeptide crosslinks by human excision nuclease. *PNAS.* **103** (0027-8424 (Print)), 4056-4061, doi:D - NLM: PMC1449645 EDAT- 2006/03/16 09:00 MHDA- 2006/04/28 09:00 CRDT- 2006/03/16 09:00 AID - 0600538103 [pii] AID - 10.1073/pnas.0600538103 [doi] PST - ppublish, (2006).
186 Vaz, B., Popovic, M. & Ramadan, K. DNA-Protein Crosslink Proteolysis Repair. *Trends Biochem Sci.* **42** (6), 483-495, doi:10.1016/j.tibs.2017.03.005, (2017).
187 Connelly, J. C. & Leach, D. R. Repair of DNA covalently linked to protein. *Mol Cell.* **13** (3), 307-316 (2004).
188 Quinones, J. L. & Demple, B. When DNA repair goes wrong: BER-generated DNA-protein crosslinks to oxidative lesions. *DNA Repair (Amst).* **44** 103-109, doi:10.1016/j.dnarep.2016.05.014, (2016).
189 Johnson, L. A. *et al.* Formation of cyclophosphamide specific DNA adducts in hematological diseases. *Pediatr Blood Cancer.* **58** (5), 708-714, doi:10.1002/pbc.23254, (2012).
190 Ming, X. *et al.* Mass Spectrometry Based Proteomics Study of Cisplatin-Induced DNA-Protein Cross-Linking in Human Fibrosarcoma (HT1080) Cells. *Chem Res Toxicol.* **30** (4), 980-995, doi:10.1021/acs.chemrestox.6b00389, (2017).
191 Lal, D., Som, S. & Friedman, S. Survival and mutagenic effects of 5-azacytidine in Escherichia coli. *Mutat Res.* **193** (3), 229-236 (1988).
192 Bhagwat, A. S. & Roberts, R. J. Genetic analysis of the 5-azacytidine sensitivity of Escherichia coli K-12. *J Bacteriol.* **169** (4), 1537-1546 (1987).
193 Ren, X. *et al.* The impact of FANCD2 deficiency on formaldehyde-induced toxicity in human lymphoblastoid cell lines. *Arch Toxicol.* **87** (1), 189-196, doi:10.1007/s00204-012-0911-6, (2013).
194 Quievryn, G. & Zhitkovich, A. Loss of DNA-protein crosslinks from formaldehyde-exposed cells occurs through spontaneous hydrolysis and an active repair process linked to proteosome function. *Carcinogenesis.* **21** (8), 1573-1580 (2000).
195 Larminat, F., Germanier, M., Papouli, E. & Defais, M. Impairment of homologous recombination control in a Fanconi anemia-like Chinese hamster cell mutant. *Biol Cell.* **96** (7), 545-552, doi:10.1016/j.biolcel.2004.06.001, (2004).
196 Zdzienicka, M. Z., Arwert, F., Neuteboom, I., Rooimans, M. & Simons, J. W. The Chinese hamster V79 cell mutant V-H4 is phenotypically like Fanconi anemia cells. *Somat Cell Mol Genet.* **16** (6), 575-581 (1990).
197 Studzian, K., Telleman, P., van der Schans, G. P. & Zdzienicka, M. Z. Mutagenic response and repair of cis-DDP-induced DNA cross-links in the Chinese hamster V79 cell mutant V-H4 which is homologous to Fanconi anemia (group A). *Mutat Res.* **314** (2), 115-120 (1994).

198 Kadkhodayan, S. *et al.* Molecular analysis of ERCC2 mutations in the repair deficient hamster mutants UVL-1 and V-H1. *Mutat Res.* **385** (1), 47-57 (1997).
199 Huang, R., Fang, P. & Kay, B. K. Improvements to the Kunkel mutagenesis protocol for constructing primary and secondary phage-display libraries. *Methods.* **58** (1), 10-17, doi:https://doi.org/10.1016/j.ymeth.2012.08.008, (2012).
200 Mulligan, R. C. & Berg, P. Expression of a bacterial gene in mammalian cells. *Science.* **209** (4463), 1422-1427 (1980).
201 Schmittgen, T. D. & Livak, K. J. Analyzing real-time PCR data by the comparative C(T) method. *Nat Protoc.* **3** (6), 1101-1108 (2008).
202 Tang, W., Liu, J. N. & Gurewich, V. Preparation of single-stranded phagemid DNA without chromosomal DNA contamination. *Biotechniques.* **21** (1), 53-54 (1996).
203 Sambrook, J., Russell, D. W. D. W. & Laboratory, C. S. H. *Molecular cloning : a laboratory manual*. 3rd. ed edn, (Cold Spring Harbor Laboratory, 2001).
204 Atanassov, B., Velkova A Fau - Mladenov, E., Mladenov E Fau - Anachkova, B., Anachkova B Fau - Russev, G. & Russev, G. Comparison of the global genomic and transcription-coupled repair rates of different lesions in human cells. *Zeitschrift fur Naturforschung. C, Journal of biosciences.* **59** (0939-5075 (Print)), 445-453 (2004).
205 Ford, J. M., Lommel, L. & Hanawalt, P. C. Preferential repair of ultraviolet light-induced DNA damage in the transcribed strand of the human p53 gene. *Mol Carcinog.* **10** (2), 105-109 (1994).
206 Michaelson-Richie, E. D. *et al.* Mechlorethamine-induced DNA-protein cross-linking in human fibrosarcoma (HT1080) cells. *J Proteome Res.* **10** (6), 2785-2796, doi:10.1021/pr200042u, (2011).
207 Toth, A., Hegedus, L., Juhasz, S., Haracska, L. & Burkovics, P. The DNA-binding box of human SPARTAN contributes to the targeting of Poleta to DNA damage sites. *DNA Repair (Amst).* **49** 33-42, doi:10.1016/j.dnarep.2016.10.007, (2017).
208 Maskey, R. S. *et al.* Spartan deficiency causes genomic instability and progeroid phenotypes. *Nat Commun.* **5** 5744, doi:10.1038/ncomms6744, (2014).
209 Boesch, P. *et al.* DNA repair in organelles: Pathways, organization, regulation, relevance in disease and aging. *Biochimica et Biophysica Acta (BBA) - Molecular Cell Research.* **1813** (1), 186-200, doi:https://doi.org/10.1016/j.bbamcr.2010.10.002, (2011).
210 Hinz, J. M. *et al.* Repression of mutagenesis by Rad51D-mediated homologous recombination. *Nucleic Acids Research.* **34** (5), 1358-1368, doi:10.1093/nar/gkl020, (2006).
211 Reh, W. A., Nairn, R. S., Lowery, M. P. & Vasquez, K. M. The homologous recombination protein RAD51D protects the genome from large deletions.

Nucleic Acids Research. **45** (4), 1835-1847, doi:10.1093/nar/gkw1204, (2017).
212 Pujari, S. S., Zhang, Y., Ji, S., Distefano, M. D. & Tretyakova, N. Y. Site-specific cross-linking of proteins to DNA via a new bioorthogonal approach employing oxime ligation. *Chemical Communications.* doi:10.1039/C8CC01300D, (2018).
213 Huang, F. & Mazin, A. V. A Small Molecule Inhibitor of Human RAD51 Potentiates Breast Cancer Cell Killing by Therapeutic Agents in Mouse Xenografts. *PLoS ONE.* **9** (6), e100993, doi:10.1371/journal.pone.0100993, (2014).
214 Jessberger, R. & Berg, P. Repair of deletions and double-strand gaps by homologous recombination in a mammalian in vitro system. *Molecular and Cellular Biology.* **11** (1), 445-457 (1991).
215 Klein, J. C. *et al.* Repair and replication of plasmids with site-specific 8-oxodG and 8-AAFdG residues in normal and repair-deficient human cells. *Nucleic Acids Research.* **20** (17), 4437-4443 (1992).
216 Yoon, Y. G. & Koob, M. D. Efficient cloning and engineering of entire mitochondrial genomes in Escherichia coli and transfer into transcriptionally active mitochondria. *Nucleic Acids Research.* **31** (5), 1407-1415, doi:10.1093/nar/gkg228, (2003).
217 Lakshmipathy, U. & Campbell, C. Mitochondrial DNA ligase III function is independent of Xrcc1. *Nucleic Acids Research.* **28** (20), 3880-3886 (2000).
218 Li, J., Bhat, A. & Xiao, W. Regulation of nucleotide excision repair through ubiquitination. *Acta Biochimica et Biophysica Sinica.* **43** (12), 919-929, doi:10.1093/abbs/gmr088, (2011).
219 He, J. *et al.* Ubiquitin-specific Protease 7 Regulates Nucleotide Excision Repair through Deubiquitinating XPC Protein and Preventing XPC Protein from Undergoing Ultraviolet Light-induced and VCP/p97 Protein-regulated Proteolysis. *The Journal of Biological Chemistry.* **289** (39), 27278-27289, doi:10.1074/jbc.M114.589812, (2014).
220 Machida, Y. J. *et al.* UBE2T is the E2 in the Fanconi anemia pathway and undergoes negative autoregulation. *Mol Cell.* **23**, doi:10.1016/j.molcel.2006.06.024, (2006).
221 Suwaki, N., Klare K Fau - Tarsounas, M. & Tarsounas, M. RAD51 paralogs: roles in DNA damage signalling, recombinational repair and tumorigenesis. *Semin Cell Dev Biol.* **8** (1096-3634 (Electronic)), 898-905 (2011).
222 Cardarelli, F. *et al.* The intracellular trafficking mechanism of Lipofectamine-based transfection reagents and its implication for gene delivery. *Scientific Reports.* **6** 25879, doi:10.1038/srep25879
https://http://www.nature.com/articles/srep25879 - supplementary-information, (2016).

223 Van Houten, B., Hunter, S. E. & Meyer, J. N. Mitochondrial DNA damage induced autophagy, cell death, and disease. *Frontiers in bioscience (Landmark edition).* **21** 42-54 (2016).
224 Cline, S. D. Mitochondrial DNA Damage and its Consequences for Mitochondrial Gene Expression. *Biochimica et biophysica acta.* **1819** (9-10), 979-991, doi:10.1016/j.bbagrm.2012.06.002, (2012).
225 Caston, R. A. & Demple, B. Risky repair: DNA-protein crosslinks formed by mitochondrial base excision DNA repair enzymes acting on free radical lesions. *Free Radical Biology and Medicine.* **107** 146-150, doi:https://doi.org/10.1016/j.freeradbiomed.2016.11.025, (2017).
226 Morrow, B. & Kucherlapati, R. Gene targeting in mammalian cells by homologous recombination. *Current Opinion in Biotechnology.* **4** (5), 577-582, doi:https://doi.org/10.1016/0958-1669(93)90080-G, (1993).
227 Smithies O Fau - Koralewski, M. A., Koralewski Ma Fau - Song, K. Y., Song Ky Fau - Kucherlapati, R. S. & Kucherlapati, R. S. Homologous recombination with DNA introduced into mammalian cells. *Cold Spring Harb Symp Quant Biol.* **49** (0091-7451 (Print)), 161-170 (1984).
228 Kucherlapati, R. S., Eves, E. M., Song, K. Y., Morse, B. S. & Smithies, O. Homologous recombination between plasmids in mammalian cells can be enhanced by treatment of input DNA. *Proceedings of the National Academy of Sciences of the United States of America.* **81** (10), 3153-3157 (1984).
229 Rouet, P., Smih, F. & Jasin, M. Expression of a site-specific endonuclease stimulates homologous recombination in mammalian cells. *Proceedings of the National Academy of Sciences of the United States of America.* **91** (13), 6064-6068 (1994).
230 Rouet, P., Smih, F. & Jasin, M. Introduction of double-strand breaks into the genome of mouse cells by expression of a rare-cutting endonuclease. *Molecular and Cellular Biology.* **14** (12), 8096-8106 (1994).
231 Bernstein, K. A. & Rothstein, R. At Loose Ends: Resecting a Double-Strand Break. *Cell.* **137** (5), 807-810, doi:10.1016/j.cell.2009.05.007, (2009).
232 Mechilli, M., Schinoppi, A., Kobos, K., Natarajan, A. T. & Palitti, F. DNA repair deficiency and acetaldehyde-induced chromosomal alterations in CHO cells. *Mutagenesis.* **23** (1), 51-56, doi:10.1093/mutage/gem042, (2008).
233 Grafstrom, R. C., Fornace, A. J., Autrup, H., Lechner, J. F. & Harris, C. C. Formaldehyde damage to DNA and inhibition of DNA repair in human bronchial cells. *Science.* **220** (4593), 216 (1983).
234 Masson, J.-Y. *et al.* Identification and purification of two distinct complexes containing the five RAD51 paralogs. *Genes & Development.* **15** (24), 3296-3307, doi:10.1101/gad.947001, (2001).
235 Chun, J., Buechelmaier, E. S. & Powell, S. N. Rad51 Paralog Complexes BCDX2 and CX3 Act at Different Stages in the BRCA1-BRCA2-Dependent Homologous Recombination Pathway. *Molecular and Cellular Biology.* **33** (2), 387-395, doi:10.1128/MCB.00465-12, (2013).

236 Feng, Z. *et al.* Rad52 inactivation is synthetically lethal with BRCA2 deficiency. *Proceedings of the National Academy of Sciences.* **108** (2), 686 (2011).
237 Kaufman, B. A. *et al.* In organello formaldehyde crosslinking of proteins to mtDNA: Identification of bifunctional proteins. *Proceedings of the National Academy of Sciences of the United States of America.* **97** (14), 7772-7777 (2000).
238 Borisov Am Fau - Guliaeva, N. A., Guliaeva Na Fau - Rasskazova, E. A., Rasskazova Ea Fau - Ploskonosova, I. I., Ploskonosova Ii Fau - Gaznev, A. I. & Gaznev, A. I. [DNA-protein cross-links in nuclei and mitochondria of tissue cells from rats of various age exposed to gamma-radiation]. *Radiats Biol Radioecol.* **44** (0869-8031 (Print)), 377-382 (2004).
239 Song, K. Y., Chekuri, L., Rauth, S., Ehrlich, S. & Kucherlapati, R. Effect of double-strand breaks on homologous recombination in mammalian cells and extracts. *Molecular and Cellular Biology.* **5** (12), 3331-3336 (1985).
240 Chamberlain, G. R., Tulumello, D. V. & Kelley, S. O. Targeted Delivery of Doxorubicin to Mitochondria. *ACS Chemical Biology.* **8** (7), 1389-1395, doi:10.1021/cb400095v, (2013).
241 Fonseca, Sonali B. *et al.* Rerouting Chlorambucil to Mitochondria Combats Drug Deactivation and Resistance in Cancer Cells. *Chemistry & Biology.* **18** (4), 445-453, doi:https://doi.org/10.1016/j.chembiol.2011.02.010, (2011).
242 Yousif Lema, F., Stewart Kelly, M. & Kelley Shana, O. Targeting Mitochondria with Organelle‐Specific Compounds: Strategies and Applications. *ChemBioChem.* **10** (12), 1939-1950, doi:10.1002/cbic.200900185, (2009).
243 Dahal, S., Dubey, S. & Raghavan, S. C. Homologous recombination-mediated repair of DNA double-strand breaks operates in mammalian mitochondria. *Cellular and Molecular Life Sciences.* **75** (9), 1641-1655, doi:10.1007/s00018-017-2702-y, (2018).
244 Arora, S., Kothandapani, A., Tillison, K., Kalman-Maltese, V. & Patrick, S. M. Downregulation of XPF–ERCC1 enhances cisplatin efficacy in cancer cells. *DNA Repair.* **9** (7), 745-753, doi:https://doi.org/10.1016/j.dnarep.2010.03.010, (2010).
245 Gavande, N. S. *et al.* DNA repair targeted therapy: The past or future of cancer treatment? *Pharmacology & Therapeutics.* **160** 65-83, doi:https://doi.org/10.1016/j.pharmthera.2016.02.003, (2016).
246 Remmen, H. V. & Richardson, A. Oxidative damage to mitochondria and aging. *Experimental Gerontology.* **36** (7), 957-968, doi:https://doi.org/10.1016/S0531-5565(01)00093-6, (2001).
247 Quinn, J. A. *et al.* Phase II Trial of Temozolomide Plus O(6)-Benzylguanine in Adults With Recurrent, Temozolomide-Resistant Malignant Glioma. *Journal of Clinical Oncology.* **27** (8), 1262-1267, doi:10.1200/JCO.2008.18.8417, (2009).
248 Dolan, M. E., Mitchell, R. B., Mummert, C., Moschel, R. C. & Pegg, A. E. Effect of O⁶-Benzylguanine Analogues

on Sensitivity of Human Tumor Cells to the Cytotoxic Effects of Alkylating Agents. *Cancer Research.* **51** (13), 3367 (1991).
249 Li, W. & Ye, Y. Polyubiquitin chains: functions, structures, and mechanisms. *Cellular and molecular life sciences : CMLS.* **65** (15), 2397-2406, doi:10.1007/s00018-008-8090-6, (2008).
250 Busso, C. S., Iwakuma, T. & Izumi, T. Ubiquitination of mammalian AP endonuclease (APE1) regulated by the p53–MDM2 signaling pathway. *Oncogene.* **28** 1616, doi:10.1038/onc.2009.5
https://http://www.nature.com/articles/onc20095 - supplementary-information, (2009).
251 Hirasawa, M., Nakayama, M., Kim, S.-K., Hase, T. & Knaff, D. B. Chemical modification studies of tryptophan, arginine and lysine residues in maize chloroplast ferredoxin:sulfite oxidoreductase. *Photosynthesis Research.* **86** (3), 325-336, doi:10.1007/s11120-005-6966-y, (2005).
252 Barker, S., Weinfeld, M., Zheng, J., Li, L. & Murray, D. Identification of Mammalian Proteins Cross-linked to DNA by Ionizing Radiation. *Journal of Biological Chemistry.* **280** (40), 33826-33838 (2005).
253 Davis, A. J. & Chen, D. J. DNA double strand break repair via non-homologous end-joining. *Translational cancer research.* **2** (3), 130-143, doi:10.3978/j.issn.2218-676X.2013.04.02, (2013).